THE ANALYSIS OF AUTOGRAPHA CALIFORNICA MULTIPLE NUCLEOPOLYHEDROVIRUS EXONO (ORF141) FUNCTION AND ITS ROLE IN VIRUS BUDDING

by
Minggang Fang

B.Sc, Huazhong Agricultural University, Wuhan, China, 1999

M.Sc, Wuhan Institute of Virology, Chinese Academy of Sciences, Wuhan, China, 2002

A THESIS SUBMITTED IN PARTIAL FULFILLMENT OF THE

REQUIREMENTS FOR THE DEGREE OF

Doctor of Philosophy

in

THE FACULTY OF GRADUATE STUDIES

(Plant Science)

UNIVERSITY OF BRITISH COLUMBIA

November, 2007

Abstract

Baculoviruses have a biphasic replication cycle producing two types of virions, budded virus (BV) and occlusion derived virus (ODV) which are required for the systemic spread or oral infection with the insect host respectively. Little is known about the events of the BV pathway and the mechanism by which nucleocapsids are selected and directed from the nucleus to plasma membrane to form BV. The *Autographa californica* Multiple Nucleopolyhedrovirus (AcMNPV) gene *exon0* (*orf141*) is known to be required for the efficient production of BV and in this study the function and mechanism by which EXON0 affects BV production was investigated.

Confocal microscopic analysis showed that EXON0 localized in the nucleus in the ring zone of virogenic stroma where nucleocapsids are assembled. In addition EXON0 also concentrated in the cytoplasm at the plasma membrane. Analysis of virions revealed that EXON0 copurified with nucleocapsid fractions of both BV and ODV. In support of this yeast 2-hybrid screening, co-immunoprecipitation, and confocal microscopy revealed that EXON0 interacted with the known nucleocapsid proteins FP25 and BV/ODV-C42. Transmission electron microscopy showed that deletion of *exon0* results in nucleocapsids being unable to efficiently egress from the nucleus to the cytoplasm.

Cellular protein interaction analyzed by tandem affinity purification and co-immunoprecipitation showed that β-tubulin co-purified with EXON0. Immunofluorescence also showed that EXON0 and microtubules co-localized during virus infection. The microtubule inhibitors colchicine and nocodazole affected the localization of EXON0 and significantly reduced BV production. These data support the conclusion that egress of AcMNPV nucleocapsids is facilitated by interaction of EXON0 with β-tubulin and microtubules.

Deletion and point mutation analysis mapped domains of EXON0 required for efficient budding, dimer formation and association with FP25, BV/ODV-C42 and β-tubulin. The

Leucine zipper domain was required for dimer formation, β-tubulin and BV/ODV-C42 interaction and also reduced interaction with FP25. Multiple domains were also shown to affect BV production.

This study provides a detailed analysis of EXON0 which is one of the first baculovirus genes shown to be specific for the BV pathway. The results extend our understanding of the BV pathway which is a major determinant of baculovirus pathogenesis.

Table of Contents

List of Tables

List of Figures

Appendix

List of Abbreviations

aa	amino acid
A	alanine
Ab	antibody
AcMNPV	*Autographa californica* multiple nucleopolyhedrovirus
AD	activating domain
ATP	adenosine tri-phosphate
BmNPV	*Bombyx mori* nucleopolyhedrovirus
B	basic domain
BD	binding domain
bp	base pair
BV	budded virus
CIP	calf intestinal phosphatase
C-terminal	carboxy-terminal
Δ	deletion
DNA	deoxyribonucleic acid
dNTP	deoxynucleotide triphophatases
DO	dropout
DTT	dithiothreitol
Fig.	Figure
GFP	green fluorescent protein
g	gram in the context of weight
g	gravitiy force in the context of speed
GP64	glycoprotein 64
His	Histidine
HLH	helix-loop-helix
hpi	hour(s) post infection
hpt	hour(s) post transfection
HSV-1	herpes simplex virus 1
G	Glycine
Gly	Glycine
GV	Granulovirus
IE	immediate early
IPTG	isopropyl-β-D-thiogalactopyranoside
K	Lysine
kb	kilobase
kDa	kilodalton
L	Leucine
Ld	*Lymantria dispar*
lef	late expression factor
Leu	Leucine
Lys	Lysine
Leu	leucine zipper domain

µ	micro
M	molar in the context of concentration; methionine in the context of protein sequence
MAb	monoclonal antibody
ml	millilitre
mM	millimolar
NaCl	sodium chloride
nt	nucleotides
N-terminal	amino-terminal
NPV	Nucleopolyhedrovirus
OB	occlusion body
ODV	occlusion derived virus
OpMNPV	*Orgyia pseudosugata* multiple nucleopolyhedrovirus
ORF	open reading frame
PBS	phosphate buffered saline
PCNA	proliferating cell nuclear antigen
PCR	polymerase chain reaction
PSMC1	proteasome (macropain) 26S subunit ATPase 1
RING	Really Interesting New Gene, RING finger domain
RNA	ribonucleic acid
S	Serine
SDS	sodium dodecyl sulfate
Sf	*Spodoptera frugiperda*
$TCID_{50}$	tissue culture infections dose 50%
TEM	transmission electron microscope
Tris	Tris-hydroxymethyl amino methane
Trp	Tryptophan
WT	wild type

Acknowledgements

I would like to thank my supervisor Dr. David A. Theilmann for giving me the opportunity to pursue my doctoral studies in his lab and for his guidance during my thesis. I would also like to express my gratitude to his family for their support and help in my research, especially for their hospitality and friendship. I would also like to thank other members of my supervisory committee, Dr. Murray Isman, Dr. Janet Chantler and Dr. Brian Ellis for attending my annual progress meeting and providing valuable suggestions to my research.

I am grateful to Les Willis for his endless effort to always help me and great advice. I appreciate his excellent organization of the lab and technical assistance which contributed a lot to my research. My thanks also go to Joan Chisholm for her always warm-hearted and timely help. Many thanks to everybody that are currently or have worked in the Theilmann lab, including Xiaojiang, Ilse, Taryn, Kevin, and Christina, for their assistance and advice. I am grateful to Michael Weis for his expert help with transmission electron microscopy and confocal microscopy. I would like to thank Rob Linning, Ron Reade for their valuable suggestions in research. I would also like to thank many other people in the research station for their help. Thank the Pacific Agri-Food Research Centre for allowing me to conduct the research for my thesis and using their facility.

The work presented in this thesis would not have been completed without the help of many other scientists. Thank Dr. Henry Krause (University of Toronto, Toronto,

Canada) and Dr. Elisa Izaurralde (EMBL, Heidelberg, Germany) for their kindly providing the plasmids for the tandem affinity purification; Dr. Sharon Braunagel (Texas A&M University, Texas, USA) and Dr. George Rohrmann (Oregon State University, Oregon, USA) for providing valuable antibodies. I also like to thank Suzanne Perry (Protein Core Facility, UBC, Vancouver) for her assistance in protein identification.

I would like to express my gratitude to Lia Maria, Kirsten Cameron and Alina Yukhymets for helping me with all the administration.

I would like to thank all my friends in the beautiful Okanagan Valley for their help and sharing much fun time together. They are John and Ikeda Laurie, Juan and his family, Guangzhi Zhang and his family, Changwen Lu and his family, Yu Xiang and his family, Xin Hu and his family, Juanhuan Xu, Collin Ho and Shawkat Ali. My sincere gratitude is extended to our landlord Zhila and Peter Scholfield for their kindness over the years.

Finally, I would like to thank my dear family for their continuous support. I am indebted to my wife, Yingchao and like to express my sincerest gratitude and love to her. Thank you very much for your understanding, day to day encouragement, moral support and help in daily life and research.

Co-Authorship Statement

Dr. Xiaojiang Dai is a co-author as the materials she helped develop on the initial study of EXON0 provided part of the foundation for the research in this study. Yingchao Nie performed some of the protein sample preparations that were used for mass spectrometry analysis.

Chapter 1: Introduction

1.1 Introduction to the baculovirus

Insects are ubiquitous on this planet and they represent over one million different species, of which many are infected by a diverse spectrum of viruses. Viral diseases of beneficial insect can lead to ecological loss, while baculoviruses are beneficial viruses by their potential to control important pests of crops and trees. Insect pathogenic viruses can be classified into 12 viral families of which the *Baculoviridae* is the most intensely studied (Miller and Ball, 1998). The baculoviruses are large DNA viruses that infect the larval stages of arthropods, mainly from the orders of Lepidoptera, Hymenoptera and Diptera (Theilmann et al., 2005). The *Baculoviridae* traditionally includes two genera: the nucleopolyhedroviruses (NPVs) and granuloviruses (GVs). With more phylogenetic evidence from the available viral genomes, baculoviruses have been proposed to comprise four genera: alphabaculovirus (lepidopteran-specific NPV), betabaculovirus (lepidopteran-specific GV), gammabaculovirus (hymenopteran-specific NPV) and deltabaculovirus (dipteran-specific NPV) (Jehle et al., 2006). However, for the purpose of this thesis the currently officially accepted NPV and GV genera will be used. Phylogenetic analysis based on the polyhedrin gene and genome sequence comparisons further suggests that the lepidopteran NPVs might be subdivided into two groups: the group I NPVs including *Autographa californica* multiple NPV (AcMNPV) and *Orgyia pseudosugata* MNPV (OpMNPV), and the group II NPVs typically including *Lymantria dispar* MNPV (LdMNPV) and *Spodoptera exigua* MNPV (SeMNPV) (Chen et al., 1997; Herniou et al., 2003; Herniou et al., 2004; Zanotto et al, 1993).

Some baculoviruses have been successfully used to control pests, notably OpMNPV for the Douglas fir tussock moth in North America and *Anticarsia gemmatalis* NPV for the velvet bean caterpillar in Brazil (Martignoni, 1999; Moscardi, 1999). However, a slower

killing ability of target insects and a narrow host range relative to chemical insecticides has limited their use as pesticides. Due to environmental concerns the use of baculoviruses as biocontrol agents remains high. To accelerate their speed of action baculoviruses have been genetically engineered by insertion of insect specific scorpion neurotoxin genes such as AaIT (Maeda et al., 1991; Stewart et al., 1991) or deletion of viral ecdysteroid UDP-glucosyltransferase (*egt)* gene (O'Reilly and Miller, 1991), which reduced the lethal time up to 25% compared to those of wild-type virus (Stewart et al, 1991).

Baculoviruses are also used extensively as a eukaryotic expression system for the production of biologically active proteins at very high levels (Douris et al., 2006). The baculovirus expression system is one of the most successful and widely used protein production systems in the biotechnology industry. Expression of proteins in insect cells permits proper folding, post-translational modifications (e.g. glycosylation, phosphorylation, internal cleavage) and oligomerization like their authentic counterparts (Vialard et al, 1995). Two types of insect cell based systems are in use: the baculovirus expression system and stably transformed insect cell lines.

Baculoviruses are also a major focus of interest since the discovery that baculoviruses can efficiently transduce mammalian cells and become potential vectors for gene therapy (Boyce and Bucher, 1996; Hofmann and Strauss, 1998). Particular advantages of baculovirus vectors are lack of toxicity and replication, large cloning capacity, ease of construction and production (Hu, 2006).

1.1.1 Structure

Baculoviruses are large, enveloped double-stranded DNA viruses which are characterized by the formation of the large proteinaceous occlusion bodies (OBs) which are stable for years in the environment. NPV or GV OBs can be distinguished by their morphology: the NPVs have large (ranging in size from 0.15-15 μm) polyhedron-shaped OBs (called polyhedra) which contain many virions, while GVs produce smaller (about 0.13×0.5 μm)

ovicylindrical-shaped OBs (called granules) that commonly contain a single virion. The occluded virions of NPVs are packaged with either single (S) or multiple (M) nucleocapsids with a single viral envelope. Nucleocapsids are rod-shaped and contain a single molecule of circular supercoiled dsDNA of approximately 80-180 kilobasepair (kbp) in size.

Two virion phenotypes can be commonly found in the baculovirus replication cycle (Fig. 1.1). Occlusion derived virus (ODV) initiates infection in the midgut epithelium of insects. If infections are not restricted to the gut epithelium a second virion phenotype, termed budded virus (BV), is generated when nucleocapsids bud through the plasma membrane at the surface of infected cells. BV typically contains a single nucleocapsid within an envelope and spreads the infection throughout the larval body. ODVs and BVs have similar nucleocapsids but are morphological distinct and have specific polypeptides (Braunagel and Summers, 1994; Funk et al, 1997).

1.1.2 Infection cycle

The primary infection cycle in animals begins in the midgut cell when OBs are taken up (Fig. 1.2). Upon ingestion the OBs dissolve in the alkaline environment of the midgut and the ODVs are released into the lumen of midgut. The virions pass through the peritrophic membrane and subsequently fuse directly with the microvilli of midgut columnar epithelial cells (Granados, 1978; Granados and Lawler, 1981; Horton and Burand, 1993). The nucleocapsids are transported to the nucleus of the midgut cells, where gene expression, DNA replication and assembly of progeny nucleocapsids occur. In the late phase of infection, newly formed nucleocapsids are transported to the cell membrane, bud from the cell and acquire a new envelope from the basal membrane. The BVs spread via the hemolymph (Granados and Lawler, 1981) and the tracheal system (Engelhard et al., 1994) into the other tissues of the insect causing the secondary infection. In the very late stage of infection, the nucleocapsids are assembled in *de novo* formed envelopes to become ODV. The enveloped ODV are then incorporated into OBs which are also referred to as polyhedra. At the end of infection cycle, the cells and tissues disintegrate

and OBs are released into the environment. Baculoviruses encode proteins such as fibrillin, chitinase and cathepsin which have been reported to facilitate the process (Hawtin et al., 1995; Hawtin et al., 1997; Hill et al., 1995; Slack et al., 1995; Van Oers and Vlak, 1997a).

In cultured cells the baculovirus infection cycle starts by the attachment of a BV to the cell membrane. BVs enter the cells by endocytosis and the acidification of the endosome triggers the fusion of BV envelope and endosome vesicle. Following release from the endosome the nucleocapsids are transported to the nucleus, where viral transcription and DNA replication occur. Newly assembled nucleocapsids one of two fates, they either move out of the nucleus into the cytoplasm and bud through the plasma membrane or are enveloped *de novo* in the nucleus and occluded into polyhedra (Williams and Faulkner, 1997).

1.1.3 Genome and gene expression

Baculoviruses contain a circular, supercoiled dsDNA genome with sizes ranging from 80-180 kbp, encoding approximately 90 to 180 proteins (Jehle et al., 2006). These genes are tightly packed with minimal intergenic region and are almost evenly distributed on both strands. Baculovirus-encoded proteins can be grouped into five functional classes, namely, proteins involved in transcription, replication, virion structure and proteins with auxiliary or unknown functions (O'Reilly, 1997). More than 800 different orthologous gene groups were identified from sequenced baculovirus genomes, only 29 genes called baculovirus core genes are common to all baculoviruses (Jehle et al., 2006). One unique feature of most baculovirus genomes is the presence of several homologous regions (*hrs*) with repeated sequences, which are suggested to function as the origin of DNA replication and the enhancer of transcription. These were first identified in the genome of the best studied baculovirus, AcMNPV, which is composed of 133,894 bp, potentially encoding 154 proteins (Ayres et al., 1994).

Baculovirus gene expression is temporally regulated in a sequential, cascade-like fashion in which each sequential phase is dependent on the previous one (Blissard and Rohrmann, 1990). Two main classes of genes are recognized: early and late. Early genes are transcribed by the host RNA polymerase II and contain the typical eukaryotic consensus TATA box and a CAGT motif at the transcriptional start site. One of the early genes is the major transactivator, *ie-1*, which plays an essential role in gene transactivation and DNA replication. Once DNA replication starts, late gene expression is initiated. Late genes are transcribed by a viral RNA polymerase. This viral polymerase is α-amanitin resistant and composed of at least four viral proteins, namely Late Expression Factor 4 (LEF4), LEF8, LEF9 and P47 (Guarino et al., 1998). The transcription of late genes start at a consensus A/TAAG motif and the majority of the late genes encode viral structural proteins or proteins involved in virion morphogenesis. Approximately nineteen viral proteins known as LEFs are identified and are necessary for late gene transcription.

1.1.4 Viral entry

BVs and ODVs have different envelope proteins and enter cells by different mechanisms. In midgut the polyhedra dissolve quickly in the highly alkaline environment (Granados, 1978; Granados and Lawler, 1981). Virions released from the occlusion bodies (ODVs) pass through the peritrophic membrane. Enhancins, a group of metalloproteases, are believed to disrupt the structural integrity of the peritrophic membrane and facilitate the passage (Hashimoto et al, 1991; Lepore et al, 1996; Wang et al, 1994). After crossing the peritrophic membrane, the virion envelope contacts and fuses with the microvillar membrane of columnar midgut epithelial cells (Granados and Lawler, 1981; Summers, 1971). The entry of ODV is via a non-endocytic pathway involving direct membrane fusion. A specific cellular receptor is involved because the attachment is saturable and protease pre-treatment results in a major reduction of binding (Horton and Burand, 1993). Nucleocapsids enter the microvilli and travel to nucleus where nucleocapsids uncoat, releasing the viral DNA to initiate the replication. Microtubules have been proposed to aid the transport of nucleocapsids in the epithelial cells based on their apparent

coalignment from the electron micrographs (Granados, 1978; Granados and Lawler, 1981).

BVs enter cells in culture primarily by adsorptive endocytosis, including two steps, namely, clathrin-mediated endocytosis and low-pH-dependent membrane fusion (Blissard and Wenz, 1992; Long et al., 2006; Volkman and Goldsmith, 1985). Glycoprotein GP64 is the major envelope fusion protein found in the BVs of AcMNPV and other members of the group I NPVs (Blissard, 1996; Volkman and Goldsmith, 1985; Volkman et al., 1984; Whitford et al., 1989). Previous studies showed that GP64 is involved in BV binding to target cells, is necessary for low-pH-dependent membrane fusion to allow entry, and is important for efficient budding from the cell surface (Blissard and Wenz, 1992; Monsma and Blissard, 1995; Oomens and Blissard, 1999a). BVs also bind to specific receptors on the cellular membrane in a saturable manner (Wickham et al., 1992), and GP64 was shown to be a host cell receptor-binding protein by a specific competition assay (Hefferon et al., 1999). A monoclonal antibody specific to GP64 MAb AcV1 was shown to neutralize virion entry by blocking membrane fusion, a step after virion binding (Chernomordik et al., 1995; Volkman and Goldsmith, 1985). However, the host cell receptors have not been identified for the entry of either BV or ODV. After the fusion of the BV envelope with membranes of a late endosome, nucleocapsids are released and traverse in the cytoplasm. Nucleocapsids can induce the formation of F-actin bundles and single nucleocapsids were observed to be associated with one end of the F-actin cables (Charlton and Volkman, 1991a; 1993). These actin cables are thought to facilitate the transport of nucleocapsids to the nucleus (Lanier and Volkman, 1998a). The uncoating of nucleocapsids is believed to occur at the nuclear pore complex or just inside the nuclear pore, and the phosphorylation of the basic DNA-binding core protein (BDBP) P6.9 by a capsid-associated kinase results in the release of viral genome (Funk and Consigli, 1993; Wilson and Consigli, 1985). The release of viral genome into the nucleoplasm of a susceptible cell is rapidly followed by the transcription of viral genes and protein synthesis in a cascade-like fashion.

1.1.5 Nucleocapsids assembly, egress and budding

The virogenic stroma is a *de novo* product of virus infected nucleus within which viral DNA is replicated and the progeny nucleocapsids are assembled in this "virus factory". The formation of this virogenic stroma coincides with viral DNA replication and late gene expression. At late times post-infection, the virogenic stroma matures and has two distinct regions, a fibrillar electron-dense stromal matte which is interspersed by intrastromal spaces. These spaces can be intensely stained by DNA-specific fluorescent dyes and are the places where the progeny nucleocapsids are assembled (MacKinnon et al., 1974a; Summers, 1971). The region surrounding the virogenic stroma between the centrally placed virogenic stroma and the nuclear membrane is called the ring zone, where the nucleocapsids are enveloped and packaged into occlusion bodies (Charlton and Volkman, 1991a; MacKinnon et al., 1974a; Xeros, 1956). The fine structure and molecular components of the virogenic stroma are not well known. However, two viral proteins P6.9, pp31 and DNA are known to be constituents. Some DNase-sensitive filament bundles which localize throughout the stromal matte are postulated to consist of viral DNA and basic DNA-binding protein P6.9 and be the precondensed viral genomes (Wilson et al., 1987; Young et al, 1993). The 39K gene product pp31 has also been found to localize, accumulate in the virogenic stroma and bind to dsDNA (Broussard et al, 1996; Guarino et al., 1992).

Baculovirus nucleocapsids have specialized end structures, with a flat plate on the basal end and a nipple-shaped structure on the other apical end (Kawamoto et al., 1977; Summers, 1971). According to Fraser (1986), the empty capsid sheaths are formed by sequential addition to the basal plate, and the apical end cap may mediate the packing of the nucleoprotein into the capsids. The supercoiled viral genome is prepackaged with the basic DNA-binding protein P6.9 and assembly of the nucleoprotein may be regulated by the state of phosphorylation of P6.9 (Funk and Consigli, 1993). Highly basic polyamines and spermidine may also play a role to neutralize the phosphate of viral DNA and are packaged with viral genome into nucleoproteins (Elliot and Kelly, 1977). The nucleoprotein complex is subsequently inserted into the preformed capsids shell at the edge of stromal matte.

Multiple approaches including proteomic identification has revealed that the ODV of AcMNPV contains 31 to 44 proteins and the nucleocapsids of AcMNPV ODV may consist of up to 29 polypeptides (Braunagel et al., 2003). Eight proteins including P78/83 (Russell et al, 1997), VP1054 (Olszewski and Miller, 1997a), FP25 (Braunagel et al., 1999), VLF-1 (Yang and Miller, 1998b), VP39 (Thiem and Miller, 1989), BV/ODV-C42 (Braunagel et al., 2001), P87 (Lu and Carstens, 1992) and P24 (Wolgamot et al., 1993) have been identified as the components of both BV and ODV nucleocapsids in AcMNPV. The assembly of nucleocapsids may involve extensive protein-protein and protein-DNA interactions and little is known about it. The nucleocapsid proteins P78/83, VP1054, and VLF-1 have been shown to be required for nucleocapsid assembly and in their absence there is either no nucleocapsid production or nucleocapsids are malformed (Olszewski and Miller, 1997a; Possee et al., 1991; Vanarsdall et al, 2006).

The intranuclear assembly of baculovirus nucleocapsids and the production of infectious progeny require the actin filaments because the presence of Cytochalasin D which specifically inhibits actin microfilament elongation results in aberrant tubular structures that lack the nucleoprotein core (Volkman, 1988). The actin filaments are induced in the nucleus upon baculovirus infection and localize in the peristromal space during the time of active nucleocapsid morphogenesis (Charlton and Volkman, 1991a). Removal of Cytochalasin D the morphogenic process is restored even in the absence of new protein synthesis (Volkman et al., 1992).

Mature nucleocapsids are able to migrate into the ring zone surrounding the virogenic stroma, where they have one of two possible destinations. At the early stages of an infection cycle, progeny nucleocapsids are believed to be destined to form BV and egress from the nucleus to cytoplasm and bud at the cytoplasmic membranes (Williams and Faulkner, 1997). At very late times p.i. nucleocapsids are also retained in the nucleus and enveloped by *de novo* membrane and finally become occluded in occlusion bodies. For AcMNPV, the maximum production of BV is achieved at about 24 hpi, while later BV production declines after the intranuclear envelopment of nucleocapsids begins (Williams

and Faulkner, 1997). The molecular events that occur during baculovirus replication have been extensively studied, but the mechanisms by which the nucleocapsids are shuttled to either ODV or BV and how the nucleocapsids are transported to the cell membrane are still unknown. It seems that some structural proteins of nucleocapsids can trigger the transport of nucleocapsids out of the ring zone to the cytoplasmic membrane, and the intranuclear envelopment of nucleocapsids later blocks the access of nucleocapsids to the cellular transport machinery.

Although the molecular mechanism of the transport of baculovirus nucleocapsids is unknown, electron microscopy studies suggest the following routes of nucleocapsid egress from the ring zone to cytoplasmic membrane. The nucleocapsids are found to penetrate the nuclear membrane in direct contact with the inner nuclear membrane. The curvature of the nuclear membrane results in packaging of nucleocapsids in the nuclear membrane, followed by vesicle "pinch off" from nuclear membrane to form transport vesicles in the cytoplasm with the nucleocapsids inside. A few changes occur to the nuclear membrane during the NPV infection. According to Williams and Faulkner (1997), "nuclear cisternae become swollen and extend into the cytoplasm; electron dense patches are often observed along the nucleoplasmic face of the inner nuclear membrane". The nuclear membrane-derived vesicle is lost during egress by an unknown mechanism and naked nucleocapsids are found in the cytoplasm. Multivesicular aggregates with many nucleocapsids which may result from a series of membrane fusions are often seen in the cytoplasm. The unenveloped nucleocapsids migrate to the plasma membrane and align their apical end with the plasma membrane in the process of budding (Adams et al, 1977; Kawamoto et al., 1977). The sites of budding are pre-enriched with BV envelope proteins and the prominent peplomers or spikes which contain the major envelope fusion protein GP64 are observed on the apical end of budding nucleocapsids (Volkman, 1986; Volkman et al., 1984). Usually a single nucleocapsid buds at the plasma membrane acquiring a loose-fitting envelope. GP64 has been shown to be required for the efficient budding and cell-to-cell propagation but does not affect normal formation of occlusion bodies (Monsma et al., 1996; Oomens and Blissard, 1999a).

1.1.6 Baculovirus proteins including EXON0 that affect BV egress

Several baculovirus genes have been shown to affect the synthesis of BV. For example the AcMNPV P78/83, VLF-1 and VP1045, are nucleocapsid proteins of both BV and ODV, and have been shown to be required for the assembly of progeny nucleocapsids in the nucleus (Olszewski and Miller, 1997a; Vanarsdall et al, 2006; Yang and Miller, 1998b). P78/83 has been shown to localize at the basal end of the nucleocapsid and bind directly to actin, thereby nucleating actin polymerization (Goley et al., 2006; Lanier and Volkman, 1998a; Vialard and Richardson, 1993). P78/83 contains WASP–homology 2 (WH2 or W) domains conserved in Wiskott-Aldrich syndrome protein (WASP) family proteins. The WH2 domain binds G-actin along with a connector and acidic region (CA) that binds the Arp2/3 complex (Machesky et al, 2001). The Arp2/3 complex is a key player of actin polymerization and nucleates new actin filaments upon activation by nucleation promoting factors (NPFs) such as the WASP and Scar protein family (Welch and Mullins, 2002). The infection of baculovirus induces nuclear actin polymerization which is essential for the production of progeny virions (Volkman et al., 1992). The P78/83 mutants that have a defect in the nucleation promoting activities of filament actins fail to produce viable BV, and the nuclear actin assembly by p78/83 and Arp2/3 complex is essential for viral progeny production (Goley et al., 2006). In addition to the requirement of nuclear actin filament assembly for progeny virion assembly, the release of BV nucleocapsids from endosomes into the cytoplasm induces the formation of thick actin cables and the polymerization of actin cables behind the nucleocapsids are postulated to facilitate their transport into the nucleus (Charlton and Volkman, 1993; Lanier and Volkman, 1998a).

Conserved in all the members of baculovirus sequenced so far, the VLF-1 has originally been found to stimulate the hyper-expression of two very late genes, *polyhedron* and *p10* (McLachlin and Miller, 1994; Yang and Miller, 1998a). As a transcriptional activator, VLF-1 binds to a burst sequence enhancing the expression of very late genes (Mistretta and Guarino, 2005; Yang and Miller, 1999). VLF-1 has the conserved motif of a tyrosine recombinase protein and binds in a non-sequence-specific manner to DNA substrates mimicking recombination junctions, but fails to exhibit enzymatic activity (Mikhailov

and Rohrmann, 2002). VLF-1 localizes on one end of nucleocapsids and its absence results in aberrant tubular structures. Mutation of the highly conserved tyrosine (Y355F) of VLF-1 produces nucleocapsids with a normal appearance, but no infectious virus is produced. The data therefore suggest that VLF-1 is required for normal capsid assembly and serves an essential function during the final stages of the DNA packaging process (Vanarsdall et al,2006).

GP41 is an O-glycosylated protein that affects BV production but is only a structural component of ODV (Olszewski and Miller, 1997b). ODV fractionation shows that GP41 does not associate with either nucleocapsids or envelope and is the only protein proposed to reside in the tegument (Whitford and Faulkner, 1992). Electron microscopy showed that nucleocapsids of a *gp41* temperature-sensitive mutant are produced within the nucleus but fail to egress from the nucleus. In addition, polyhedra also failed to form therefore suggesting that GP41 is required for both ODV and BV synthesis even though it is only found associated with ODV. The baculovirus core gene *38K* (*ac98*) that expresses a nuclear protein, has been shown to be essential for the formation of normal nucleocapsids and affects both BV and ODV production but has not been shown to be a structural component of the nucleocapsid (Wu et al., 2006). GP64 is required for the efficient virion budding from the plasma membrane and is essential for BV attachment and membrane fusion (Blissard and Wenz, 1992; Hefferon et al., 1999; Monsma et al, 1996b; Oomens and Blissard, 1999b).

The subject of this thesis is AcMNPV *exon0* which is a highly conserved late gene that encodes a protein of 261 amino acids and is found in all the members of lepidopteran NPVs. *exon0* (*orf141*) locates in the *Eco*RI B fragment of AcMNPV genome and the intron region of ie0 transcript (Fig. 1.3A). Northern blot analysis revealed that *exon0* was transcribed as a late gene (Dai et al., 2004) (Fig. 1.3B). At very early times post infection the 5' 114 nucleotides of *exon0* form the first exon of *ie0* which is the only known baculovirus spliced gene that produces multiple protein products. The splicing event results in the first 37 amino acids of IE0 being identical to the first 37 amino acids of EXON0. IE0 and IE1 are essential regulatory genes that are required for both DNA

replication and transcription (Stewart et al., 2005). EXON0 has a predicted leucine-rich coiled-coil domain and a novel RING finger motif. At the N-terminal, three more domains, Acidic I, Charged and Acidic II domain, were defined in this study due to the abundance of charged residues (Fig. 1.3C). The recent studies from our laboratory show that the deletion of *exon0* reduces the BV production over 99.99%, and infection of the *exon0* knockout virus is restricted to a single or a few neighbouring cells (Dai et al., 2004). However in the infected cells, DNA replication and polyhedra formation are not affected, indicating that EXON0 has a key and specific role in the BV production pathway.

1.2 Mechanisms of the egress of other animal viruses

Assembly and egress are one of the most important steps in a viral life cycle and the mechanisms by which viruses accomplish this process have similarities between virus families. As a well-orchestrated process, the assembly and egress usually involves extensive protein-protein interactions requiring various cellular structures, especially for large DNA viruses. Many viruses have been reported to move and depend on microtubules for the egress of progeny virions (reviewed by Dohner et al. (2005), Smith and Enquist (2002)). In addition, the nuclear targeting and entry of herpes simplex virus (Sodeik et al, 1997), human cytomegalovirus (Ogawa-Goto et al., 2003), adenovirus (Suomalainen et al., 1999), parvoviruses (Seisenberger et al., 2000), simian virus 40 (SV40) (Pelkmans et al, 2001) and other RNA viruses require microtubules. Vaccinia virus and african swine fever virus even utilize both microtubule and actin filaments for egress, transitting from microtubule-dependent movement toward, and actin polymerization motility away, from the plasma membrane (Jouvenet et al., 2004; Jouvenet et al., 2006; Smith et al., 2003). The well studied egress of herpesvirus and vaccinia virus disscussed below may shed light on the mechanism of baculovirus egress.

1.2.1 Herpesvirus

Herpesviruses are large DNA viruses with a genome of 125 to 240 kbp in size. The mature virions of herpesviruses contain over 30 proteins which are organized in four structures, the core, capsid, tegument, and envelope (Roizman and Knipe, 2001). The inner nucleoprotein core comprises a linear dsDNA molecule, which is included in an icosahedral capsid shell of 150 hexons and 12 pentons. A mature capsid is composed of 6 proteins and surrounded by a layer of proteinaceous tegument which contains at least 15 different proteins. The viral envelope is derived from host cell lipids containing at least 10 virus-encoded integral membrane proteins (Davison et al., 2005).

Herpesvirus infection of a host cell starts from the interaction of extracellular viral glycoproteins with their cell surface receptors and entry is achieved by the fusion between the virion envelope and the plasma membrane (Spear and Longnecker, 2003). After the fusion of viral and cellular membrane, the nucleocapsid is transported to the nuclear pore and viral genome is released to the nucleus, where viral gene transcription and DNA replication occurs. Many tegument proteins dissociate from the incoming nucleocapsid and modify cellular metabolism. In herpes simplex virus-1, the UL41 (VHS) inhibits host protein synthesis and UL48 (VP16) is a potent transcription factor that activates the immediate early (α) genes (Batterson and Roizman, 1983; Kwong and Frenkel, 1989). The expression of early (β) genes and late (γ) genes are regulated by the products of immediate early genes and are transcribed sequentially by host RNA polymerase II. Viral DNA replication occurs from one or more origins of replication probably by a rolling circle mechanism. The assembly of capsids occurs in the nucleus after viral gene expression and DNA synthesis. Capsids bud at the inner nuclear membrane and are translocated to the cytoplasm after the fusion of the primary viral envelope with the outer nuclear membrane. Nucleocapsids obtain their final envelope by budding into the glycoprotein-containing Golgi- derived vesicles and are released out of cell (Reviewed by Mettenleitter (2002b; 2004).

Two viral products UL31 and UL34 are required for production of the primary envelop after the capsids are assembled in the nucleus (Chang et al., 1997; Roller et al., 2000).

UL34 is a type II membrane protein and rich on the nuclear membrane (Klupp et al, 2000). UL34 interacts with UL31 and directs UL31 to the nuclear membrane (Bjerke et al., 2003; Reynolds et al., 2001). UL34 recruits cellular protein kinase C to the primary envelope sites which phosphorylates lamin B and causes the local dissolution of the nuclear lamin network (Muranyi et al., 2002a; Park and Baines, 2006; Sanchez and Spector, 2002; Simpson-Holley et al., 2005). Deletion of either UL34 or UL31 results in a defect in primary envelopment and accumulation of capsids in the nucleus (Chang et al., 1997; Fuchs et al., 2002a; Fuchs et al., 2002b; Klupp et al, 2000; Roller et al., 2000). The budding of nucleocapsids at inner nuclear membrane results in the localization of primary enveloped virions in the perinuclear space. The envelope of primary virions differs from that of mature virions. UL31 and UL34 are components of primary enveloped virions but not mature virus particles, whereas major tegument proteins of mature virions UL46, UL47 are absent from primary enveloped virions (Fuchs et al., 2002b; Klup et al, 2000; Naldinho-Souto et al, 2006; Reynolds et al., 2002). The US3 kinase seems to trigger the "de-envelopment" because a US3 deletion mutant was deficient in this process (Klupp et al, 2001; Reynolds et al., 2002; Schumacher et al., 2005). After translocation into the cytosol, nucleocapsids undergo tegumentation by incorporating more than 15 tegument proteins. A highly ordered network of protein–protein interactions drives tegumentation and secondary envelopment (reviewed by Mettenleiter (2002b; 2004)). The final envelopment is often observed in the trans-Golgi network (Granzow et al., 2001; McMillan and Johnson, 2001).

Like its entry into the nucleus, the egress of herpesvirus nucleocapsids is microtubule-dependent. Nucleocapsid transport has been shown to be at rates consistent with the microtubule-based movement and is sensitive to the microtubule inhibitory drug nocodazole (Miranda-Saksena et al., 2000b; Penfold et al, 1994). Herpesvirus particles tagged with GFP-VP11/12 or GFP-VP26 have been found to translocate along microtubules over long distances in neuronal axons (Smith et al., 2001; Willard, 2002). Potentially facilitating this movement it has been found that the major capsid protein VP5 and the tegument proteins VP16, VP22 and US11 interact with the heavy chain of kinesin motors from an infected cell lysate (Diefenbach et al., 2002a).

1.2.2 Vaccinia virus

Vaccinia virus (VV) is the prototypic member of the *Poxviridae* and possesses a large double-stranded DNA genome of approximately 200 kb, many virus-encoded enzymes for transcription and DNA replication and a complex morphogenic pathway (Moss, 2001). Unique from other DNA viruses, vaccinia virus has a cytoplasmic site of replication. The vaccinia virus produces four types of virions which play different roles in the virus life cycle (Smith et al, 2002). Intracellular mature viruses (IMV) are the first infectious particles assembled in the viral factories of infected cells. IMV are transported on microtubules near the microtubule-organizing center (MTOC) where they become intracellular enveloped virions (IEV) by wrapping with viral modified membrane. IEV are transported to the cell periphery on microtubules and the fusion of outer IEV membrane with the plasma membrane produces cell-associated enveloped virions (CEV) on the cell surface. The polymerization of actin drives the CEV away from the cell and spreads cell-to-cell infection. Extracellular enveloped virus (EEV) is released from the cell and mediates the long-range dissemination of virus (reviewed by Smith et al.(2003)).

After formation IMV may be wrapped by membranes of the *trans*-Golgi network or early endosomes close the microtubule-organizing center to form IEV (Schmelz et al., 1994; Tooze et al., 1993; van Eijl et al., 2002). The movement of IMV particles from the factory to the MTOC is on microtubules and the A27L protein which localizes on the surface of IMV is required (Rodriguez et al, 1985; Sanderson et al, 2000). The absence of A27L produces smaller plaque and reduces the level of EEV by 20 fold (Rodriguez and Smith, 1990). The enveloping of IMV by modified *trans*-Golgi network or endosome membranes results in the formation of IEV. Two proteins F12L and A36R, called transport proteins, are specifically present on the IEV envelope but not on CEV or EEV and are involved in the IEV movement (Smith et al, 2002). F12L has been observed to co-localize with microtubules and is believed to have a role in the microtubule-dependent egress of IEV (van Eijl et al., 2002). Deletion mutants of either F12L or A36R cause smaller plaques, produce five to seven folds less EEV (van Eijl et al., 2002; van

Eijl et al, 2000; Zhang et al, 2000). Green fluorescent protein (GFP) tagged IEV shows colocalization with microtubules and the movement of IEV was inhibited by microtubule depolymerzation drugs and the velocity (~60 μm/min) is the characteristic of microtubule transport (Hollinshead et al., 2001; Rietdorf et al., 2001; Ward and Moss, 2001a). At the cell surface the fusion of the IEV envelope with the cytoplasmic membrane exposes CEV on the cell surface. The A36R protein is the key protein required for actin polymerization which drives CEV away from the cell surface. Phosphorylation of A36R by the Src family of kinases results in the recruitment of Nck, the Wiskott-Aldrich syndrome protein (WASP) family member N-WASP and Arp2/3 complex to the site of actin assembly, which nucleates the actin monomers to form actin filaments (Frischknecht et al., 1999; Moreau et al., 2000).

1.3 Microtubules

1.3.1 Microtubule dynamics

As described in the previous section the cytoskeleton network plays a key role in virion transport. In uninfected cells the cytoskeleton polymers, consisting of actin microfilaments, intermediate filaments, and microtubules help to determine cell shape and subcellular architecture (Soldati and Schliwa, 2006). In addition, in eukaryotic cells there are two types of motility systems for the movement of organelles, namely actin filament- and microtubule- dependent transport (Langford, 1995). The microtubule network is usually involved in long-range transport of components while the actin network is used for short-range transport, but the mechanism(s) by which these two transport systems are coordinated is largely unknown (Huang et al., 1999). Microtubules, the key components of the cytoskeleton, are long, hollow cylindrical structures that are essential in all eukaryotic cells. They are vital for the development and maintenance of cell shape, intracellular transport of vesicles, organelles and protein and crucial in cell signalling, cell division and mitosis (reviewed by Kirschner (1987); Nogales (2000); and Jordan and Wilson (2004a)).

A microtubule is usually built from 13 parallel protofilaments in a diameter of about 24 nm and can be many micrometers long. Protofilaments are composed of alternating α-tubulin and β-tubulin heterodimers in a head-to-tail fashion. The two tubulins are found only in the complex and are bound together by noncovalent bonds. Each α or β monomer has a binding site for one molecule of GTP. GTP bound to α subunit is trapped at dimer interface and is nonexchangeable. The nucleotide on the β subunit can be GTP or GDP. Microtubule assembly requires GTP: β-tubulin which is hydrolysed upon addition of the tubulin dimer to the elongating microtubule. In the GTP cap model, free tubulin–GTP dimers have a straight conformation, but following GTP hydrolysis in the protofilaments, dimer conformation changes to a curved form, such that the tubulin-GDP in microtubule core is in a strained conformation. The plus end of the microtubule is stabilized by the GTP or GDP-Pi cap. When the GTP cap is lost, the metastable microtubules rapidly depolymerize (reviewed by Caplow (1994); Wilson and Jordon (1995); Nogales (2001a); and Nogales and Wang (2006)). The GDP at the E-site of released tubulin dimers can be exchanged for GTP and GTP-dimers participate in another cycle of polymerization.

Microtubules are highly dynamic and switch between phases of polymerization and depolymerization. The two ends of a microtubule are not equivalent; one end, termed the "plus" end grows and shrinks more rapidly and more extensively than the "minus" end. In many cell types, the minus end of microtubules is fixed at the microtubule-organizing center (MTOC) and the plus end extends toward to cell periphery (Orr et al., 2003). Transport on microtubules is directional. Movement to the microtubule plus end (anterograde transport) is often facilitated by a kinesin-family (KIF) motor, whereas movement to the minus end (retrograde transport) usually requires the dynein motor.

Microtubule dynamics are tightly regulated both spatially and temporally: by expression of different tubulin isotypes, which have different functions; and through several post-translational modifications of tubulin; by the control of tubulin monomer folding and formation of functional dimers; through the binding of various regulatory proteins, including microtubule-associated proteins (MAPs). For homo sapiens, 6 forms of α-tubulin and 7 forms of β-tubulin are expressed at varying levels in different cells and

tissues (Hirokawa and Takemura, 2005). In *Bombyx mori*, three α– and four β–tubulins have been cloned (Kawasaki et al., 2003). Microtubule diversity is also generated by an extensive array of reversible post-translational modifications, such as acetylation, polyglycylation, tyrosination, polyglutamylation, phosphorylation and palmitoylation (Westermann and Weber, 2003). The cytosolic chaperonin CCT and a series of folding cofactors are required for the correct folding of tubulin monomer and subsequent dimer formation (Nogales, 2000). There are many different MAPs that are broadly classified as microtubule stabilizers or destabilizers, including the dynein and kinesin motor protein families and many microtubule-regulatory proteins, such as survivin, stathmin, TOG, dynactin *et al.* (reviewed by Jordan and Wilson (2004a); Cassimeris (1999); and Desai and Mitchison (1997)).

Kinesins and dyneins are the major microtubule motor proteins which usually direct the anterograde and retrograde transport on microtubules, respectively. Kinesins are composed of two heavy chains (KHCs) and two light chains (KLCs). The N-terminal of KHCs is a global motor head domain, followed by a coiled-coil region that mediates the dimerization. The C-terminal of KLC and the tail of KHC bind to cargo. Different kinesins share a common motor domain but diverge considerably in their cargo-binding tail domains (Dohner et al., 2005; Miki et al., 2005). The retrograde transport on microtubules is catalyzed by the dynein motors with assistance of dynactin complex which functions in both cargo binding and motor processivity (Schroer, 2004). Dynein is a large protein complex consisting of two dynein heavy chains, two dynein intermediate chains, light intermediate chains and light chains (Dohner et al., 2005).

1.3.2 Molecular structure of tubulin

The α and β tubulins are highly conserved, but they also display extensive molecular heterogeneity at their C-termini. Electron crystallography reveals that the tubulin monomer has three domains (Nogales, 2000; Nogales et al., 1998). Residues 1–206 form a domain consisting of alternative parallel beta strands and helices which is the binding site of GTP. The smaller central domain (residues 207-384) is formed by three helices

and a mixed beta sheet that participates in both longitudinal/lateral contacts between tubulin monomers present in protofilaments. Taxol binds to a hydrophobic pocket within this central domain and strengthens the lateral contacts of protofilaments and stabilizes microtubules (Nogales, 2000; Rao et al., 1999). The last domain is on the outside of the protofilament which consists of two antiparallel helices that cover the previous N-terminal and central domains.

The N-site (Non-exchangeable) in α-tubulin is buried at the intradimer interface while the guanine nucleotide at the E-site (Exchangeable) of β-tubulin is at the surface of the dimer allowing for exchange. After polymerization, the E-site is buried at the interdimer interface and becomes nonexchangeable. From Nogales's 3D structure model (Nogales, 2000), "the bumpy, inside surface of the microtubule is dominated by the H1-S2 loop; the flatter, outside surface is dominated by the C-terminal helices H11 and H12"and "the main elements forming this interface are the M (Microtubule) loop and helix H3".

Colchicine and nocodazole are two commonly used microtubule-specific drugs. Both of them destabilize microtubules by binding to tubulin subunits and preventing microtubule polymerization. The possible binding site of colchicine to tubulin has been mapped at the monomer-monomer interface of the heterodimer (Uppuluri et al., 1993). Nocodazole has been proposed to increase GTPase activity upon binding tubulin dimers and result in increase of GTP hydrolysis (Vasquez et al., 1997).

1.4 Hypothesis and objectives

Viruses are obligate intracellular parasites and depend on cellular machinery for different steps of their life cycles, including assembly and egress, which are two of the most essential steps of a virus life cycle. How viruses organize their egress strategies to promote cell-to-cell spread is an important question. Eukaryotic cells are compartmentalized by cytoskeleton, organelles and intracellular membrane systems

which inhibit Brownian movement of macromolecules over 500 kDa (Luby-Phelps, 2000). If viruses had to depend on diffusional translocation, the time requirement would be prohibitory. For example, Sodeik (2000) estimated that a HSV capsid would take 231 years to move 1 cm in the axonal cytoplasm. Therefore, the movement of virions cannot depend on passive diffusion and they have to utilize cellular transport machinery to provide an active motility.

As indicated in the previous sections extensive studies from herpesvirus and vaccinia virus have unravelled how large DNA viruses remodel cytoskeletal structures to facilitate entry into, transport within and egress from target cells. Exciting progress has been made in understanding how herpesvirus and vaccinia virus control microtubule organization and actin polymerization to spread the progeny viruses.

The release of baculovirus nucleocapsids from the endosomes induces actin cables which may propel the transport of nucleocapsids into the nucleus (Charlton and Volkman, 1993; Lanier and Volkman, 1998a). Following uncoating within the nucleus, the actin cytoskeleton assumes a second configuration and forms the ventral aggregates at the plasma membrane and an early gene product ARIF-1 mediates this second change (Charlton and Volkman, 1991a; Dreschers et al, 2001; Roncarati and Knebel-Morsdorf, 1997). The nuclear actin assembly is required for the morphogenesis of normal nucleocapsids (Goley et al., 2006; Volkman, 1988). The disappearance of Arif-1-induced actin rearrangement correlates with the appearance of nuclear F-actin. These studies demonstrate the actin filaments are involved in the baculovirus life cycle extensively and may also have a role in the transport of nucleocapsids into the nucleus. However, how the baculovirus nucleocapsids are transported out of the nucleus to plasma membrane is unknown.

In this study, we investigate the egress mechanisms of baculovirus nucleocapsids by studying the function of EXON0 and its roles in BV production. As with other viruses, the baculoviruses must use host cellular actin or/and microtubule transport systems to achieve the delivery of progeny nucleocapsids to the plasma membrane for budding. The

early electron micrographs have revealed the frequent association of nucleocapsids with microtubules (Granados, 1978; Granados and Lawler, 1981). The treatment of microtubule drugs colchicine and taxol can reduce the BV production over 75% (Volkman and Zaal, 1990a).

EXON0 has been shown in previous studies to play a key role in BV production. Following preliminary evidence that EXON0 is required for efficient production of BV (Dai et al, 2004), it is the central hypothesis of this thesis that AcMNPV EXON0 must interact with the cellular cytoskeleton or other viral proteins to facilitate the viral budding process. This study was therefore designed based on this hypothesis to analyze the functions of EXON0 and its role in BV production with the following objectives:

1. Determine the cellular localization of EXON0 during infection
2. Determine if EXON0 is a structural component of virions
3. If EXON0 is a structural protein, determine if nucleocapsid proteins interact with EXON0
4. Determine by electron microscopy analysis at which step in the BV pathway that viral egress is blocked in the absence of EXON0
5. Identify the cellular proteins which interact with EXON0 by tandem affinity purification
6. Investigate the effect of cellular partners on BV production
7. Perform a deletion and point mutational analysis of the domains of EXON0 required for the efficient BV production and association with other viral and cellular proteins

Figure 1.1 Structural composition of baculovirus virions.

Nucleocapsid proteins common to both BV and ODV are indicated between BV and ODV, protein specific to BV or ODV are indicated on the left and right, respectively. (Adapted from Dwight Lynn, Baculovirus Wikipedia, 2006, http://en.wikipedia.org/wiki/Image:Nucleopolyhedrovirus.jpg).

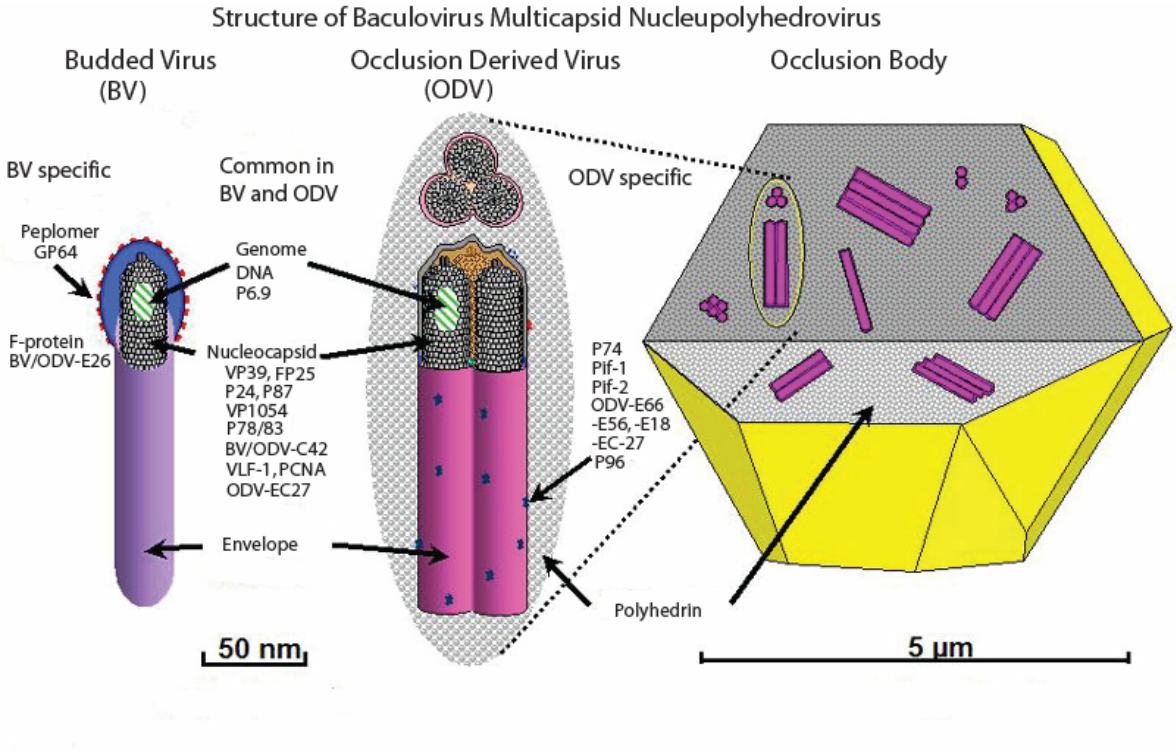

Figure 1.2 The life cycle of baculovirus.

(A) The process of BV infection of a cultured cell. BV attaches to cell surface (1), fuses with plasma membrane and enters by endocytosis (2). The nucleocapsid is released (3) after the fusion of viral membrane with late endosome. After nucleocapsid interacts with a nuclear pore (4), the viral core is released (5) and viral genes transcribed (6), replicated and packaged into nucleocapsids (7) in virogenic stroma (VS). At late phase nucleocapsids exit in BV pathway (8-10) or are enveloped in the nucleus and embedded in occlusion bodies (OB) (11). NM, nuclear membrane. (B) The process of ODV infection of a midgut epithelial cell. The ODV attaches the microvilli (1). The ODV membrane fuses directly with the membrane of microvilli of the cell, releasing nucleocapsids into the cytoplasm (2). Nucleucapsid moves in the cytoplasm (3) and targets to a nuclear pore (4). The remaining events appear to be similar to those in cultured cells. (Adapted from Miller (1996)).

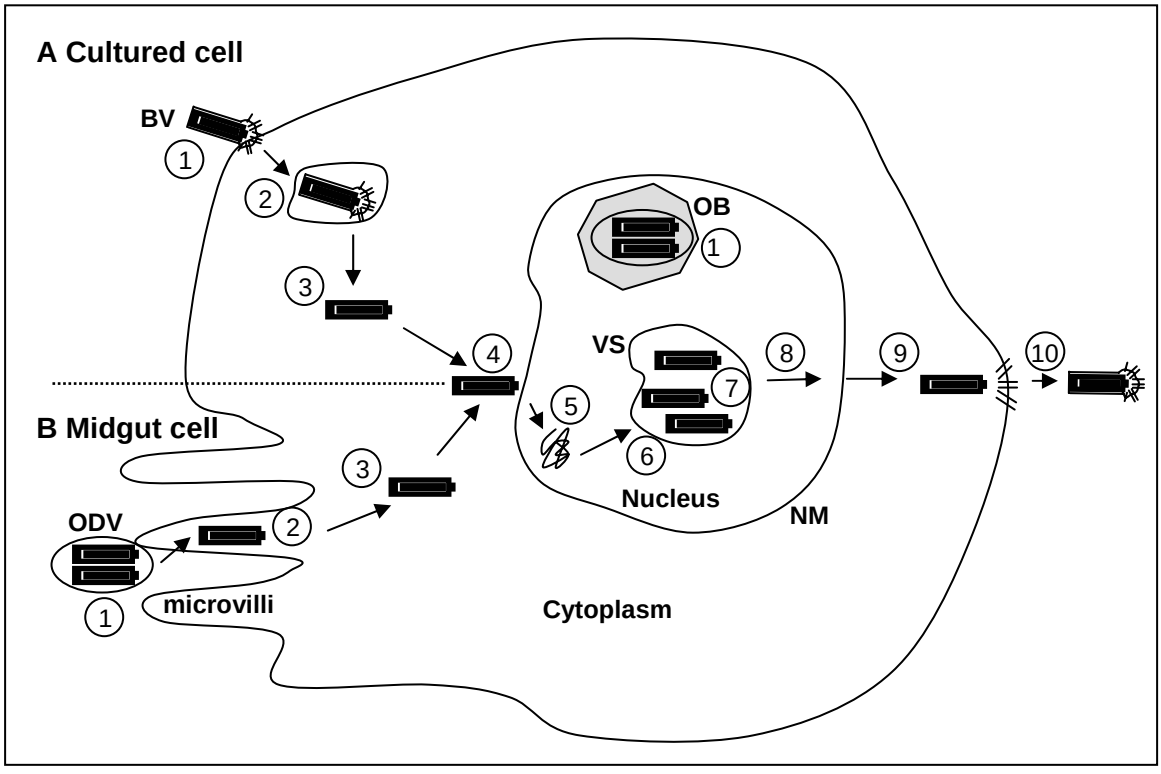

Figure 1.3 The location of exon0 gene and its transcription.

(A) The location of *exon0* (*orf141*) gene in AcMNPV genome. *Exon0* (black) is in the *ie0* intron region and the relative positions and orientations of the *exon0* and adjoining ORFs are shown. Three polyadenylation signals downstream *exon0* are indicated along with the three transcripts observed in Northern blots shown in B. (B) Transcriptional analysis of *exon0*. Sf9 cells were infected WT AcMNPV and total RNA was extracted from 3 to 72 hpi. The northern blot was probed with an *exon0* strand specific RNA probe and three transcripts are detected. The sizes of *exon0* mRNAs are indicated on the right. (C) The predicted domains of EXON0. (A and B are adapted from Dai et al., 2004)

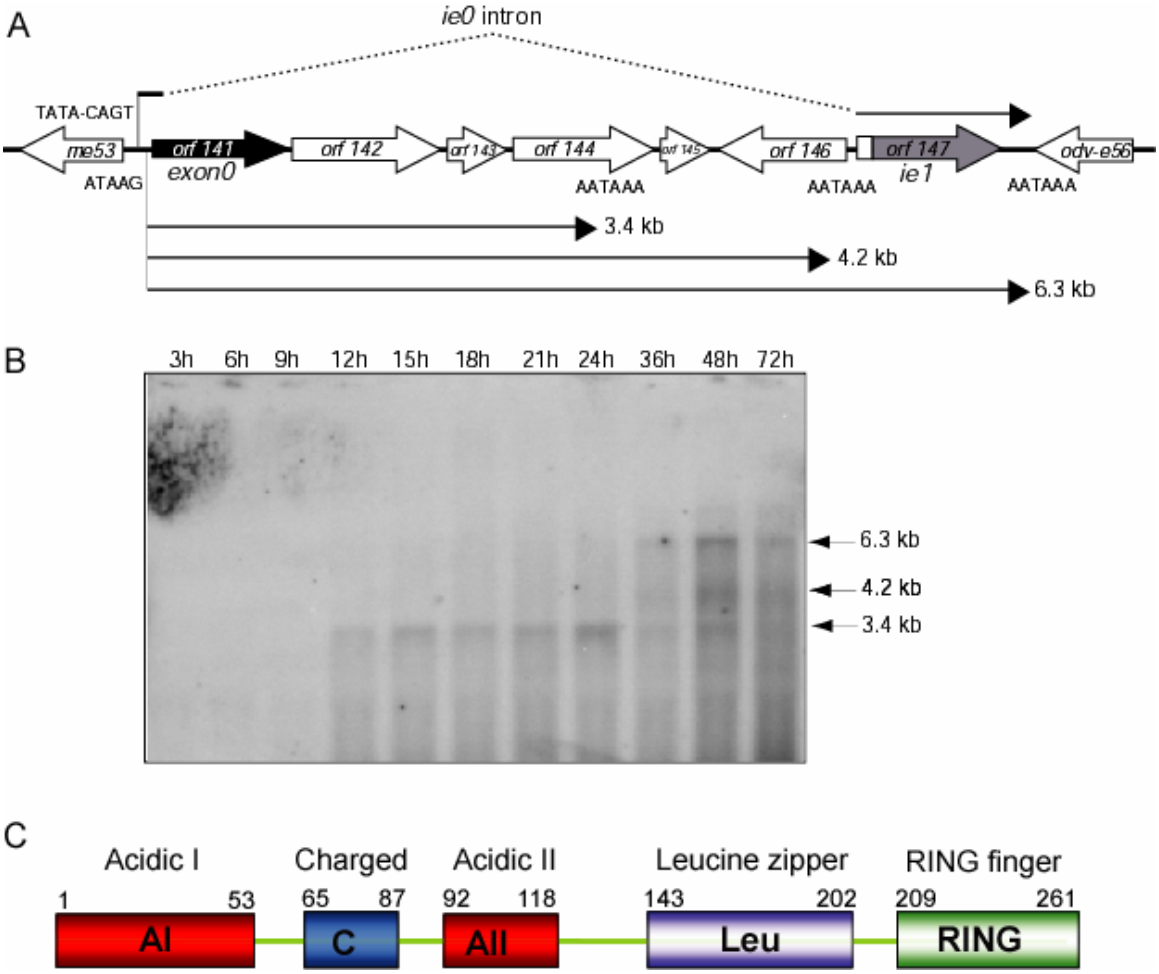

1.5 References

Adams, J. R., Goodwin, R. H., and Wilcox, T. A. (1977). Electron microscopic investigations on invasion and replication of insect baculoviruses in vivo and in vitro. *Biologie Cellulaire* **28**(3)**,** 261-268.

Ayres, M. D., Howard, S. C., Kuzio, J., Lopez-Ferber, M., and Possee, R. D. (1994). The complete DNA sequence of *Autographa californica* nuclear polyhedrosis virus. *Virology* **202**(2)**,** 586-605.

Batterson, W., and Roizman, B. (1983). Characterization of the herpes simplex virion-associated factor responsible for the induction of alpha genes. *J. Virol.* **46,** 371-377.

Bjerke, S. L., Cowan, J. M., Kerr, J. K., Reynolds, A. E., Baines, J. D., and Roller, R. J. (2003). Effects of charged cluster mutations on the function of herpes simplex virus type 1 UL34 protein. *J. Virol.* **77**(13)**,** 7601-7610.

Blissard, G. W. (1996). Baculovirus--insect cell interactions. *Cytotechnology* **20**(1-3)**,** 73-93.

Blissard, G. W., and Rohrmann, G. F. (1990). Baculovirus diversity and molecular biology. *Annu. Rev. Entomol.* **35,** 127-155.

Blissard, G. W., and Wenz, J. R. (1992). Baculovirus GP64 envelope glycoprotein is sufficient to mediate pH-dependent membrane fusion. *J. Virol.* **66**(11)**,** 6829-6835.

Boyce, F. M., and Bucher, N. L. R. (1996). Baculovirus-mediated gene transfer into mammalian cells. *Proc. Natl. Acad. Sci. U. S. A.* **93,** 2348-2352.

Braunagel, S. C., Burks, J. K., Rosas-Acosta, G., Harrison, R. L., Ma, H., and Summers, M. D. (1999). Mutations within the *Autographa californica* nucleopolyhedrovirus FP25K gene decrease the accumulation of ODV-E66 and alter its intranuclear transport. *J. Virol.* **73**(10)**,** 8559-8570.

Braunagel, S. C., Guidry, P. A., Rosas-Acosta, G., Engelking, L., and Summers, M. D. (2001). Identification of BV/ODV-C42, an *Autographa californica* nucleopolyhedrovirus *orf101*-encoded structural protein detected in infected-cell complexes with ODV-EC27 and p78/83. *J. Virol.* **75**(24)**,** 12331-12338.

Braunagel, S. C., Russell, W. K., Rosas-Acosta, G., Russell, D. H., and Summers, M. D. (2003). Determination of the protein composition of the occlusion-derived virus of *Autographa californica* nucleopolyhedrovirus. *Proc. Natl. Acad. Sci. U. S. A.* **100**(17)**,** 9797-9802.

Braunagel, S. C., and Summers, M. D. (1994). *Autographa californica* nuclear polyhedrosis virus, PDV, and ECV viral envelopes and nucleocapsids: structural proteins, antigens, lipid and fatty acid profiles. *Virology* **202**(1)**,** 315-328.

Broussard, D. R., Guarino, L. A., and Jarvis, D. L. (1996). Dynamic phosphorylation of *Autographa californica* nuclear polyhedrosis virus pp31. *J. Virol.* **70**(10)**,** 6767-6774.

Caplow, M., Ruhlen, R. L., and J., S. (1994). The free energy for hydrolysis of a microtubule-bound nucleotide triphosphate is near zero: all of the free energy for hydrolysis is stored in the microtubule lattice. *J. Cell Biol.* **127,** 779-788.

Cassimeris, L. (1999). Accessory protein regulation of microtubule dynamics throughout the cell cycle. *Curr. Opinion Cell Biol.* **11,** 134-141.

Chang, Y. E., Van Sant, C., Krug, P. W., Sears, A. E., and Roizman, B. (1997). The null mutant of the U(L)31 gene of herpes simplex virus 1: construction and phenotype in infected cells. *J. Virol.* **71**(11)**,** 8307-8315.

Charlton, C. A., and Volkman, L. E. (1991). Sequential rearrangement and nuclear polymerization of actin in baculovirus-infected *Spodoptera frugiperda* cells. *J. Virol.* **65,** 1219-1227.

Charlton, C. A., and Volkman, L. E. (1993). Penetration of *Autographa californica* nuclear polyhedrosis virus nucleocapsids into IPLB Sf 21 cells induces actin cable formation. *Virology* **197,** 245-254.

Chen, X., Hu, Z., Jehle, J. A., Zhang, Y., and Vlak, J. M. (1997). Analysis of the ecdysteroid UDP-glucosyltransferase gene of *Heliothis armigera* single-nucleocapsid baculovirus. *Virus Genes* **15**(3)**,** 219-225.

Chernomordik, L., Leikina, E., Cho, M., and Zimmerberg, J. (1995). Control of baculovirus GP64-induced syncytium formation by membrane lipid composition. *J. Virol.* **69**(5)**,** 3049-3058.

Dai, X., Stewart, T. M., Pathakamuri, J. A., Li, Q., and Theilmann, D. A. (2004). *Autographa californica* multiple nucleopolyhedrovirus *exon0* (*orf141*), which encodes a RING finger protein, is required for efficient production of budded virus. *J. Virol.* **78**(18)**,** 9633-9644.

Davison, A., Eberle, R., Hayward, G. S., McGeoch, D. J., Minson, A. C., Pellett, P. E., Roizman, B., Studdert, M. J., and Thiry, E. (2005). Herpesviridae. *In* "Virus Taxonomy - Eighth Report of the International Committee on Taxonomy of Viruses" (M. M. A. Fauquet C.M., Maniloff J., Desselberger U., and B. L.A. (ed.), Ed.), pp. 199-212. Elsevier/Academic Press, London.

Desai, A., and Mitchison, T. J. (1997). Microtubule polymerization dynamics. *Annu. Rev. Cell Dev. Biol.* **13,** 83-117.

Diefenbach, R. J., Miranda-Saksena, M., Diefenbach, E., Holland, D. J., Boadle, R. A., Armati, P. J., and Cunningham, A. L. (2002). Herpes simplex virus tegument protein US11 interacts with conventional kinesin heavy chain. *J. Virol.* **76,** 3282-3291.

Dohner, K., Nagel, C. H., and Sodeik, B. (2005). Viral stop-and-go along microtubules: taking a ride with dynein and kinesins. *Trends Microbiol.* **13,** 320-327.

Douris, V., Swevers, L., Labropoulou, V., Andronopoulou, E., Georgoussi, Z., and K., I. (2006). Stably transformed insect cell lines: tools for expression of secreted and membrane-anchored proteins and high-throughput screening platforms for drug and insecticide discovery. *Adv. Virus Res.* **68,** 113-156.

Dreschers, S., Roncarati, R., and Knebel-Morsdorf, D. (2001). Actin rearrangement-inducing factor of baculoviruses is tyrosine phosphorylated and colocalizes to F-actin at the plasma membrane. *J. Virol.* **75,** 3771-3778.

Elliot, R. M., and Kelly, D. C. (1977). The polyamine content of a nuclear polyhedrosis virus from *Spodoptera littoralis*. *Virology* **76,** 472-474.

Engelhard, E. K., Kam-Morgan, L. N., Washburn, J. O., and Volkman, L. E. (1994). The insect tracheal system: a conduit for the systemic spread of *Autographa californica* M nuclear polyhedrosis virus. *Proc. Natl. Acad. Sci. U. S. A.* **91,** 3224-3227.

Fraser, M. J. (1986). Ultrastructural observations of virion maturation in *Autographa californica* nuclear polyhedrosis virus infected *Spodoptera frugiperda* cell cultures. *J. Ultrastruct. Mol. Struct. Res.* **95,** 189–195.

Frischknecht, F., Moreau, V., Rottger, S., Gonfloni, S., Reckmann, I., Superti-Furga, G., and M., W. (1999). Actin-based motility of vaccinia virus mimics receptor tyrosine kinase signalling. *Nature* **401,** 926–929.

Fuchs, W., Granzow, H., Klupp, B. G., Kopp, M., and Mettenleiter, T. C. (2002a). The UL48 tegument protein of pseudorabies virus is critical for intracytoplasmic assembly of infectious virions. *J. Virol.* **76,** 6729-6742.

Fuchs, W., Klupp, B. G., Granzow, H., Osterrieder, N., and Mettenleiter, T. C. (2002b). The interacting UL31 and UL34 gene products of pseudorabies virus are involved in egress from the host-cell nucleus and represent components of primary enveloped but not mature virions. *J. Virol.* **76**(1)**,** 364-378.

Funk, C. J., Braunagel, S. C., and Rohrmann, G. F. (1997). Baculovirus structure. *In* "The Baculoviruses" (L. K. Miller, Ed.), pp. 7-32. Plenum, New York.

Funk, C. J., and Consigli, R. A. (1993). Phosphate cycling on the basic protein of *Plodia interpunctella* granulosis virus. *Virology* **193,** 396-402.

Goley, E. D., Ohkawa, T., Mancuso, J., Woodruff, J. B., D'Alessio, J. A., Cande, W. Z., Volkman, L. E., and Welch, M. D. (2006). Dynamic nuclear actin assembly by Arp2/3 complex and a baculovirus WASP-like protein. *Science* **314,** 464-467.

Granados, R. R. (1978). Early events in the infection of Hiliothis zea midgut cells by a baculovirus. *Virology* **90**(1)**,** 170-174.

Granados, R. R., and Lawler, K. A. (1981). *In vivo* pathway of *Autographa californica* baculovirus invasion and infection. *Virology* **l08,** 297-308.

Granzow, H., Klupp, B. G., Fuchs, W., Veits, J., Osterrieder, N., and Mettenleiter, T. C. (2001). Egress of alphaherpesviruses: comparative ultrastructural study. *J. Virol.* **75**(8)**,** 3675-3684.

Guarino, L. A., Dong, W., Xu, B., Broussard, D. R., Davis, R. W., and Jarvis, D. L. (1992). Baculovirus phosphoprotein pp31 is associated with virogenic stroma. *J. Virol.* **66**(12)**,** 7113-7120.

Guarino, L. A., Xu, B., Jin, J., and Dong, W. (1998). A virus-encoded RNA polymerase purified from baculovirus-infected cells. *J. Virol.* **72**(10)**,** 7985-91.

Hashimoto, Y., Corsaro, B. G., and Granados, R. R. (1991). Location and nucleotide sequence of the gene encoding the viral enhancing factor of the *Trichoplusia ni* granulosis virus. *J. Gen. Virol.* **72**(11)**,** 2645-2652.

Hawtin, R. E., Arnold, K., Ayres, M. D., Zanotto, P. M., Howard, S. C., Gooday, G. W., Chappell, L. H., Kitts, P. A., King, L. A., and Possee, R. D. (1995). Identification and preliminary characterization of a chitinase gene in the *Autographa californica* nuclear polyhedrosis virus genome. *Virology* **212**(2)**,** 673-685.

Hawtin, R. E., Zarkowska, T., Arnold, K., Thomas, C. J., Gooday, G. W., King, L. A., Kuzio, J. A., and Possee, R. D. (1997). Liquefaction of *Autographa californica* nucleopolyhedrovirus-infected insects is dependent on the integrity of virus-encoded chitinase and cathepsin genes. *Virology* **238**(2)**,** 243-253.

Hefferon, K. L., Oomens, A. G., Monsma, S. A., Finnerty, C. M., and Blissard, G. W. (1999). Host cell receptor binding by baculovirus GP64 and kinetics of virion entry. *Virology* **258,** 455-468.

Herniou, E. A., Olszewski, J. A., Cory, J. S., and O'Reilly, D. R. (2003). The genome sequence and evolution of baculoviruses. *Annu. Rev. Entomol.* **48,** 211-234.

Herniou, E. A., Olszewski, J. A., O'Reilly, D. R., and Cory, J. S. (2004). Ancient coevolution of baculoviruses and their insect hosts. *J. Virol.* **78**(7)**,** 3244-3251.

Hill, J. E., Kuzio, J., and Faulkner, P. (1995). Identification and characterization of the *v-cath* gene of the baculovirus, CfMNPV. *Biochim. Biophys. Acta.* **1264**(3)**,** 275-278.

Hirokawa, N., and Takemura, R. (2005). Molecular motors and mechanisms of directional transport in neurons. *Nat. Rev. Neurosci.* **6**(3)**,** 201-214.

Hofmann, C., and Strauss, M. (1998). Baculovirus-mediated gene transfer in the presence of human serum or blood facilitated by inhibition of the complement system. *Gene Ther.* **5**(4)**,** 531-536.

Hollinshead, M., Rodger, G., Van Eijl, H., Law, M., Hollinshead, R., Vaux, D. J., and Smith, G. L. (2001). Vaccinia virus utilizes microtubules for movement to the cell surface. *J. Cell. Biol.* **154**(2)**,** 389-402.

Horton, H. M., and Burand, J. P. (1993). Saturable attachment sites for polyhedron-derived baculovirus on insect cells and evidence for entry via direct membrane fusion. *J. Virol.* **67**(4)**,** 1860-1868.

Hu, Y. C. (2006). Baculovirus vectors for gene therapy. *Adv. Virus Res.* **68,** 287-320.

Huang, J. D., Brady, S. T., Richards, B. W., Stenolen, D., Resau, J. H., Copeland, N. G., and Jenkins, N. A. (1999). Direct interaction of microtubule- and actin-based transport motors. *Nature* **397**(6716)**,** 267-270.

Jehle, J. A., Blissard, G. W., Bonning, B. C., Cory, J. S., Herniou, E. A., Rohrmann, G. F., Theilmann, D. A., Thiem, S. M., and Vlak, J. M. (2006). On the classification and nomenclature of baculoviruses: a proposal for revision. *Arch. Virol.* **151**(7)**,** 1257-1266.

Jordan, M. A., and Wilson, L. (2004). Microtubules as a target for anticancer drugs. *Nat. Rev. Cancer* **4**(4)**,** 253-265.

Jouvenet, N., Monaghan, P., Way, M., and Wileman, T. (2004). Transport of African swine fever virus from assembly sites to the plasma membrane is dependent on microtubules and conventional kinesin. *J. Virol.* **78**(15)**,** 7990-8001.

Jouvenet, N., Windsor, M., Rietdorf, J., Hawes, P., Monaghan, P., Way, M., and Wileman, T. (2006). African swine fever virus induces filopodia-like projections at the plasma membrane. *Cell Microbiol.* **8**(11)**,** 1803-1811.

Kawamoto, F., Suto, C., Kumada, N., and Kobayashi, M. (1977). Cytoplasmic budding of a nuclear polyhedrosis virus and comparative ultrastructural studies of envelopes. *Microbiol. Immunol.* **21**(5)**,** 255-265.

Kawasaki, H., Sugaya, K., Quan, G. X., Nohata, J., and Mita, K. (2003). Analysis of alpha- and beta-tubulin genes of Bombyx mori using an EST database. *Insect Biochem. Mol. Biol.* **33**(1)**,** 131-137.

Kirschner, M. W. (1987). Biological implications of microtubule dynamics. *Harvey Lect.* **83,** 1-20.

Klupp, B. G., Granzow, H., and Mettenleiter, T. C. (2000). Primary envelopment of pseudorabies virus at the nuclear membrane requires the UL34 gene product. *J. Virol.* **74**(21)**,** 10063-10073.

Klupp, B. G., Granzow, H., and Mettenleiter, T. C. (2001). Effect of the pseudorabies virus US3 protein on nuclear membrane localization of the UL34 protein and virus egress from the nucleus. *J. Gen. Virol.* **82**(Pt 10)**,** 2363-2371.

Kwong, A. D., and Frenkel, N. (1989). The herpes simplex virus virion host shutoff function. *J. Virol.* **63**(11)**,** 4834-4839.

Langford, G. M. (1995). Actin- and microtubule-dependent organelle motors: interrelationships between the two motility systems. *Curr. Opin. Cell Biol.* **7**(1)**,** 82-88.

Lanier, L. M., and Volkman, L. E. (1998). Actin binding and nucleation by *Autographa california* M nucleopolyhedrovirus. *Virology* **243**(1)**,** 167-177.

Lepore, L. S., Roelvink, P. R., and Granados, R. R. (1996). Enhancin, the granulosis virus protein that facilitates nucleopolyhedrovirus (NPV) infections, is a metalloprotease. *J. Invertebr. Pathol.* **68**(2)**,** 131-140.

Long, G., Pan, X., Kormelink, R., and Vlak, J. M. (2006). Functional entry of baculovirus into insect and mammalian cells is dependent on clathrin-mediated endocytosis. *J. Virol.* **80**(17)**,** 8830-8803.

Lu, A., and Carstens, E. B. (1992). Nucleotide sequence and transcriptional analysis of the *p80* gene of *Autographa californica* nuclear polyhedrosis virus: a homologue of the *Orgyia pseudotsugata* nuclear polyhedrosis virus capsid-associated gene. *Virology* **190,** 201-209.

Luby-Phelps, K. (2000). Cytoarchitecture and physical properties of cytoplasm: volume, viscosity, diffusion, intracellular surface area. *Int. Rev. Cytol.* **192,** 189-221.

Machesky, L. M., Insall, R. H., and Volkman, L. E. (2001). WASP homology sequences in baculoviruses. *Trends Cell Biol.* **11**(7)**,** 286-287.

MacKinnon, E. A., Henderson, J. F., Stoltz, D. B., and Faulkner, P. (1974). Morphogenesis of nuclear polyhedrosis virus under conditions of prolonged passage in vitro. *J. Ultrastruct. Res.* **49**(3)**,** 419-435.

Maeda, S., Volrath, S. L., Hanzlik, T. N., Harper, S. A., Majima, K., Maddox, D. W., Hammock, B. D., and Fowler, E. (1991). Insecticidal effects of an insect-specific neurotoxin expressed by a recombinant baculovirus. *Virology* **184**(2)**,** 777-780.

Martignoni, M. E. (1999). History of TM Biocontrol-1: the first registered virus-based product for control of a forest insect. *Am. Entomol.* **45,** 30-37.

McLachlin, J. R., and Miller, L. K. (1994). Identification and characterization of *vlf-1*, a baculovirus gene involved in very late gene expression. *J. Virol.* **68**(12)**,** 7746-7756.

McMillan, T. N., and Johnson, D. C. (2001). Cytoplasmic domain of herpes simplex virus gE causes accumulation in the trans-Golgi network, a site of virus envelopment and sorting of virions to cell junctions. *J. Virol.* **75**(4)**,** 1928-1940.

Mettenleiter, T. C. (2002). Herpesvirus assembly and egress. *J. Virol.* **76**(4)**,** 1537-1547.

Mettenleiter, T. C. (2004). Budding events in herpesvirus morphogenesis. *Virus Res.* **106**(2)**,** 167-180.

Mikhailov, V. S., and Rohrmann, G. F. (2002). Baculovirus replication factor LEF-1 is a DNA primase. *J. Virol.* **76**(5)**,** 2287-2297.

Miki, H., Okada, Y., and Hirokawa, N. (2005). Analysis of the kinesin superfamily: insights into structure and function. *Trends Cell Biol.* **15**(9)**,** 467-476.

Miller, L. K. (1996). Insect Viruses. *In* "Field Virology" (K. D. M. Field B.N., Howley P., eds, Ed.), pp. 33-59. Lippincott-Raven, New York.

Miller, L. K., and Ball, L. A. (1998). "The Insect Viruses." Plenum Press, New York.

Miranda-Saksena, M., Armati, P., Boadle, R. A., Holland, D. J., and Cunningham, A. L. (2000). Anterograde transport of herpes simplex virus type 1 in cultured, dissociated human and rat dorsal root ganglion neurons. *J. Virol.* **74,** 1827-1839.

Mistretta, T. A., and Guarino, L. A. (2005). Transcriptional activity of baculovirus very late factor 1. *J. Virol.* **79**(3)**,** 1958-1960.

Monsma, S. A., and Blissard, G. W. (1995). Identification of a membrane fusion domain and an oligomerization domain in the baculovirus GP64 envelope fusion protein. *J. Virol.* **69**(4)**,** 2583-2595.

Monsma, S. A., Oomens, A. G., and Blissard, G. W. (1996). The GP64 envelope fusion protein is an essential baculovirus protein required for cell-to-cell transmission of infection. *J. Virol.* **70**(7)**,** 4607-4616.

Moreau, V., Frischknecht, F., Reckmann, I., Vincentelli, R., Rabut, G., Stewart, D., and Way, M. (2000). A complex of N-WASP and WIP integrates signalling cascades that lead to actin polymerization. *Nat. Cell Biol.* **2**(7)**,** 441-448.

Moscardi, F. (1999). Assessment of the application of baculoviruses for control of Lepidoptera. *Annu. Rev. Entomol.* **44,** 257-289.

Moss, B. (2001). Poxviridae. *In* "Field Virology" (K. D. M. Field B.N., Howley P., eds, Ed.), Vol. 2, pp. 2849-2883. Lippincott-Raven Publishers, Philadelphia.

Muranyi, W., Haas, J., Wagner, M., Krohne, G., and Koszinowski, U. H. (2002). Cytomegalovirus recruitment of cellular kinases to dissolve the nuclear lamina. *Science* **297**(5582)**,** 854-857.

Naldinho-Souto, R., Browne, H., and Minson, T. (2006). Herpes simplex virus tegument protein VP16 is a component of primary enveloped virions. *J. Virol.* **80**(5)**,** 2582-2584.

Nogales, E. (2000). Structural insights into microtubule function. *Annu. Rev. Biochem.* **69,** 277-302.

Nogales, E. (2001). Structural insight into microtubule function. *Annu. Rev. Biophys. Biomol. Struct.* **30,** 397-420.

Nogales, E., and Wang, H. W. (2006). Structural intermediates in microtubule assembly and disassembly: how and why? *Curr. Opin. Cell Biol.* **18**(2)**,** 179-184.

Nogales, E., Wolf, S. G., and Downing, K. H. (1998). Structure of the alpha beta tubulin dimer by electron crystallography. *Nature* **391**(6663)**,** 199-203.

O'Reilly, D. R. (1997). Auxiliary Genes of Baculoviruses. *In* "*The Baculoviruses*. " (L. K. Miller, Ed.), pp. 267-300. Plenum press., New York.

O'Reilly, D. R., and Miller, L. K. (1991). Improvement of a baculovirus pesticide by the deletion of the EGT gene. *Biotechnology* **9,** 1086-1089.

Ogawa-Goto, K., Tanaka, K., Gibson, W., Moriishi, E., Miura, Y., Kurata, T., Irie, S., and Sata, T. (2003). Microtubule network facilitates nuclear targeting of human cytomegalovirus capsid. *J. Virol.* **77**(15)**,** 8541-8547.

Olszewski, J., and Miller, L. K. (1997a). Identification and characterization of a baculovirus structural protein, VP1054, required for nucleocapsid formation. *J. Virol.* **71**(7)**,** 5040-5050.

Olszewski, J., and Miller, L. K. (1997b). A role for baculovirus GP41 in budded virus production. *Virology* **233**(2)**,** 292-301.

Oomens, A. G., and Blissard, G. W. (1999a). Requirement for GP64 to drive efficient budding of *Autographa californica* multicapsid nucleopolyhedrovirus. *Virology* **254**(2)**,** 297-314.

Oomens, A. G. P., and Blissard, G. W. (1999b). Requirement for GP64 to Drive Efficient Budding of *Autographa californica* Multicapsid Nucleopolyhedrovirus. *Virology* **254,** 297-314.

Orr, G. A., Verdier-Pinard, P., McDaid, H., and Horwitz, S. B. (2003). Mechanisms of Taxol resistance related to microtubules. *Oncogene* **22**(47)**,** 7280-7295.

Park, R., and Baines, J. D. (2006). Herpes simplex virus type 1 infection induces activation and recruitment of protein kinase C to the nuclear membrane and increased phosphorylation of lamin B. *J. Virol.* **80**(1)**,** 494-504.

Pelkmans, L., Kartenbeck, J., and Helenius, A. (2001). Caveolar endocytosis of simian virus 40 reveals a new two-step vesicular-transport pathway to the ER. *Nat. Cell Biol.* **3,** 473-483.

Penfold, M. E., Armati, P., and Cunningham, A. L. (1994). Axonal transport of herpes simplex virions to epidermal cells: evidence for a specialized mode of virus transport and assembly. *Proc. Natl. Acad. Sci. U. S. A.* **91**(14)**,** 6529-6533.

Possee, R. D., Sun, T. P., Howard, S. C., Ayres, M. D., Hill-Perkins, M., and Gearing, K. L. (1991). Nucleotide sequence of the *Autographa californica* nuclear polyhedrosis 9.4 kbp *Eco*RI-I and -R (*polyhedrin* gene) region. *Virology* **185**(1)**,** 229-241.

Rao, S., He, L., Chakravarty, S., Ojima, I., Orr, G. A., and Horwitz, S. B. (1999). Characterization of the Taxol binding site on the microtubule. Identification of Arg(282) in beta-tubulin as the site of photoincorporation of a 7-benzophenone analogue of Taxol. *J. Biol. Chem.* **274**(53)**,** 37990-37994.

Reynolds, A., Ryckman, B., Baines, J., Zhou, Y., Liang, L., and Roller, R. (2001). UL31 and UL34 proteins of herpes simplex virus type 1 form a complex that accumulates at the nuclear rim and is required for envelopment of nucleocapsids. *J. Virol.* **75,** 8803-8817.

Reynolds, A., Wills, E. G., Roller, R., Ryckman, B. J., and Baines, J. D. (2002). Ultrastructural localization of the herpes simplex virus type 1 UL31, UL34, and US3 proteins suggests specific roles in primary envelopment and egress of nucleocapsids. *J. Virol.* **76,** 8939–8952.

Rietdorf, J., Ploubidou, A., Reckmann, I., Holmstrom, A., Frischknecht, F., Zettl, M., Zimmermann, T., and Way, M. (2001). Kinesin-dependent movement on microtubules precedes actin-based motility of vaccinia virus. *Nat. Cell Biol.* **3**(11)**,** 992-1000.

Rodriguez, J. F., Janeczko, R., and Esteban, M. (1985). Isolation and characterization of neutralizing monoclonal antibodies to vaccinia virus. *J Virol* **56**(2)**,** 482-488.

Rodriguez, J. F., and Smith, G. L. (1990). IPTG-dependent vaccinia virus: identification of a virus protein enabling virion envelopment by Golgi membrane and egress. *Nucleic Acids Res* **18**(18)**,** 5347-5351.

Roizman, B., and Knipe, D. (2001). Herpes simplex viruses and their replication. *In* "Field Virology" (K. D. M. Field B.N., Howley P., eds, Ed.), Vol. 2, pp. 2399-2460. Lippincott-Raven Publishers, Philadelphia.

Roller, R., Zhou, Y., Schnetzer, R., Ferguson, J., and DeSalvo, D. (2000). Herpes simplex virus type 1 UL34 gene product is required for viral envelopment. *J. Virol.* **74,** 117–129.

Roncarati, R., and Knebel-Morsdorf, D. (1997). Identification of the early actin-rearrangement-inducing factor gene, arif-1, from Autographa californica multicapsid nuclear polyhedrosis virus [published erratum appears in J. Virol. 1998 Jan;72(1):888-9]. *J. Virol.* **71**(10)**,** 7933-7941.

Russell, R. L., Funk, C. J., and Rohrmann, G. F. (1997). Association of a baculovirus-encoded protein with the capsid basal region. *Virology* **227**(1)**,** 142-152.

Sanchez, V., and Spector, D. H. (2002). CMV makes a timely exit. *Science* **297,** 778–779.

Sanderson, C. M., Hollinshead, M., and Smith, G. L. (2000). The vaccinia virus A27L protein is needed for the microtubule-dependent transport of intracellular mature virus particles. *J. Gen. Virol.* **81**(Pt 1)**,** 47-58.

Schmelz, M., Sodeik, B., Ericsson, M., Wolffe, E. J., Shida, H., Hiller, G., and Griffiths, G. (1994). Assembly of vaccinia virus: the second wrapping cisterna is derived from the trans Golgi network. *J. Virol.* **68**(1)**,** 130-147.

Schroer, T. A. (2004). Dynactin. *Annu. Rev. Cell Dev. Biol.* **20,** 759-779.

Schumacher, D., Tischer, B. K., Trapp, S., and Osterrieder, N. (2005). The protein encoded by the US3 orthologue of Marek's disease virus is required for efficient de-envelopment of perinuclear virions and involved in actin stress fiber breakdown. *J. Virol.* **79**(7)**,** 3987-3997.

Seisenberger, G., Ried, M. U., Endress, T., Buning, H., Hallek, M., and Brauchle, C. (2000). Real-time single-molecule imaging of the infection pathway of an adeno-associated virus. *Science* **294,** 1929-1932.

Simpson-Holley, M., Colgrove, R. C., Nalepa, G., Harper, J. W., and Knipe, D. M. (2005). Identification and functional evaluation of cellular and viral factors involved in the alteration of nuclear architecture during herpes simplex virus 1 infection. *J. Virol.* **79**(20)**,** 12840-12851.

Slack, J. M., Kuzio, J., and Faulkner, P. (1995). Characterization of v-cath, a cathepsin L-like proteinase expressed by the baculovirus *Autographa californica* multiple nuclear polyhedrosis virus. *J. Gen. Virol.* **76 (Pt 5),** 1091-1098.

Smith, G. A., and Enquist, L. W. (2002). Break ins and break outs: viral interactions with the cytoskeleton of Mammalian cells. *Annu. Rev. Cell Dev. Biol.* **18,** 135-161.

Smith, G. A., Gross, S. P., and Enquist, L. W. (2001). Herpesviruses use bidirectional fast-axonal transport to spread in sensory neurons. *Proc. Natl. Acad. Sci. U. S. A.* **98**(6)**,** 3466-3470.

Smith, G. L., Murphy, B. J., and Law, M. (2003). Vaccinia virus motility. *Annu. Rev. Microbiol.* **57,** 323-342.

Smith, G. L., Vanderplasschen, A., and Law, M. (2002). The formation and function of extracellular enveloped vaccinia virus. *J. Gen. Virol.* **83**(Pt 12)**,** 2915-2931.

Sodeik, B. (2000). Mechanisms of viral transport in the cytoplasm. *Trends Microbiol.* **8**(10)**,** 465-472.

Sodeik, B., Ebersold, M. W., and Helenius, A. (1997). Microtubule-mediated transport of incoming herpes simplex virus 1 capsids to the nucleus. *J. Cell Biol.* **136,** 1007-1021.

Soldati, T., and Schliwa, M. (2006). Powering membrane traffic in endocytosis and recycling. *Nat. Rev. Mol. Cell Biol.* **7**(12)**,** 897-908.

Spear, P. G., and Longnecker, R. (2003). Herpesvirus entry: an update. *J. Virol.* **77**(19)**,** 10179-10185.

Stewart, L. M., Hirst, M., Lopez, F. M., Merryweather, A. T., Cayley, P. J., and Possee, R. D. (1991). Construction of an improved baculovirus insecticide containing an insect-specific toxin gene. *Nature (Lond)* **352**(6330)**,** 85-88.

Stewart, T. M., Huijskens, I., Willis, L. G., and Theilmann, D. A. (2005). The *Autographa californica* multiple nucleopolyhedrovirus *ie0-ie1* gene complex is essential for wild-type virus replication, but either IE0 or IE1 can support virus growth. *J. Virol.* **79**(8)**,** 4619-4629.

Summers, M. D. (1971). Electron microscopic observations on granulosis virus entry, uncoating and replication processes during infection of the midgut cells of Trichoplusia ni. *J. Ultrastruct. Res.* **35**(5)**,** 606-625.

Suomalainen, M., Nakano, M. Y., Keller, S., Boucke, K., Stidwill, R. P., and Greber, U. F. (1999). Microtubule-dependent plus- and minus end-directed motilities are competing processes for nuclear targeting of adenovirus. *J. Cell Biol.* **144,** 657-672.

Theilmann, D. A., Blissard, G. W., Bonning, B., Jehle, J. A., O'Reilly, D. R., Rohrmann, G. F., Thiem, S., and Vlak, J. M. (2005). Baculoviridae. *In* "Virus Taxonomy - Eighth Report of the International Committee on Taxonomy of Viruses" (M. M. A. Fauquet C.M., Maniloff J., Desselberger U., and B. L.A. (ed.), Ed.), pp. 177-185. Elsevier/Academic Press, London.

Thiem, S. M., and Miller, L. K. (1989). Identification, sequence, and transcriptional mapping of the major capsid protein gene of the baculovirus *Autographa californica* nuclear polyhedrosis virus. *J. Virol.* **63,** 2008-2018.

Tooze, J., Hollinshead, M., Reis, B., Radsak, K., and Kern, H. (1993). Progeny vaccinia and human cytomegalovirus particles utilize early endosomal cisternae for their envelopes. *Eur. J. Cell Biol.* **60**(1)**,** 163-178.

Uppuluri, S., Knipling, L., Sackett, D. L., and Wolff, J. (1993). Localization of the colchicine-binding site of tubulin. *Proc. Natl. Acad. Sci. U. S. A.* **90**(24)**,** 11598-11602.

van Eijl, H., Hollinshead, M., Rodger, G., Zhang, W. H., and Smith, G. L. (2002). The vaccinia virus F12L protein is associated with intracellular enveloped virus particles and is required for their egress to the cell surface. *J. Gen. Virol.* **83**(Pt 1)**,** 195-207.

van Eijl, H., Hollinshead, M., and Smith, G. L. (2000). The vaccinia virus A36R protein is a type Ib membrane protein present on intracellular but not extracellular enveloped virus particles. *Virology* **271**(1)**,** 26-36.

Van Oers, M. M., and Vlak, J. M. (1997). The baculovirus 10-kDa protein. *J Invertebr Pathol* **70**(1)**,** 1-17.

Vanarsdall, A. L., Okano, K., and Rohrmann, G. F. (2006). Characterization of the role of very late expression factor 1 in baculovirus capsid structure and DNA processing. *J. Virol.* **80**(4)**,** 1724-1733.

Vasquez, R. J., Howell, B., Yvon, A. M., Wadsworth, P., and Cassimeris, L. (1997). Nanomolar concentrations of nocodazole alter microtubule dynamic instability in vivo and in vitro. *Mol. Biol. Cell* **8**(6)**,** 973-985.

Vialard, J. E., Arif, B. M., and Richardson, C. D. (1995). Introduction to the molecular biology of baculoviruses. *Methods Mol. Biol.* **39,** 1-24.

Vialard, J. E., and Richardson, C. D. (1993). The 1629-nucleotide open reading frame located downstream of the *Autographa californica* Nuclear Polyhedrosis Virus polyhedrin gene encodes a nucleocapsid-associated phosphoprotein. *J. Virol.* **67**(10)**,** 5859-5866.

Volkman, L. E. (1986). The 64K envelope protein of budded *Autographa californica* nuclear polyhedrosis virus. *Curr. Top. Microbiol. Immunol.* **131,** 103-118.

Volkman, L. E. (1988). *Autographa californica* MNPV nucleocapsid assembly: inhibition by cytochalasin D. *Virology* **163**(2)**,** 547-553.

Volkman, L. E., and Goldsmith, P. A. (1985). Mechanism of neutralization of budded *Autographa californica* nuclear polyhedrosis virus by a monoclonal antibody: inhibition of entry by adsorptive endocytosis. *Virology* **143,** 143-185.

Volkman, L. E., Goldsmith, P. A., Hess, R. T., and Faulkner, P. (1984). Neutralization of budded *Autographa californica* NPV by a monoclonal antibody: Identification of the target antigen. *Virology* **133**(2)**,** 354-362.

Volkman, L. E., Talhouk, S. N., Oppenheimer, D. I., and Charlton, C. A. (1992). Nuclear F Actin a Functional Component Of Baculovirus-Infected Lepidopteran Cells? *J. Cell Sci.* **103**(1)**,** 15-22.

Volkman, L. E., and Zaal, K. J. (1990). Autographa californica M nuclear polyhedrosis virus: microtubules and replication. *Virology* **175**(1)**,** 292-302.

Wang, P., Hammer, D. A., and Granados, R. R. (1994). Interaction of *Trichoplusia ni* granulosis virus-encoded enhancin with the midgut epithelium and peritrophic membrane of four lepidopteran insects. *J. Gen. Virol.* **75**(8)**,** 1961-1967.

Ward, B. M., and Moss, B. (2001). Vaccinia virus intracellular movement is associated with microtubules and independent of actin tails. *J Virol* **75**(23)**,** 11651-63.

Welch, M. D., and Mullins, R. D. (2002). Cellular control of actin nucleation. *Annu. Rev. Cell Dev. Biol.* **18,** 247-288.

Westermann, S., and Weber, K. (2003). Post-translational modifications regulate microtubule function. *Nat. Rev. Mol. Cell Biol.* **4**(12)**,** 938-947.

Whitford, M., and Faulkner, P. (1992). Nucleotide sequence and transcriptional analysis of a gene encoding gp41 a structural glycoprotein of the baculovirus *Autographa californica* nuclear polyhedrosis virus. *J. Virol.* **66**(8)**,** 4763-4768.

Whitford, M., Stewart, S., Kuzio, J., and Faulkner, P. (1989). Identification and sequence analysis of a gene encoding *gp67,* an abundant envelope glycoprotein of the baculovirus *Autographa californica* nuclear polyhedrosis virus. *J. Virol.* **63**(3)**,** 1393-1399.

Wickham, T. J., Shuler, M. L., Hammer, D. A., Granados, R. R., and Wood, H. A. (1992). Equilibrium and kinetic analysis of *Autographa californica* Nuclear Polyhedrosis Virus attachment to different insect cell lines. *J. Gen. Virol.* **73,** 3185-3194.

Willard, M. (2002). Rapid directional translocations in virus replication. *J. Virol.* **76**(10)**,** 5220-5232.

Williams, G. V., and Faulkner, P. (1997). Cytological changes and viral morphogenesis during baculovirus infection. *In* "The Baculoviruses" (L. K. Miller, Ed.), pp. 61-107. Plenum Press, New York.

Wilson, L., and Jordan, M. A. (1995). Microtubule dynamics: taking aim at a moving target. *Chem. Biol.* **2**(9)**,** 569-573.

Wilson, M. E., and Consigli, R. A. (1985). Functions of a protein kinase activity associated with purified capsids of the granulosis virus infecting *Plodia interpunctella*. *Virology* **143,** 526-535.

Wilson, M. E., Mainprize, T. H., Friesen, P. D., and Miller, L. K. (1987). Location, transcription, and sequence of a baculovirus gene encoding a small arginine-rich polypeptide. *J. Virol.* **61**(3)**,** 661-666.

Wolgamot, G. M., Gross, C. H., Russell, R. L., and Rohrmann, G. F. (1993). Immunocytochemical characterization of P24, a baculovirus capsid-associated protein. *J. Gen. Virol.* **74,** 103-107.

Wu, W., Lin, T., Pan, L., Yu, M., Li, Z., Pang, Y., and Yang, K. (2006). *Autographa californica* multiple nucleopolyhedrovirus nucleocapsid assembly is interrupted upon deletion of the 38K gene. *J. Virol.* **80,** 11475-11485.

Xeros, N. (1956). The virogenic stroma in nuclear and cytoplasmic polyhedrosis. *Nature* **178,** 412-413.

Yang, S., and Miller, L. K. (1998a). Expression and mutational analysis of the baculovirus very late factor 1 (*vlf-1*) gene. *Virology* **245,** 99-109.

Yang, S., and Miller, L. K. (1998b). Expression and mutational analysis of the baculovirus very late factor 1 (*vlf-1*) gene. *Virology* **245,** 99-109.

Yang, S., and Miller, L. K. (1999). Activation of baculovirus very late promoters by interaction with very late factor 1. *J. Virol.* **73**(4)**,** 3404-3409.

Young, J. C., Mackinnon, E. A., and Faulkner, P. (1993). The architecture of the virogenic stroma in isolated nuclei of *Spodoptera frugiperda* cells in vitro infected by *Autographa californica* nuclear polyhedrosis virus. *J. Struct. Biol.* **110**(2)**,** 141-153.

Zanotto, P. M., Kessing, B. D., and Maruniak, J. E. (1993). Phylogenetic interrelationships among baculoviruses: evolutionary rates and host associations. *J. Invertebr. Pathol.* **62**(2)**,** 147-164.

Zhang, W. H., Wilcock, D., and Smith, G. L. (2000). Vaccinia virus F12L protein is required for actin tail formation, normal plaque size, and virulence. *J. Virol.* **74**(24)**,** 11654-62.

Chapter 2: Autographa californica Multiple Nucleopolyhedrovirus EXON0 (ORF141) is required for the efficient egress of nucleocapsids from the nucleus[1]

2.1 Introduction

Autographa californica Multiple Nucleopolyhedrovirus (AcMNPV), the archetype of the *Baculoviridae,* has a large double-stranded DNA genome of approximately 134 kbp and encodes 154 predicted genes. AcMNPV has a nuclear site of replication, many virus-encoded enzymes for DNA transcription and replication, and a complex morphogenic pathway that produces two distinct forms of infectious virions in infected cells budded virus (BV) and occlusion derived virus (ODV) (Theilmann et al., 2005). *Exon0* (*orf141*) is a highly conserved gene found in all lepidopteran baculoviruses of the genus *Nucleopolyhedrovirus*. The deletion of *exon0* reduces the level of BV production up to 99% and the infection of Sf9 cells with the *exon0* KO virus is restricted to a single cell or a few neighbouring cells. However, viral replication and polyhedra production are unaffected (Dai et al., 2004), suggesting that *exon0* plays a key role in the pathway that is specific for the synthesis of BV.

Baculovirus BVs are thought to enter insect and mammalian cells *via* adsorptive endocytosis (Hefferon et al., 1999; Volkman and Goldsmith, 1985), including clathrin-mediated endocytosis and low-pH-dependent membrane fusion (Blissard and Wenz, 1992; Kingsley et al., 1999; Leikina et al., 1992; Long et al., 2006). After the nucleocapsids are released from the endosomes, they are transported into the nuclei, where viral transcription and DNA replication occur resulting in the production of BV and ODV (Fraser, 1986). These two virion forms have different functions in the viral life cycle. ODV is required for inter-host transmission whereas BV is required for the

[1] A version of this chapter has been published as: Fang M, Dai X, and Theilmann D. A. (2007). *Autographa californica* Multiple Nucleopolyhedrovirus EXON0 (ORF141) is required for the efficient egress of nucleocapsids from the nucleus. J. Virol.: 9859-69.

dissemination of a viral infection throughout the tissues of an infected host. Both virion forms are genetically identical but differ in their envelope composition and tissue tropisms, and are produced at different times during infection (Braunagel and Summers, 1994; Funk et al., 1997). At the late times post infection (pi) nucleocapsids are synthesized in the nucleus and are initially shuttled out of the nucleus and transported to the cytoplasmic membrane from which they bud forming BVs. At very late times pi nucleocapsids are retained in the nucleus to form ODVs where they become occluded in occlusion bodies. The molecular events that occur during baculovirus replication have been extensively studied (Okano et al., 2006), but the mechanisms by which the nucleocapsids are determined to be shuttled to either ODV or BV and how the nucleocapsids are transported to the cell membrane are still unknown.

Several viral genes have been shown to affect the synthesis of BV and ODV. For example the AcMNPV VP1045 and VLF-1 are nucleocapsid proteins of both BV and ODV, and have been shown to be required for the assembly of progeny nucleocapsids in the nucleus (Olszewski and Miller, 1997a; Vanarsdall et al., 2006; Yang and Miller, 1998b). GP41 is an O-glycosylated protein that affects both BV and ODV but is only a structural component of ODV (Olszewski and Miller, 1997b). The baculovirus core gene *38K* (*ac98*) that expresses a nuclear protein, has been shown to be essential for the formation of normal nucleocapsids affecting both BV and ODV production but has not been shown to be a structural component of the nucleocapsid (Wu et al., 2006). Other than EXON0 very few proteins have been shown to be specific for the synthesis of BV but one of the most intensively studied is the envelope glycoprotein GP64. GP64 is required for the efficient virion budding from the plasma membrane and is essential for BV attachment and membrane fusion (Blissard and Wenz, 1992; Hefferon et al., 1999; Monsma et al., 1996; Oomens and Blissard, 1999b).

In this study, we present evidence to show that EXON0 is a structural component of both BV and ODV and a component of the BV nucleocapsid. Using yeast 2-hybrid screening, immunoprecipitation and confocal microscopy we show that EXON0 interacts with the known nucleocapsid proteins FP25 and BV/ODV-C42. In the absence of EXON0

nucleocapsids are not efficiently transported from the nucleus to the cytoplasm, but the nucleocapsid assembly remains unchanged.

2.2 Materials and Methods

2.2.1 Cells and Viruses

Spodoptera frugiperda Sf9 cells were maintained in 10% fetal bovine serum-supplemented TC100 medium at 27°C. AcMNPV recombinant bacmids were derived from the commercially available bacmid bMON14272 (Invitrogen Life Technologies) and propagated in *Escherichia coli* strain DH10B.

2.2.2 Construction of HA-tagged EXON0

To tag EXON0 with the influenza HA epitope (CYPYDVPDYASL) at the N-terminus, *exon0* was amplified using primers 608 (5'-AGATCTATGTACCCCTACGACGTGCCCGACTACGCCATAAGAACCAGCAGTCACGTG-3') and 609 (5'-GTTGCGTTGCCCGTTATC -3') and p2ZeoKS-exon0 (Dai et al., 2004) as a template. Inverse polymerase chain reaction (PCR) was used to amplify the linear fragments which were then treated with T4 polynucleotide kinase and gel purified. Amplified fragments were self-ligated overnight at 16°C and transformed into DH5α competent cells. Zeocin resistant colonies were picked and identified by restriction digestion and confirmed by sequencing. The resulting plasmid was named p2Zeo-HA-exon0.

2.2.3 Construction of bMON 14272 exon0 KO and HA-exon0 repaired bacmid

The first 114 bp of exon0 are shared with and spliced to ie0 mRNA. In addition, the TAA stop codon of *exon0* overlaps with the putative *orf142* late transcription initiation motif DTAAG, which is one of the 29 core baculovirus genes and encodes a structural protein of ODV (Braunagel et al., 2003). To prevent any possible intragenomic homologous recombination we ensured that no homologous sequences were present between the wild type (WT) locus and repair constructs inserted at the *polyhedrin* locus. To accomplish this, we constructed a new KO bacmid in which both the complete open reading frame (ORF) of *exon0* and the promoters of *exon0* and *ie0* were deleted. The late promoter *gp64* L2 (Garrity et al., 1997) was inserted upstream of *orf142* to drive this

gene and so avoid any possible disruption of its expression. IE0 is not essential for viral replication and in addition the *ie0* KO virus *ie1* KO-IE1 produces WT levels of BV (Lu et al., 2005; Stewart et al., 2005), thus the new KO virus provided the backbone genome for the analysis of *exon0* presented in this study. The AcMNPV bacmid (bMON 14272) was used to generate the KO virus by recombination in *E. coli*, as previously described (Hou et al., 2002; Lin and Blissard, 2002; Lung et al., 2003). A zeocin resistance gene was amplified using primers 665 (5'-GGTCACGTAGGCACTTTGCGCACGGCACTAGGGCTGTGGAGGGGACAGGCGGATCTCTGCAGCACGTGTT-3') and 666 (5'-CTCTTTCCAGAGTCAACAAGTTGCCGCCACCACTCATTTTGCGTTGCGTGCTTATCTTTTTATCTTAGACATGATAAGATACATTGATGA-3') and p2ZeoKS as template. These primers contain 50 bp and 43 bp homologous to the upstream and downstream flanking regions of *exon0*, respectively. The PCR fragment of the zeocin resistance gene amplified with primers 665 and 666 was gel purified and electroporated into *E. coli* BW25113-pKD46 cells, which already contained the AcMNPV bacmid bMON14272 DNA. The electroporated cells were incubated at 37°C for 4 h in 3 ml of SOC medium and placed onto agar medium containing 30 μg of zeocin per ml and 50 μg of kanamycin per ml. These plates were incubated at 37°C overnight, and colonies resistant to zeocin and kanamycin were selected for further confirmation by PCR.

Two different pairs of primers were used to confirm that *exon0* had been deleted from the *exon0* locus of the AcMNPV bacmid genome (Fig. 2.1A). Primers 183 (5'-CGCAACAGGATCCGAACCAGCAGTC-3') and 520 (5'-CTTTTGGATCCACAACAGGCAATTTGAT-3') were used to detect the correct insertion of the *zeocin* gene cassette. A fragment of 1855 bp which was amplified with primers 183/520 from the *exon0* KO bacmid confirmed the correct insertion of *zeocin* in the *exon0* locus. Primers 626 and 630 (5'-TGTATATGCGTAGGAGAGCC-3' and 5'-CTCGCAACTGTTTCAAGTAC-3', respectively) were used to confirm the absence of the *exon0* ORF. These primers amplify a 250 bp fragment from the WT AcMNPV bacmid (Fig. 2.1B). One of the recombinant bacmids confirmed by PCR was selected and named bMON 14272 *exon0* KO.

To introduce HA-tagged *exon0* back into bMON 14272 *exon0* KO, rescue transfer vectors were constructed using the plasmid backbone pFAcT (Dai et al., 2004). pFAcT contains two Tn*7* transposition excision sites that allow the genes cloned between the sites to be transposed into the mini ATT region located in the AcMNPV bacmid. p2Zeo-HA-exon0 was digested with *Xho*I and *Xba*I. The excised fragment, containing the native late promoter of *exon0*, *exon0* ORF and an *Orgyia pseudotsugata* MNPV *ie1* polyadenylation signal, was cloned into the *Xho*I and *Xba*I sites of pFAcT to generate pFAcT-HA-exon0. In the pFAcT backbone, the AcMNPV *polyhedrin* is included in the transposed DNA cassette. bMON 14272 *exon0* KO bacmids containing the pFAcT or pFAcT-HA-exon0 cassettes were generated by Tn*7*-mediated transposition as previously described by Luckow *et al* (1993), the resulting viruses were named *exon0* KO and *exon0* KO-HA-EXON0.

2.2.4 Time course analysis of BV production

Sf9 cells (1.0 x 10^6 cells/35mm diameter well of a six-well plate) were transfected with 1.0 μg of each bacmid construct (*exon0* KO, *exon0* KO-HA-EXON0 or the control virus *ie1* KO-IE1). At various hours post transfection (hpt), the supernatant containing the BV was harvested and cell debris was removed by centrifugation (8,000 x *g* for 5 min). The supernatant BV titers were determined in duplicate by end point dilution in Sf9 cells using 96-well microtiter plates.

2.2.5 Cellular localization of EXON0 by nuclear and cytoplasmic fractionation

Sf9 cells (2.0 x 10^6/35-mm-diameter six-well plate) were infected with the *exon0* KO-HA-EXON0 virus at a multiplicity of infectivity (MOI) of 10. At 6, 12, 18, 24, 36, 48, and 72 hours post infection (hpi), cells were washed with phosphate-buffered saline (PBS, 137 mM NaCl, 10 mM Phosphate, 2.7 mM KCl, pH 7.4), scraped with a rubber policeman and collected (800 x g for 5 min). Cells were resuspended in 0.2 ml NP-40 lysis buffer (10 mM Tris, pH7.9, 10 mM NaCl, 5 mM $MgCl_2$, 1 mM dithiothreitol, 0.5% NP40 (V/V)), gently mixed and kept on ice for 5 min. Nuclei were pelleted by

centrifugation at 1000 x *g* for 3 min. The supernatant containing the cytosolic fraction was transferred to a new tube and mixed with an equal volume of 2× Protein Sample Buffer (PSB) (0.25 M Tris-Cl, pH6.8, 4% SDS, 20% glycerol, 10% 2-mercaptoethanol, 0.02% bromophenol blue). The nuclei were resuspended in the original volume of lysis buffer and mixed with an equal volume of 2× PSB. The nuclear fraction was sheared with a 25 G syringe and analyzed by a 10% sodium dodecyl sulfate-polyacrylamide gel electrophoresis (SDS-PAGE) and Western blot.

2.2.6 Immunofluorescence

Sf9 cells were infected with *exon0* KO-HA-EXON0 using a MOI of 10. At 12, 18, 24, 36, 48 and 72 hpi, the supernatant was removed and the cells were washed three times in PBS, followed by fixation in 3% paraformaldehyde in PBS for 10 min. The fixed cells were washed three times in PBS for 15 min, followed by permeabilization in 0.15% Triton X-100 in PBS for 15 min. The cells were then blocked for 60 min in blocking buffer (2% bovine serum albumin in PBS), followed by 1 hr incubation with either mouse monoclonal anti-HA antibody (1:200) (Covance, HA11) alone, or with mouse monoclonal anti-HA antibody (1:200) coupled with either rabbit anti-FP25 antibody (1:1000) or rabbit anti-BV/ODV-C42 antibody (1:1000) (Braunagel et al., 1999; Braunagel et al., 2001). The cells were washed three times for 10 min each time in blocking buffer, followed by 1 hr incubation with a fluorescently tagged antibody. Samples incubated with HA antibody alone were further incubated with an Alexa 635-conjugated goat anti-mouse antibody (1:500) (Molecular Probes). Samples incubated with rabbit anti-FP25 or anti-BV/ODV-C42 antibodies were further incubated with Alexa 488-conjugated goat anti-rabbit IgG (1:500) (Molecular Probes). The cells were subsequently washed three times for 10 min each time in PBS, followed by staining with 200 ng/ml 4', 6-diamidino-2-phenylindole (DAPI) (Sigma) and examined using a Leica confocal Microscope.

2.2.7 Purification of BV and ODV

Sf9 cells were infected with *exon0* KO-HA-EXON0 with a MOI of 0.1. Six days post infection (pi), 80 ml of media were collected and centrifuged at 8,000 x g in a Beckman JA 17 rotor. The supernatant was then centrifuged at 100,000 x g (Beckman SW28, 21,000 rpm) at 4 °C to pellet the BV. The BV pellet was resuspended in 0.4 ml 0.1xTE, loaded on a 25-60% sucrose gradient and centrifuged at 100,000 x g (Beckman SW41, 24,000 rpm) for 90 min. The BV band was collected, diluted twice, and centrifuged at 100,000 *g* for 30 min at 4°C (Beckman SW41, 24000 rpm). The virus pellet was resuspended in 200 µl 0.1x TE. Protein concentration was determined by Bradford assay (Bradford, 1976).

In a 250 µl reaction, 250 µg of BV was incubated in 1.0% NP-40 and 10 mM Tris, pH 8.5 at room temperature for 30 min with gentle agitation. The solution was then layered onto a 4 ml 30% (w/v) glycerol/10 mM Tris (pH 8.5) cushion and centrifuged at 150,000 *g* for 60 min at 4°C (Beckman SW60, 34,000 rpm). The envelope proteins were recovered from the top of the cushion, trichloroacetic acid (TCA) precipitated. The pelleted nucleocapsids were dissolved in 10 mM Tris (pH 7.4).

Polyhedra and ODV were purified from the cells infected with *exon0* KO-HA-EXON0 at 6 days pi and purified as previously described (Braunagel and Summers, 1994).

2.2.8 Immunoprecipitation (IP)

Sf9 cells (3 x 10^8) were infected with either WT AcMNPV E2 or *exon0* KO-HA-EXON0 at a MOI of 10. At 24 hpi, the cells were collected and washed with PBS, pelleted at 800 x g for 5 min and resuspended in 2 ml EBC (50 mM Tris-Cl pH 8.0, 120 mM NaCl, 0.5% Nonidet P-40, 0.2 mM sodium orthovanadate, 1% sodium fluoride, 1% protease inhibitor cocktail (Sigma)), and placed on ice for 10 min. The cells were passed through a cold French press cell twice at 1000 PSI. Fifteen µl of the lysate was removed for Western blot. The lysate was centrifuged at 13,000 x rpm on a benchtop centrifuge at 4 °C for 10

min. Forty µl of anti-HA antibody-immobilized agarose beads (Sigma) were equilibrated with EBC buffer and mixed with the 2 ml of lysate supernatant, incubated overnight on a orbital shaker at 4 °C. The incubation mix was then transferred to a Bio-Rad column and the beads were washed once with 0.5 ml EBC buffer, followed by 5 washes with 0.5 ml NETN buffer (20 mM Tris-Cl pH 8.0, 1 mM EDTA, 0.5% NP-40) containing 400 mM NaCl. The beads were eluted twice using 60 µl 100 mM glycine-HCl (pH 2.2) after 1 min incubation. Two eluates were combined and the pH was raised with 1.5 M Tris-HCl (pH8.8) to a final pH of 8.0. The eluate was vacuum concentrated to 45 µl, mixed with 45 µl 2× PSB, boiled for 10 min at 100 °C, and subjected to SDS-PAGE and examined by Western blot.

2.2.9 Western blot analysis

Protein samples from the nuclear and cytoplasmic fractionation, purified BV or ODV and the protein immunoprecipitation eluates from the HA agarose beads, were mixed with equal volumes of 2× sodium dodecyl sulfate PSB, and incubated at 100°C for 10 min. Protein samples were separated by 10% SDS-PAGE and transferred to Millipore Immobilon-P membrane with the Bio-Rad Mini-Protean II and Liquid Transfer apparatuses, respectively, in accordance with the manufacturers' recommended protocols. Western blots were probed with one of the following primary antibodies: (i) mouse monoclonal HA antibody (Covance, HA11), 1:1,000; (ii) mouse monoclonal OpMNPV VP39, 1:3,000; (iii) mouse monoclonal IE1 antibody (1: 5,000); (iv) rabbit polyclonal FP25 antibody (1:5,000); (v) rabbit polyclonal BV-ODV C42 antibody (1:5,000); (vi) mouse monoclonal GP64 AcV5 antibody (1:5,000); (vii) OpMNPV polyhedrin mouse monoclonal at (1:10,000). Horseradish peroxidase-conjugated rabbit anti-mouse secondary antibody (1:15,000) or horseradish peroxidase-conjugated goat anti-rabbit antibody (1:10,000) were used with the Enhanced Chemiluminescence System (Amersham).

2.2.10 Yeast 2-hybrid screening

The *S. cerevisiae* strain YRG2 (MATa *ura3-52 his3-200 ade2-101lys2-801 trp1-901 leu2-3 112 gal4-542gal80-538* LYS2::UAS GAL1-TATA GAL1-HIS3URA3::UAS GAL4 17mers(x3)-TATACYC1-*lacZ*) (Stratagene) and the vectors pBD-GAL4 Cam (Stratagene) and pAD-GAL4-2.1 (Stratagene) were used for yeast two-hybrid tests. When cloned into the binding domain vector pBD-GAL4 Cam EXON0 transactivates the histidine reporter gene (data not shown). Therefore for all analyses EXON0 was cloned into the activation domain vector (pAD-GAL4-2.1). Eight known nucleocapsid proteins previously identified in both BV and ODV and non-nucleocapsid proteins, ME53, as control were analyzed as candidate interacting partners of EXON0 and fused with the binding domain vector pBD-GAL4. The following primers were used for amplifying these genes: primer 1175 (5'- GCGGGAATTCATGACGAATCGTAGATATG -3') and 1176 (5'- GCGGCTGCAGTTAAGCGCTAGATTCTGTG-3') for *p78/83*, primer 1177 (5'- GCGGCTCGAGCATGTGTTCGACCAAGAAAC-3') and 1178 (5'- GCGGCTGCAGCTACACGTTGTGTGCGTGC-3') for *vp1054*, primer 1179 (5'- GCGGGAATTCATGGATCAATTTGAACAGTT-3') and 1180 (5'- GCGGCTGCAGTTAAATTAAATTTTGAAGCATTT -3') for *fp25*, primer 1181 (5'- GCGGGAATTCATGAACGGTTTTAATGTTCG-3') and 1182 (5'- GCGGCTGCAGCTATTCGTTGCGATAGTAC-3') for *vlf-1*, and 1183 (5'- GCGGGAATTCATGGCGCTAGTGCCCGT-3') and 1184 (5'- GCGGCTGCAGTTAGACGGCTATTCCTCC-3') for *vp39*, primer 1185 (5'- GCGGGAATTCATGAGCGCTATCGCGTTG-3') and 1186 (5'- GCGGCTGCAGTTAATATTTTTTACGCTTTGCA-3') for *bv/odv-c42*, primer 1187 (5'- GCGGCTCGAGCATGAACGATTCCAATTCTCT-3') and 1188 (5'- GCGGCTGCAGTTATATAACATTGTAGTTTGCG-3') for *p87*, primer 1189 (5'- GCGGGAATTCATGAACACGGACGCTCAG-3') and 1190 (5'- GCGGCTGCAGTTATTTATTCAGGCACATTAAA-3') for *p24*, primer 1195 (5'- GCGGGAATTCATGAACCGTTTTTTTCGAGA-3') and 1196 (5'- GCGGCTGCAGTTAGACATTGTTATTTACAATA-3') for *me53*. The resulting AD and BD fusion plasmids were introduced into the YRG2 yeast strain by the lithium acetate method according to the manufacturers' instructions (Stratagene). Transformants

were screened on medium lacking the appropriate amino acids, and selection for histidine reporter gene activation was performed on histidine, tryptophan, or histidine, tryptophan, leucine-deficient agar plates.

2.2.11 Transmission electron microscopy (TEM)

Sf9 cells (2.0 x 106 cells/60-mm-diameter plate) were transfected with 1.0 µg of either exon0 KO or exon0 KO-HA-EXON0. At 24, 36, 48 and 96 hpt, the supernatant was removed and the cells washed once with PBS (pH 7.2) and then fixed in 2.5% glutaradehyde in PBS for 2 hrs. Cells were then dislodged with a rubber policeman, transferred into eppendorf tubes and washed twice for 15 min in PBS. Cells were then immobilized with 50 µl of 3% low melting point agarose and placed on ice for 30 min. The agarose fraction was then removed and the cells were fixed with 1% Osmium for 1 hr, followed by staining with 2% uranyl acetate for 1 hr. After dehydration through a series of 30-100% ethanol washes, cells were embedded in Spur resin. Ultra thin sections were obtained and subsequently stained with 1% uranium acetate and Sato's lead (Takagi et al., 1990). Images were obtained using a Hitachi transmission electron microscope.

2.3 Results

2.3.1 Construction of *exon0* KO bacmid and growth curve of the repaired virus

The *exon0* gene is essential for the efficient production of BV which was previously shown using an *exon0* KO bacmid which retained 142 bp and 261 bp of the 5' and 3' ends of the *exon0* coding region respectively in order to preserve the *ie0* splice site and the *orf142* promoter (Dai et al., 2004). With this previous construct intragenomic recombination could occur between the *exon0* KO locus and the repair locus. To prevent any possible intragenomic homologous recombination events between the *exon0* locus and repair constructs, a new *exon0* KO bacmid was constructed in which the complete ORF of *exon0* and the promoters of both *exon0* and *ie0* were deleted. This resulted in a bacmid construct (bMON 14272 *exon0* KO) which has both *exon0* and *ie0* knocked out but the *orf142* promoter was repaired using the *gp64* late promoter (Fig. 2.1A). It has been previously shown that *ie0* is not required for WT levels of BV production (Lu et al., 2005; Stewart et al., 2005), therefore, bMON 14272 *exon0* KO permitted the analysis of *exon0* function without the possibility of intragenomic homologous recombination. The correct deletion and repair construct were confirmed by PCR (Fig. 2.1B)

The bMON 14272 *exon0* KO bacmid was repaired by Tn7 mediated transposition at the *polyhedrin* locus with either *polyhedrin* alone or with N-terminally HA epitope tagged *exon0* and *polyhedrin* generating the viruses *exon0* KO and *exon0* KO-HA-EXON0, respectively (Fig. 2.1). To confirm the WT levels of BV production of *exon0* KO-HA-EXON0 and the reduction of BV production from *exon0* KO the viruses were compared to the *ie0* KO virus *ie1* KO-IE1 (Stewart et al., 2005) by comparing growth curves (Fig. 2.1C). As expected the BV production of *exon0* KO-HA-EXON0 virus and the control virus *ie1* KO-IE1 exhibited WT levels of BV production reaching 1.0×10^6 by 24 hpt and 1.0×10^8 $TCID_{50}$/ml by 72 hpt. BV production by the *exon0* KO was significantly lower, producing less than 200 $TCID_{50}$ by 24 hpt, with peak level of 1×10^4 $TCID_{50}$/ml by 72 hpt. This corresponded to a 99.99% reduction in BV production compared to *exon0* KO-HA-EXON0 and *ie1*KO-IE1. The growth curves confirmed that EXON0 was required for the

efficient production of BVs as previously reported (Dai et al., 2004) and that the HA-tag on the repair construct did not affect the function of EXON0.

2.3.2 Sub-cellular localization of EXON0 during infection

In order to determine the function of EXON0 it was necessary to establish its temporal expression and cellular localization. An initial time course analysis of EXON0 expression was performed using *exon0* KO-HA-EXON0. The infected Sf9 cells were collected at various times pi and the nucleus and cytoplasmic fractions were separated. Western blot analysis showed that EXON0 was translated from 12 hpi to 72 hpi and was distributed in both the nucleus and the cytoplasm. From 12 to 24 hpi, during the peak BV production, EXON0 localized to a greater extent in the cytoplasm (Fig. 2.2). As a control to test the efficiency of the fractionation process, the same samples were probed with an IE1 and GP64 antibody. The presence of IE1 and GP64 exclusively in the nuclear fraction and cytoplasmic fractions respectively, confirmed the efficiency of the cell fractionation

Cellular localization of EXON0 was also analyzed by immunofluorescence and confocal microscopy. As shown in Fig. 2.3, EXON0 could be detected more in the cytoplasm at 12 hpi with a low unevenly distributed level in the nucleus. At 18 hpi, EXON0 was detected with greater intensity in a ring pattern concentrating to the cytoplasmic membrane and more EXON0 localized in the nucleus, at the periphery of virogenic stroma (blue of DAPI) that corresponded to the ring zone of the virogenic stroma (Charlton and Volkman, 1991a; Xeros, 1956). This double ring localization continued at 24 hpi but with greater levels of expression. By 48 hpi the EXON0 fluorescence signal became diffuse and with a slightly greater intensity at the ring zone of virogenic stroma. EXON0 signal decreased in both the cytoplasm and the nucleus after 48 hpi (data not shown). The localization of EXON0 by immunofluorescence was consistent with the results obtained from the fractionation and Western blot.

2.3.3 Western blot analysis of EXON0 association with BV and ODV

As EXON0 affects the production of BV it was necessary to determine if EXON0 was associated with the viral particles. Therefore BV and ODV were purified and analyzed by Western blot for the presence of EXON0. The results (Fig. 2.4) showed that EXON0 could be detected in both BV and ODV (Lanes BV and ODV). The BV particles were also biochemically fractionated into both nucleocapsid and envelope fractions (Lanes NC and ENV) and the Western blot analysis indicated that EXON0 was localized in the nucleocapsid fraction. As a control to confirm the efficiency of the fractionation, the known nucleocapsid protein VP39 and the BV envelope specific GP64 were analyzed by western blot. Both VP39 and GP64 were observed in the expected fractions. These results show that EXON0 is associated with both BV and ODV virions and localizes in the nucleocapsids of BV.

2.3.4 Interaction of EXON0 with nucleocapsid proteins.

The Western blot results above suggest that EXON0 is a structural component of the nucleocapsid. It is therefore possible that EXON0 may physically interact with known nucleocapsid proteins. To test this we initially used a yeast 2-hybrid screening to determine if other nucleocapsid proteins interacted with EXON0. Eight nucleocapsid proteins, P78/83, VP1054, FP25, VLF1, VP39, BV/ODV-C42, P87, P24 and as a control one non-structural protein ME53 were selected. Each protein was cloned into the GAL4 binding domain vector and an initial control experiment was performed to determine whether these nucleocapsid proteins transactivated the Histidine reporter in the absence of EXON0. EXON0 was cloned into the activation domain vector and was co-transformed with the nucleocapsid protein fusion constructs as well as an empty binding domain control vector (pBD-Gal4). Based on comparison with the empty vector, medium colony growth was observed with FP25 and BV/ODV-C42 (Table 2.1).

Co-immunoprecipitation assays were performed to confirm the *in vivo* interaction between EXON0 and FP25 and BV/ODV-C42. Sf9 cells were infected with either WT AcMNPV-E2 which does not have a HA tagged EXON0 or with *exon0* KO-HA-EXON0 virus. At 24 hpi cells were collected and lysed for immunoprecipitation. Lysates were

immunoprecipitated with HA antibody and the precipitates were analyzed by Western blot and probed with FP25 and BV/ODV-C42 antibodies. The results showed that both FP25 and BV/ODV-C42 co-immunoprecipitated from cells infected with the HA-EXON0 repaired virus, but not with the WT AcMNPV-E2 virus. Controls were performed with the major nucleocapsid protein VP39, the BV envelope protein GP64 and the hyperexpressed protein polyhedrin and all gave the negative results (Fig. 2.5). These results confirmed EXON0 was specifically interacting with FP25 and BV/ODV-C42 *in vivo*.

2.3.5 Co-localization of EXON0 with FP25 and BV/ODV-C42

To determine if EXON0 co-localizes with the nucleocapsid protein FP25 and BV/ODV-C42, immunofluorescence was used to analyze their localization in infected Sf9 cells (Fig. 2.6). At 24 and 48 hpi, FP25 was predominantly detected in the cytoplasm as has been previously reported with very low levels detectable in the nucleus in the ring zone of the virogenic stroma (Braunagel et al., 1999; Rosas-Acosta et al., 2001). Analysis of the merged images show that FP25 co-localized with EXON0 in the cytoplasm as demonstrated by the yellow fluorescence (Fig. 2.6A). At 24 hpi BV/ODV-C42 was detected either in the virogenic stroma or at the ring zone of virogenic stroma, while at 48 hpi it principally localized at the edge of virogenic stroma in agreement with what has been previously reported (Fig. 2.6B) (Braunagel et al., 2001). EXON0 showed a strong co-localization with BV/ODV-C42 mainly at the edge of the virogenic stroma (yellow fluorescence) in the ring zone.

2.3.6 Cellular localization of nucleocapsids in Sf9 cells transfected with exon0 KO and the repaired virus

The last essential steps in the AcMNPV BV life cycle are the assembly of nucleocapsids and egress from the nucleus followed by transport through the cytoplasm and budding from the plasma membrane where it gains its envelope. In order to determine whether the deletion of EXON0 interferes with the assembly and egress of nucleocapsids, Sf9 cells were transfected with either *exon0* KO or *exon0* KO-HA-EXON0 and examined by TEM at 24, 36, 48 and 96 hpt. The TEM analysis showed that the nuclei of cells

transfected with either *exon0* KO or *exon0* KO-HA-EXON0 exhibited the typical baculovirus infection symptoms, namely an extensive number of nucleocapsids, enlarged nuclei and a reorganized electron-dense virogenic stroma (Fig. 2.7). No physical difference was observed between the nucleocapsids of *exon0*-KO and *exon0*-KO-HA-EXON0 indicating that EXON0 is not required for the assembly of nucleocapsids.

In most cells transfected with the *exon0* KO virus nucleocapsids were found in the nucleus, but very few of which were found to be closely associated with or passing through the nuclear membrane. In addition very few were observed in the cytoplasm or budding at the cytoplasmic membrane. In contrast, cells transfected with *exon0* KO-HA-EXON0 virus showed many nucleocapsids penetrating the nuclear membrane, in the cytoplasm and budding at the cytoplasmic membrane. To quantify this observation twenty Sf9 cells transfected with either *exon0* KO or *exon0* KO-HA-EXON0 were randomly chosen and the total number of nucleocapsids in the nucleus, in the process of egress from the nucleus, in the cytoplasm or budding from the cytoplasmic membrane were counted and summarized in Table 2.2. This analysis showed that of the 20 Sf9 cells transfected with *exon0* KO-HA-EXON0 a total of 2868 were found in the nucleus and 390 nucleocapsids were found in the BV pathway (inner nuclear membrane, cytoplasm, and cytoplasmic membrane). In contrast, the 20 Sf9 cells transfected with *exon0* KO virus presented a total of 2957 nucleocapsids in the nucleus and only 25 nucleocapsids in the process of budding. The similar numbers of nucleocapsids found in the nuclei of Sf9 cells transfected with either *exon0* KO and *exon0* KO-HA-EXON0 would indicate that *exon0* does not impact on the production or assembly of nucleocapsids. For *exon0* KO the lower numbers of nucleocapsids are observed at all steps in the budding process suggesting that EXON0 is required for the efficient egress of nucleocapsids from the nucleus.

2.4 Discussion

AcMNPV EXON0 (ORF141) is required for the efficient production of BV but its role in the BV pathway was unknown. In this study, EXON0 was shown to be a structural protein of both BV and ODV. Western blot analysis indicated that it was localized in the nucleocapsid fraction of BVs (Fig. 2.4) and was the expected size (30kDa) but is a minor component of nucleocapsids when compared to VP39 from the coomassie stain of purified virions (Appendix Fig.1). Therefore EXON0 is the ninth nucleocapsid protein identified along with P78/83 (Russell et al., 1997), VP1054 (Olszewski and Miller, 1997a), FP25 (Braunagel et al., 1999), VLF-1 (Yang and Miller, 1998b), VP39 (Thiem and Miller, 1989), BV/ODV-C42 (Braunagel et al., 2001), P87 (Lu and Carstens, 1992) and P24 (Wolgamot et al., 1993) which have been found to associate with both AcMNPV BV and ODV. Braunagel *et al* (2003) performed a very detailed proteomic analysis of ODV structural proteins but surprisingly did not identify EXON0. However, they did isolate a protein of the same size as EXON0 from ODV but they were unable to identify this protein by the methods they used.

EXON0 was shown to interact with the nucleocapsid proteins FP25 and BV/ODV C42 by yeast 2-hybrid and co-immunoprecipitation (Table 2.1 and Fig. 2.5). It was also shown to co-localize with FP25 in the cytoplasm and with BV/ODV-C42 in the nucleus (Fig. 2.6). Previous reports have shown that an FP25 mutant produced fewer occlusion bodies and fewer virions per occlusion body (Fraser and Hink, 1982; MacKinnon et al., 1974b; Potter et al., 1976; Ramoska and Hink, 1974), but released more BV into the media (Fraser and Hink, 1982; Harrison and Summers, 1995; Potter et al., 1976). The association identified between FP25 with EXON0 in this study indicates that these two proteins may be jointly involved in regulating the nucleocapsid ratio between BV and ODV, and ultimately BV production. Nevertheless, the significance of these interactions with respect to EXON0 functionality remains to be fully determined.

The nucleocapsid proteins P78/83, VP1054, and VLF-1 have been shown to be required for the nucleocapsid assembly and in their absence there is either no nucleocapsid production or nucleocapsids are malformed (Olszewski and Miller, 1997a; Possee et al., 1991; Vanarsdal et al, 2006). EXON0 as a nucleocapsid protein present in both BV and ODV could potentially affect the efficiency of nucleocapsid assembly. However this does not seem to be the case as the nuclei of cells transfected with *exon0* KO virus produced normal length nucleocapsids with an electron-dense nucleoprotein core as determined by TEM. Sections of cells transfected with *exon0* KO virus at 96 hpt showed that the nucleocapsids were packaged in polyhedra but further studies are being done to determine if there is a quantitative difference in packaging efficiency. Finally, there was no significant difference in the number of nucleocapsids found in the nuclei of Sf9 cells transfected with either *exon0* KO or *exon0* KO-HA-EXON0 viruses. These data suggest that EXON0 is not required for the assembly of nucleocapsids.

Interestingly confocal microscopy shows that EXON0 has distinct cellular localization in both the cytoplasm and the nucleus. The nuclear association of EXON0 is at the ring zone of the virogenic stroma where the nucleocapsid morphogenesis and polyhedra development occurs (Charlton and Volkman, 1991a; Xeros, 1956). This would agree with our results showing that EXON0 is a structural component of virions. It is not yet clear what function EXON0 has in second ring pattern that concentrates towards the cytoplasmic membrane. It is possible that EXON0 has multiple roles during infection and the cytoplasmic ring pattern may facilitate transport or budding of nucleocapsids to the cell surface.

The TEM results provide evidence that EXON0 is required for the efficient egress of nucleocapsids from the nucleus to the cytoplasm. The conservation of EXON0 in all lepidopteran NPVs suggests that it may play a role in facilitating a common transport pathway for nucleocapsid egress for this group of baculoviruses. However, *exon0* is not strictly essential for the production of BV, since a few nucleocapsids in the cells transfected with *exon0* KO do pass through the nuclear membrane in the *exon0* KO-transfected cells, followed by transport through the cytoplasm and bud at the plasma

membrane. Two possible explanations are that the EXON0-facilitated nucleocapsid transport process can be by-passed and/or other viral and cellular proteins can replace EXON0, although extremely inefficiently. Granulovirus (GV) genomes that have been sequenced to date do not contain an *exon0* homolog. Therefore it is interesting to note that the characterized *Cydia pomonella* GV tissue culture system produces very low titers of extracellular virus that are produced at a very different times post infection compared to lepidopteran NPVs (Winstanley and Crook, 1993). Therefore EXON0 may be a relatively recent acquisition by the lepidopteran NPVs for the rapid and high-level production of BV.

How nucleocapsids egress and transport is an important question as it represents an essential step in the viral life cycle. For other large DNA animal viruses it has been shown that egress is a complex procedure that involves many viral and cellular proteins. Previous studies showed that the deletion of herpesvirus UL34 produces virus deficient in plaque formation, and a 100-fold reduction in viral titer, similar to the AcMNPV *exon0* KO phenotype (Roller et al., 2000). UL34 has been shown to recruit the cellular protein kinase C to phosphorylate the lamin and cause local dissolution of nuclear lamin for the access of capsids to the nuclear membrane (Muranyi et al., 2002b; Sanchez and Spector, 2002; Scott and O'Hare, 2001). The UL34 and UL31 gene products have been shown to be constituents of primary enveloped virions but not mature virus particles and the absence of either protein causes the accumulation of capsids in the nucleus (Fuchs et al., 2002c). Both UL34 and UL31are required for the formation of the herpesvirus primary envelope acquired by budding through the inner nuclear membrane (Klupp et al., 2000; Reynolds et al., 2001). Nuclear egress is also affected by the US3 kinase which appears to trigger the de-envelopment of primary enveloped capsids in the perinuclear region by fusion with the outer nuclear membrane (Klupp et al., 2001; Reynolds et al., 2002). Once herpes capsids have egressed from the nucleus further movement may involve the endoplasmic reticulum and Golgi secretory pathways and interactions with microtubules. (Diefenbach et al., 2002b; Mabit et al., 2002; Martin et al., 2002b; Mettenleiter, 2002a; Miranda-Saksena et al., 2000a; Sodeik et al, 1997; Ye et al., 2000). Similarly EXON0 as a component of nucleocapsids required for the efficient egress of nucleocapsids from the

nucleus may be interacting with cellular proteins to facilitate transport similar to herpesvirus capsids. In addition, EXON0 is expressed in specific ring patterns in both the cytoplasm and the nucleus suggesting that it may have multiple functions in the BV pathway. The elucidation of additional proteins that interact with EXON0 is currently under way and will help to shed light on how BV nucleocapsids are transported during egress.

Figure 2.1 Construction of the bMON 14272 exon0 KO bacmid and viral growth curves.

(A) Schematic of *exon0* locus of WT AcMNPV and bMON 14272 *exon0* KO showing the relative locations and orientations of *me53, exon0*, and *orf142*. The linear PCR fragment (middle) consisting of EM7 promoter, zeocin resistant gene, SV40 polyA and a *gp64* late promoter L2 (Garrity et al., 1997) was amplified with a 70-mer primer (665) and 90-mer primer (666). Primer 665 contains a 50-nt region of homology (H1) complementary to the intergenic region upstream to *ie0* early promoter and primer 666 contains a 43-nt region of homology (H2) complementary to the immediate downstream region of *exon0* ORF. A 16-nt *gp64* late promoter (L2) was combined in primer 666 to replace the *orf142* promoter. In bMON 14272 *exon0* KO bacmid, the complete *exon0* ORF and the *exon0* and *ie0* promoters were replaced by the *zeocin* cassette. The bMON 14272 *exon0* KO bacmid was repaired at the polyhedrin locus with *polyhedrin* (*exon0* KO) or with *polyhedrin* and HA tagged *exon0* (*exon0* KO-HA-EXON0) as described in the Materials and Methods. (B) The deletion of *exon0* was confirmed by PCR analysis. The primers used to confirm the deletion of the *exon0* ORF and the correct insertion of the *zeocin* resistance gene cassette were shown in (A) and indicated by arrows. The presence of 1.85 kb from primers 183/520 and absence of 0.25 kb from primers 626/630 proved the right insertion of zeocin and loss of *exon0* in bMON 14272 *exon0* KO. M, 1 kb plus DNA ladder; Lane 1, negative control; Lane 2, AcMNPV-WT; Lane 3, bMON 14272 *exon0* KO. (C) Growth curves of *exon0* KO and *exon0* KO-HA-EXON0, and *ie1* KO-IE1. Sf9 cells were transfected with these bacmids; the virus supernatants were harvested at various time points post-transfection and were analyzed by end point dilution assay. Data points represent the average on two independent titrations. BV production of *exon0* KO was reduced to 0.01% from the WT virus and repaired virus.

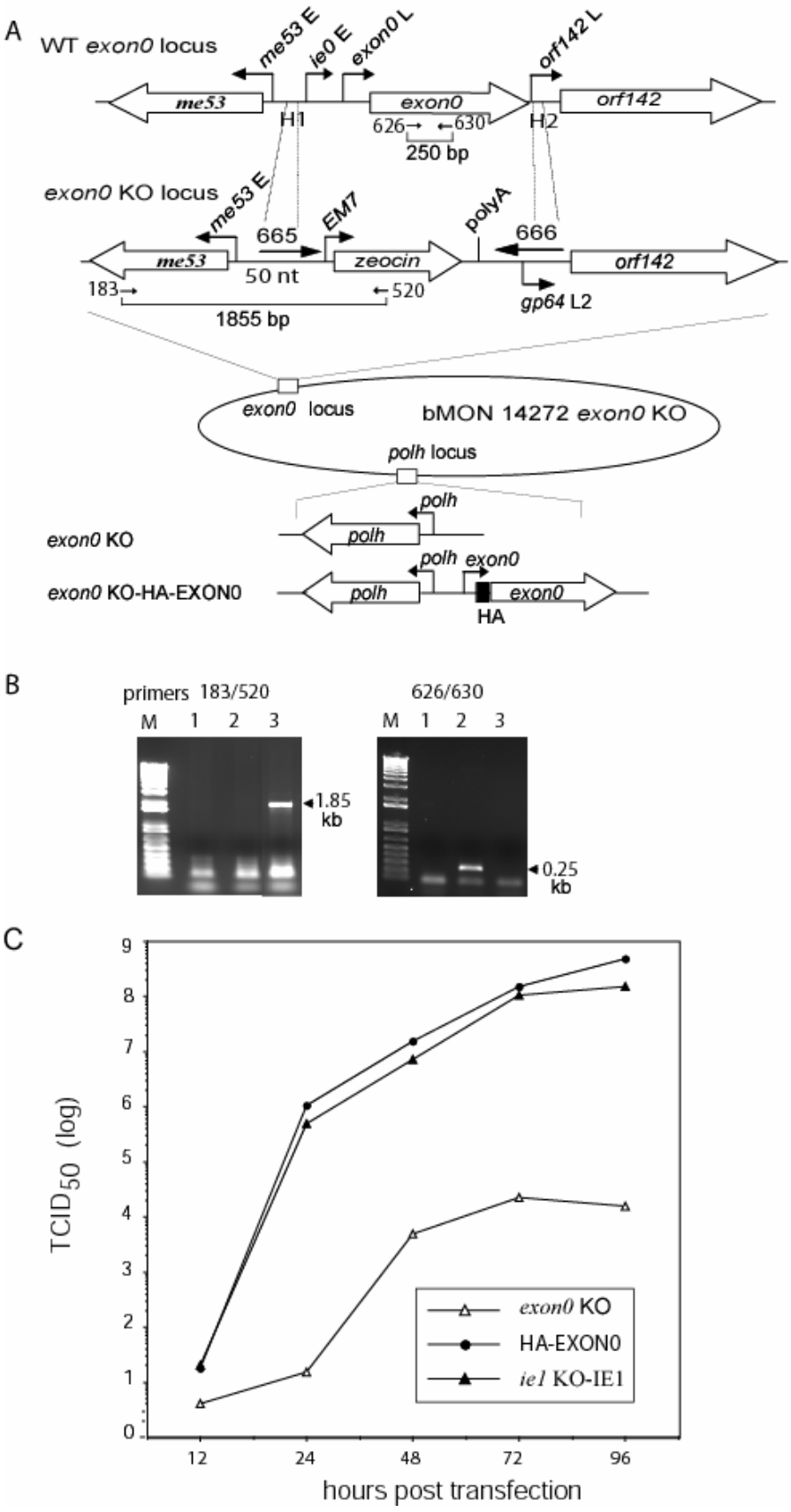
A
WT exon0 locus
me53 E
ie0 E
exon0 L
orf142 L
me53
exon0
orf142
H1
H2
626
630
250 bp
exon0 KO locus
me53 E
665
EM7
polyA
666
me53
50 nt
zeocin
orf142
183
520
gp64 L2
1855 bp
exon0 locus
bMON 14272 exon0 KO
polh locus
polh
exon0 KO
polh
polh exon0
exon0 KO-HA-EXON0
polh
exon0
HA
B
primers 183/520
626/630
M 1 2 3
M 1 2 3
1.85 kb
0.25 kb
C
TCID50 (log)
hours post transfection
exon0 KO
HA-EXON0
ie1 KO-IE1

Figure 2.2 Cellular localization of EXON0 determined by the fractionation of the cytoplasm and nucleus and Western blot.

Sf9 cells were infected with *exon0* KO-HA-EXON0 virus at an MOI of 10. Cells were harvested and separated into the nuclear and cytoplasmic fractions.
Fractions were separated by SDS-PAGE and probed with anti-HA, -IE1 and -GP64 monoclonal antibodies to detect HA tagged EXON0, IE1 and GP64 respectively.

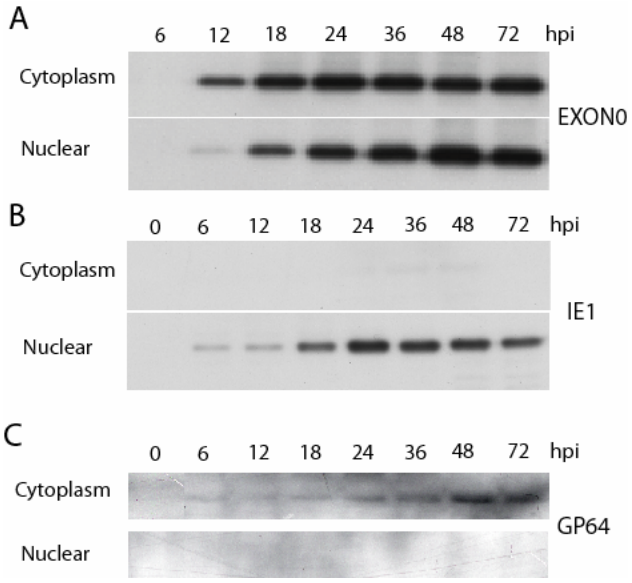

Figure 2.3 Localization of EXON0 by immunofluorescence.

Sf9 cells were infected with *exon0* KO-HA-EXON0 virus at a MOI of 10. At different times post infection, cells were fixed, probed with mouse monoclonal HA antibody to detect HA-tagged EXON0, and visualized by Alexa 635 conjugated goat anti-mouse IgG (red). Additionally, cells were stained with DAPI to directly visualize nuclear DNA (blue). The healthy Sf9 cells probed with the Alexa 635 produced very low background fluorescence, whereas the HA-EXON0 was detected from the cytoplasm and nuclei of *exon0* KO-HA-EXON0 infected cells from 12 hpi. Bars, 10 μm.

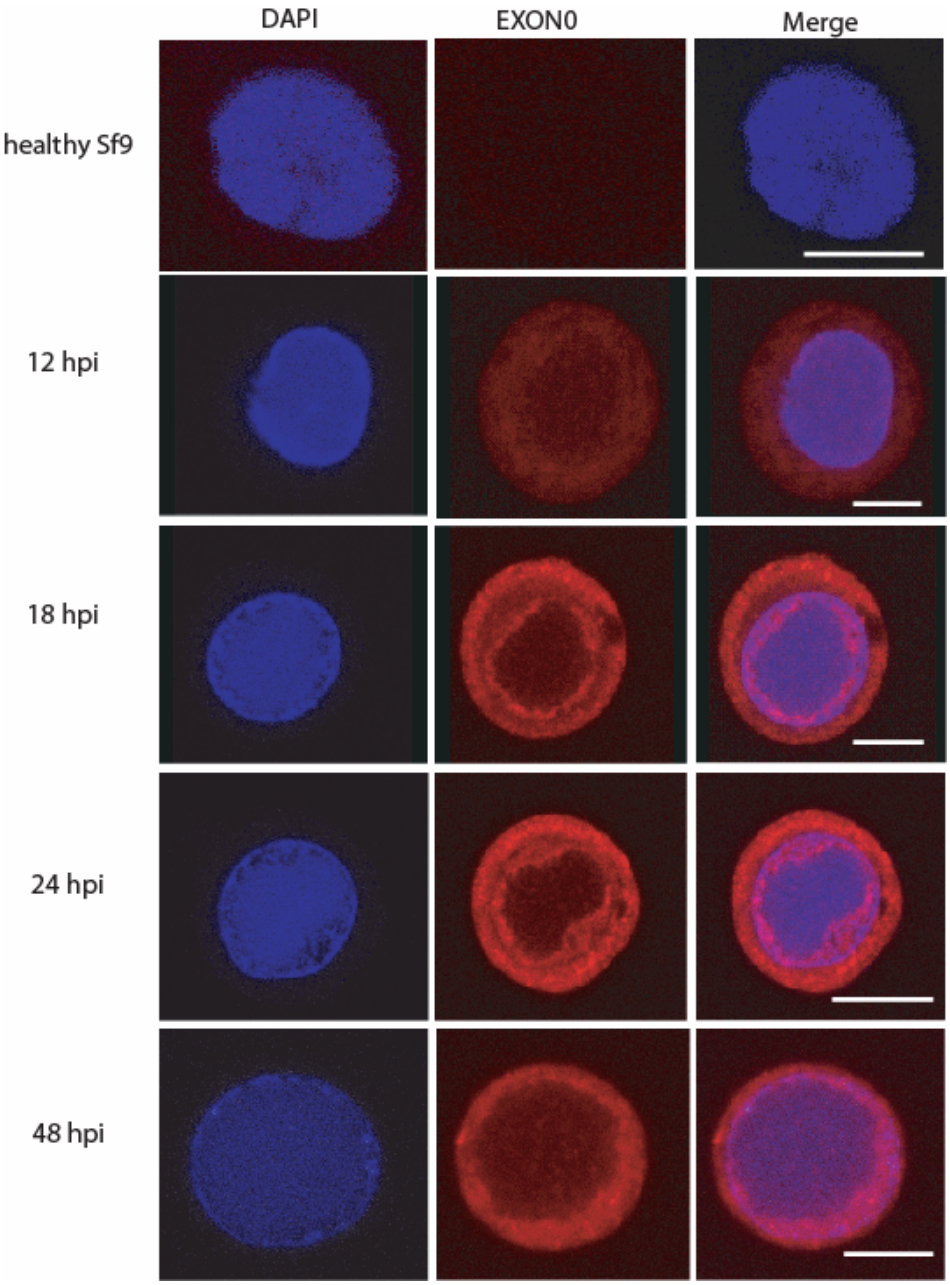
DAPI
EXON0
Merge
healthy Sf9
12 hpi
18 hpi
24 hpi
48 hpi

Figure 2.4 Analysis of EXON0 in purified and fractionated virions.
BV and ODV were purified by sucrose gradient and analyzed by SDS-PAGE and Western blot. Duplicate blots were probed with an anti-HA antibody to detect HA-tagged EXON0, MAb AcV5 to detect the BV envelope protein GP64 and anti-VP39 to detect the nucleocapsid protein VP39.

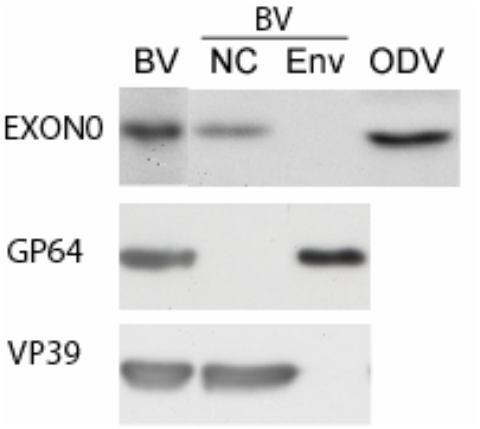

Figure 2.5 Confirmation of protein interactions of EXON0 with FP25 and BV/ODV-C42.

Protein interactions of EXON0 with FP25 and BV/ODV-C42 were confirmed by co-IP. Sf9 cells (2×10^8) were infected with either WT AcMNPV E2 or *exon0* KO-HA-EXON0 virus at an MOI of 10 and harvested at 24 hpi and lysed for co-IP. Samples were immunoprecipitated with anti-HA antibody. The cell lysate (0.025% IP input, approximately 5×10^5) and the immunoprecipitate (10% IP eluate) were separated by SDS-PAGE and duplicate blots were probed with antibodies against FP25, BV/ODV-C42, GP64, VP39 and polyhedrin (POLH).

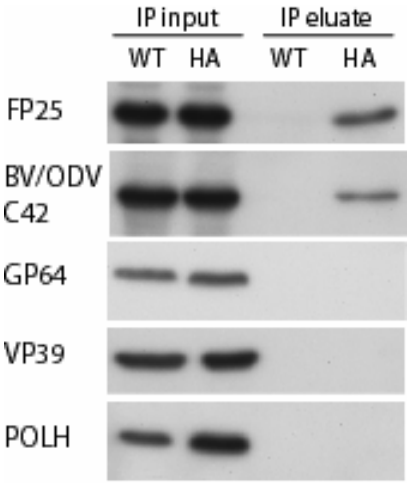

Figure 2.6 Co-localization of EXON0 with FP25 and BV/ODV-C42.
Sf9 cells were infected with *exon0* KO-HA-EXON0 virus. Cells were fixed at 24 hpi, probed with mouse MAb anti-HA (A and B) followed by anti-FP25 rabbit polyclonal antibody (A), or anti-BV/ODV-C42 rabbit polyclonal antibody (B). EXON0 displayed in red was visualized by Alexa 635 conjugated goat anti-mouse IgG. FP25 and BV/ODV-C42 displayed in green were visualized with Alexa 488 conjugated goat anti-rabbit IgG. Cells were also stained with DAPI to visualize the nucleus. In the merged micrographs yellow color indicates co-localization. The bottom panels in A and B are enlargements of the region highlighted by the square box in the upper panels. The white triangle in A points to location of small amounts of nuclear FP25 localized to the ring zone (RZ) of the virogenic stroma (VS) where nucleocapsid assembly occurs. (B) EXON0 and BV/ODV-C42 colocalized predominately in the nuclear ring zone of the virogenic stroma. Bars, 10 μm.

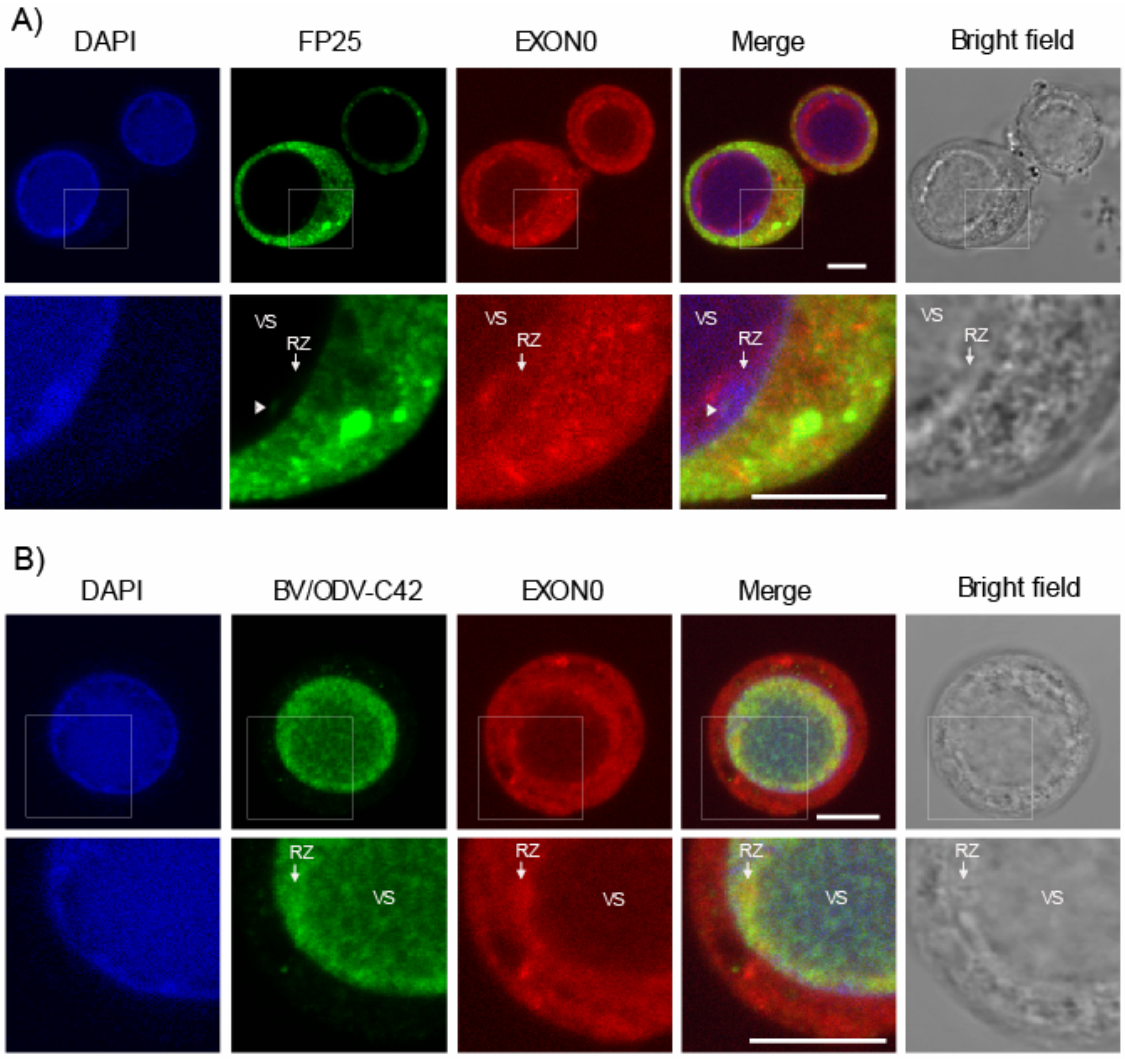
A)
DAPI
FP25
EXON0
Merge
Bright field
VS
RZ
B)
DAPI
BV/ODV-C42
EXON0
Merge
Bright field
RZ
VS

Figure 2.7 Localization of nucleocapsids by TEM in Sf9 cells.

Sf9 cells were transfected with either *exon0* KO-HA-EXON0 (A, B, F) or *exon0* KO (C, D, E) at 24 hpt (A, B, C, D) or 36 hpt (E, F). B and D are higher magnification of the rectangles in A and C respectively. Labels and arrows indicate the virogenic stroma (VS), nucleocapsids (NC), and the nucleus (Nuc). Nucleocapsids in the process of egressing that were passing through the nuclear membrane (NM), in the cytoplasm (Cyto) or budding at cytoplasmic membrane are indicated with triangles.

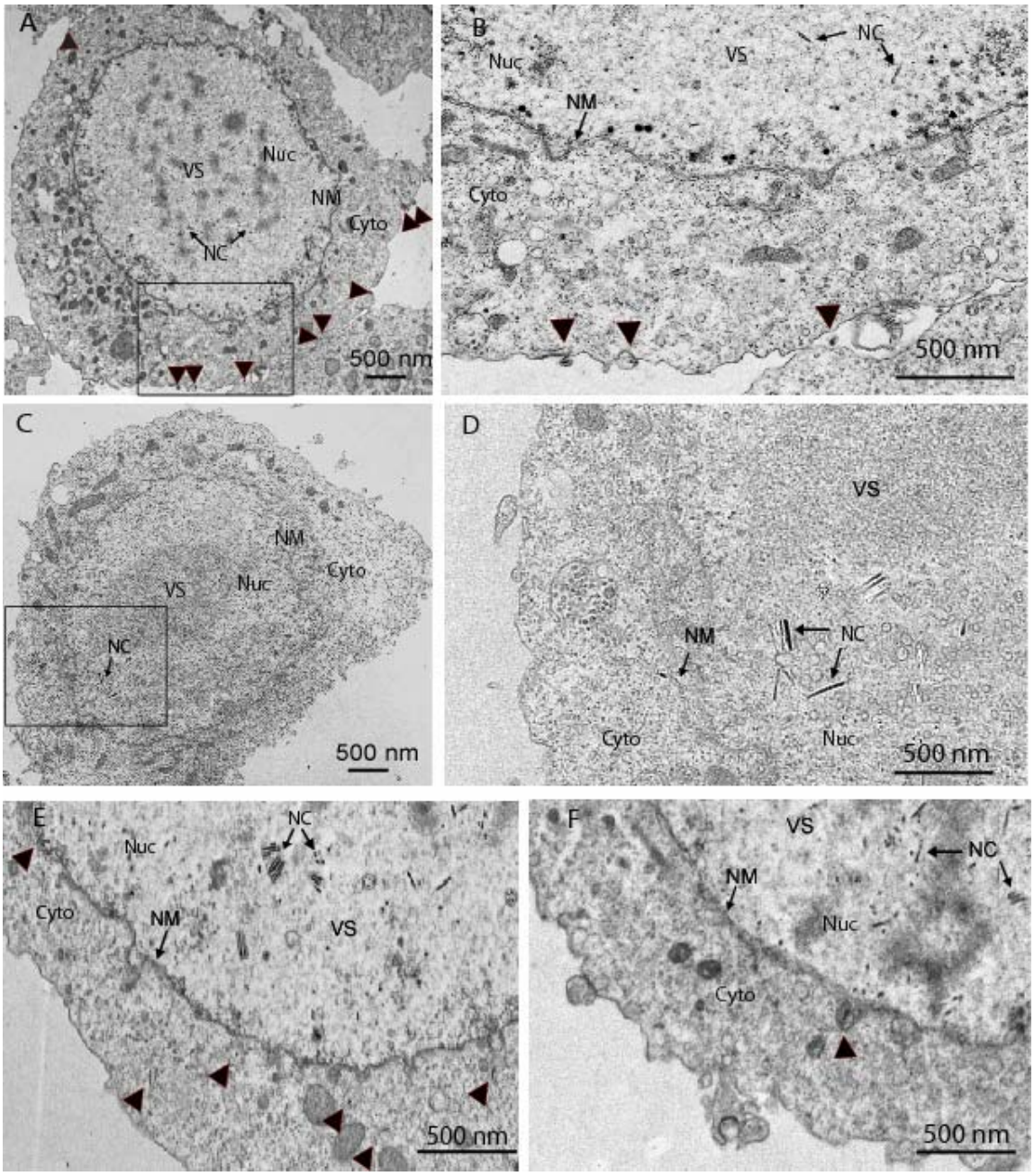
A
VS
Nuc
NM
Cyto
NC
500 nm
B
Nuc
VS
NC
NM
Cyto
500 nm
C
NM
Cyto
VS
Nuc
NC
500 nm
D
VS
NM
NC
Cyto
Nuc
500 nm
E
NC
Nuc
Cyto
NM
VS
500 nm
F
VS
NC
NM
Nuc
Cyto
500 nm

Table 2.1 Yeast 2-hybrid screening of the nucleocapsid proteins which interact with EXON0

Construct	(His-, Trp-) [a]	pAD-Gal4-EXON0[b] (His-, Trp-, Leu-)
pBD-Gal4	-[c]	-
pBD-Gal4-P78/83	-	+
pBD-Gal4-VP1054	-	-
pBD-Gal4-FP25	-	++
pBD-Gal4-VLF1	-	+
pBD-Gal4-VP39	-	+
pBD-Gal4-C42	-	++
pBD-Gal4-P87	-	+
pBD-Gal4-P24	-	+
pBD-Gal4-ME53	-	+

[a] Binding domain vector and its fusion constructs were transformed into yeast and selected on histidine and tryptophan dropout plates.

[b] Binding domain vector and its fusion constructs were co-transformed with pAD-Gal4-EXON0 into yeast and selected on histidine, tryptophan and leucine dropout plates.

[c] Growth of colonies on double (His-, Trp-) or triple (His-, Trp- and Leu-) dropout plates: -, no growth; +, weak growth; ++, medium growth.

Table 2.2 Summary of numbers of the nucleocapsids in the nucleus and in the process of budding from 20 Sf9 cells which were transfected with *exon0* KO or the *exon0* KO-HA-EXON0

Location	*exon0* KO	Total budding [b]	*exon0* repair	Total budding [b]
Nucleus	2957		2868	
Nuclear membrane	4		35	
Cytoplasm	19		193	
Cytoplasmic membrane	2		162	
		25		390

[a] The numbers of cells transfected by *exon0* KO or the *exon0* KO-HA-EXON0 are equal at each time point from 24, 36, 48 and 96 hpt.

[b] Total budding refers to the nucleocapsids in the process of budding including those associated with or penetrating the nuclear membrane, in the cytoplasm or budding from the cytoplasmic membrane.

2.5 References

Blissard, G. W., and Wenz, J. R. (1992). Baculovirus GP64 envelope glycoprotein is sufficient to mediate pH-dependent membrane fusion. *J. Virol.* **66**(11)**,** 6829-6835.

Bradford, M. M. (1976). A rapid and sensitive method for the quantitation of microgram quantities of protein utilizing the principle of protein-dye binding. *Anal. Biochem.* **72,** 248-254.

Braunagel, S. C., Burks, J. K., Rosas-Acosta, G., Harrison, R. L., Ma, H., and Summers, M. D. (1999). Mutations within the *Autographa californica* nucleopolyhedrovirus FP25K gene decrease the accumulation of ODV-E66 and alter its intranuclear transport. *J. Virol.* **73**(10)**,** 8559-8570.

Braunagel, S. C., Guidry, P. A., Rosas-Acosta, G., Engelking, L., and Summers, M. D. (2001). Identification of BV/ODV-C42, an *Autographa californica* nucleopolyhedrovirus *orf101*-encoded structural protein detected in infected-cell complexes with ODV-EC27 and p78/83. *J. Virol.* **75**(24)**,** 12331-12338.

Braunagel, S. C., Russell, W. K., Rosas-Acosta, G., Russell, D. H., and Summers, M. D. (2003). Determination of the protein composition of the occlusion-derived virus of *Autographa californica* nucleopolyhedrovirus. *Proc. Natl. Acad. Sci. U. S. A.* **100**(17)**,** 9797-9802.

Braunagel, S. C., and Summers, M. D. (1994). *Autographa californica* nuclear polyhedrosis virus, PDV, and ECV viral envelopes and nucleocapsids: structural proteins, antigens, lipid and fatty acid profiles. *Virology* **202**(1)**,** 315-328.

Charlton, C. A., and Volkman, L. E. (1991). Sequential rearrangement and nuclear polymerization of actin in baculovirus-infected *Spodoptera frugiperda* cells. *J. Virol.* **65,** 1219-1227.

Dai, X., Stewart, T. M., Pathakamuri, J. A., Li, Q., and Theilmann, D. A. (2004). *Autographa californica* multiple nucleopolyhedrovirus *exon0* (*orf141*), which

encodes a RING finger protein, is required for efficient production of budded virus. *J. Virol.* **78**(18)**,** 9633-9644.

Diefenbach, R. J., Miranda-Saksena, M., Diefenbach, E., Holland, D. J., Boadle, R. A., Armati, P. J., and Cunningham, A. L. (2002). Herpes simplex virus tegument protein US11 interacts with conventional kinesin heavy chain. .*J. Virol.* **76,** 3282-3291.

Fraser, M. J. (1986). Ultrastructural observations of virion maturation in *Autographa californica* nuclear polyhedrosis virus infected *Spodoptera frugiperda* cell cultures. *J. Ultrastruct. Mol. Struct. Res.* **95,** 189–195.

Fraser, M. J., and Hink, W. F. (1982). The isolation and characterization of the MP and FP plaque variants of *Galleria mellonella* nuclear polyhedrosis virus. *Virology* **117,** 366–378.

Fuchs, W., Klupp, B. G., Granzow, H., Osterrieder, N., and Mettenleiter, T. C. (2002). The interacting UL31 and UL34 gene products of pseudorabies virus are involved in egress from the host-cell nucleus and represent components of primary enveloped but not of mature virions. *J. Virol.***76,** 364-378.

Funk, C. J., Braunagel, S. C., and Rohrmann, G. F. (1997). Baculovirus structure. *In* "The Baculoviruses" (L. K. Miller, Ed.), pp. 7-32. Plenum, New York.

Garrity, D. B., Chang, M., and Blissard, G. W. (1997). Late Promoter Selection in the Baculovirus *gp64 Envelope Fusion Protein* Gene. *Virology* **231,** 167-181.

Harrison, R. L., and Summers, M. D. (1995). Mutations in the *Autographa californica* multinucleocapsid nuclear polyhedrosis virus 25 kDa protein gene result in reduced virion occlusion, altered intranuclear envelopment and enhanced virus production. *J. Gen. Virol.* **76,** 1451–1459.

Hefferon, K. L., Oomens, A. G., Monsma, S. A., Finnerty, C. M., and Blissard, G. W. (1999). Host cell receptor binding by baculovirus GP64 and kinetics of virion entry. *Virology* **258,** 455-468.

Hou, S., Chen, X., Wang, H., Tao, M., and Hu, Z. (2002). Efficient method to generate homologous recombinant baculovirus genomes in *E. coli*. *Biotechniques* **32**(4)**,** 783-784, 786, 788.

Kingsley, D. H., Behbahani, A., Rashtian, A., Blissard, G. W., and Zimmerberg, J. (1999). A discrete stage of baculovirus GP64-mediated membrane fusion. *Mol. Biol. Cell* **10**(12)**,** 4191-200.

Klupp, B. G., Granzow, H., and Mettenleiter, T. C. (2000). Primary envelopment of pseudorabies virus at the nuclear membrane requires the UL34 gene product. *J. Virol.* **74**(21)**,** 10063-10073.

Klupp, B. G., Granzow, H., and Mettenleiter, T. C. (2001). Effect of the pseudorabies virus US3 protein on nuclear membrane localization of the UL34 protein and virus egress from the nucleus. *J. Gen. Virol.* **82**(Pt 10)**,** 2363-2371.

Leikina, E., Onaran, H. O., and Zimmerberg, J. (1992). Acidic pH induces fusion of cells infected with baculovirus to form syncytia. *FEBS Lett.* **304**(2-3)**,** 221-224.

Lin, G., and Blissard, G. W. (2002). Analysis of an *Autographa californica* multicapsid nucleopolyhedrovirus *lef-6*-null virus: LEF-6 is not essential for viral replication but appears to accelerate late gene transcription. *J. Virol.* **76**(11)**,** 5503-5514.

Long, G., Pan, X., Kormelink, R., and Vlak, J. M. (2006). Functional entry of baculovirus into insect and mammalian cells is dependent on clathrin-mediated endocytosis. *J. Virol.* **80**(17)**,** 8830-8803.

Lu, A., and Carstens, E. B. (1992). Nucleotide sequence and transcriptional analysis of the *p80* gene of *Autographa californica* nuclear polyhedrosis virus: a homologue of the *Orgyia pseudotsugata* nuclear polyhedrosis virus capsid-associated gene. *Virology* **190,** 201-209.

Lu, L., Rivkin, H., and Chejanovsky, N. (2005). The immediate-early protein IE0 of the *Autographa californica* nucleopolyhedrovirus is not essential for viral replication. *J. Virol.* **79**(15)**,** 10077-10082.

Luckow, V. A., Lee, S. C., Barry, G. F., and Olins, P. O. (1993). Efficient generation of infectious recombinant baculoviruses by site-specific transposon-mediated insertion of foreign genes into a baculovirus genome propagated in *Escherichia coli*. *J. Virol.* **67**(8)**,** 4566-4579.

Lung, O. Y., Cruz-Alvarez, M., and Blissard, G. W. (2003). Ac23, an envelope fusion protein homolog in the baculovirus *Autographa californica* multicapsid nucleopolyhedrovirus, is a viral pathogenicity factor. *J. Virol.* **77,** 328-339.

Mabit, H., Nakano, M. Y., Prank, U., Saam, B., Dohner, K., Sodeik, B., and Greber, U. F. (2002). Intact microtubules support adenovirus and herpes simplex virus infections. *J. Virol.***76,** 9962-9971.

MacKinnon, E. A., Henderson, J. F., Stoltz, D. B., and Faulkner, P. (1974). Morphogenesis of nuclear polyhedrosis virus under conditions of prolonged passage *in vitro*. *J. Ultrastruct. Res.* **49,** 419–435.

Martin, A., O'Hare, P., McLauchlan, J., and Elliott, G. (2002). Herpes simplex virus tegument protein VP22 contains overlapping domains for cytoplasmic localization, microtubule interaction, and chromatin binding. *J. Virol.* **76,** 4961–4970.

Mettenleiter, T. C. (2002). Herpesvirus assembly and egress. *J Virol* **76**(4)**,** 1537-47.

Miranda-Saksena, M., Armati, P., Boadle, R. A., Holland, D. J., and Cunningham, A. L. (2000). Anterograde transport of herpes simplex virus type 1 in cultured, dissociated human and rat dorsal root ganglion neurons. *J. Virol.* **74,** 1827-1839.

Monsma, S. A., Oomens, A. G., and Blissard, G. W. (1996). The GP64 envelope fusion protein is an essential baculovirus protein required for cell-to-cell transmission of infection. *J. Virol.* **70,** 4607-4616.

Muranyi, W., Haas, J., Wagner, M., Krohne, G., and Koszinowski, U. H. (2002). Cytomegalovirus recruitment of cellular kinases to dissolve the nuclear lamina. *Science* **297,** 854–857.

Okano, K., Vanarsdall, A. L., Mikhailov, V. S., and Rohrmann, G. F. (2006). Conserved molecular systems of the Baculoviridae. *Virology* **344**(1)**,** 77-87.

Olszewski, J., and Miller, L. K. (1997a). Identification and characterization of a baculovirus structural protein, VP1054, required for nucleocapsid formation. *J. Virol.* **71**(7)**,** 5040-5050.

Olszewski, J., and Miller, L. K. (1997b). A role for baculovirus GP41 in budded virus production. *Virology* **233**(2)**,** 292-301.

Oomens, A. G. P., and Blissard, G. W. (1999). Requirement for GP64 to Drive Efficient Budding of *Autographa californica* Multicapsid Nucleopolyhedrovirus. *Virology* **254,** 297-314.

Possee, R. D., Sun, T. P., Howard, S. C., Ayres, M. D., Hill-Perkins, M., and Gearing, K. L. (1991). Nucleotide sequence of the *Autographa californica* nuclear polyhedrosis 9.4 kbp *Eco*RI-I and -R (*polyhedrin* gene) region. *Virology* **185**(1)**,** 229-241.

Potter, K. N., Faulkner, P., and MacKinnon, E. A. (1976). Strain selection during serial passage of *Trichoplusia ni* nuclear polyhedrosis virus. *J. Virol.* **18,** 1040–1050.

Ramoska, W. A., and Hink, W. F. (1974). Electron microscope examination of two plaque variants from a nuclear polyhedrosis virus of the alfalfa looper, *Autographa californica*. *J. Invert. Pathol.* **23,** 197–201.

Reynolds, A., Ryckman, B., Baines, J., Zhou, Y., Liang, L., and Roller, R. (2001). UL31 and UL34 proteins of herpes simplex virus type 1 form a complex that accumulates at the nuclear rim and is required for envelopment of nucleocapsids. *J. Virol.* **75,** 8803-8817.

Reynolds, A., Wills, E. G., Roller, R., Ryckman, B. J., and Baines, J. D. (2002). Ultrastructural localization of the herpes simplex virus type 1 UL31, UL34, and US3 proteins suggests specific roles in primary envelopment and egress of nucleocapsids. *J. Virol.* **76,** 8939–8952.

Roller, R., Zhou, Y., Schnetzer, R., Ferguson, J., and DeSalvo, D. (2000). Herpes simplex virus type 1 UL34 gene product is required for viral envelopment. *J. Virol.* **74,** 117–129.

Rosas-Acosta, G., Braunagel, S. C., and Summers, M. D. (2001). Effects of deletion and overexpression of the *Autographa californica* nuclear polyhedrosis virus FP25K gene on synthesis of two occlusion-derived virus envelope proteins and their transport into virus-induced intranuclear membranes. *J. Virol.* **75**(22)**,** 10829-10842.

Russell, R. L., Funk, C. J., and Rohrmann, G. F. (1997). Association of a baculovirus-encoded protein with the capsid basal region. *Virology* **227**(1)**,** 142-152.

Sanchez, V., and Spector, D. H. (2002). CMV makes a timely exit. *Science* **297,** 778–779.

Scott, E., and O'Hare, P. (2001). Fate of the inner nuclear membrane protein lamin B receptor and nuclear lamins in herpes simplex virus type 1 infection. *J. Virol.* **75,** 8818–8830.

Sodeik, B., Ebersold, M. W., and Helenius, A. (1997). Microtubule-mediated transport of incoming herpes simplex virus 1 capsids to the nucleus. *J. Cell Biol.* **136,** 1007-1021.

Stewart, T. M., Huijskens, I., Willis, L. G., and Theilmann, D. A. (2005). The *Autographa californica* multiple nucleopolyhedrovirus *ie0-ie1* gene complex is essential for wild-type virus replication, but either IE0 or IE1 can support virus growth. *J. Virol.* **79**(8)**,** 4619-4629.

Takagi, I., Yamada, K., Sato, T., Hanaichi, T., Iwamoto, T., and Jin, L. (1990). Penetration and stainability of modified Sato's lead staining solution. *J. Electron Microscopy* **39,** 67-68.

Theilmann, D. A., Blissard, G. W., Bonning, B., Jehle, J. A., O'Reilly, D. R., Rohrmann, G. F., Thiem, S., and Vlak, J. M. (2005). Baculoviridae. *In* "Virus Taxonomy - Eighth Report of the International Committee on Taxonomy of Viruses" (M. M. A. Fauquet C.M., Maniloff J., Desselberger U., and B. L.A. (ed.), Ed.), pp. 177-185. Springer, New York.

Thiem, S. M., and Miller, L. K. (1989). Identification, sequence, and transcriptional mapping of the major capsid protein gene of the baculovirus *Autographa californica* nuclear polyhedrosis virus. *J. Virol.* **63,** 2008-2018.

Vanarsdall, A. L., Okano, K., and Rohrmann, G. F. (2006). Characterization of the role of very late expression factor 1 in baculovirus capsid structure and DNA processing. *J. Virol.* **80**(4)**,** 1724-1733.

Volkman, L. E., and Goldsmith, P. A. (1985). Mechanism of neutralization of budded *Autographa californica* nuclear polyhedrosis virus by a monoclonal antibody: inhibition of entry by adsorptive endocytosis. *Virology* **143,** 143-185.

Winstanley, D., and Crook, N. E. (1993). Replication of *Cydia pomonella* granulosis virus in cell cultures. *J. Gen. Virol.* **74,** 1599-609.

Wolgamot, G. M., Gross, C. H., Russell, R. L., and Rohrmann, G. F. (1993). Immunocytochemical characterization of P24, a baculovirus capsid-associated protein. *J. Gen. Virol.* **74,** 103-107.

Wu, W., Lin, T., Pan, L., Yu, M., Li, Z., Pang, Y., and Yang, K. (2006). *Autographa californica* multiple nucleopolyhedrovirus nucleocapsid assembly is interrupted upon deletion of the 38K gene. *J. Virol.* **80,** 11475-11485.

Xeros, N. (1956). The virogenic stroma in nuclear and cytoplasmic polyhedrosis. *Nature* **178,** 412-413.

Yang, S., and Miller, L. K. (1998). Expression and mutational analysis of the baculovirus very late factor 1 (*vlf-1*) gene. *Virology* **245,** 99-109.

Ye, G. J., Vaughan, K. T., Vallee, R. B., and Roizman, B. (2000). The herpes simplex virus 1 U(L)34 protein interacts with a cytoplasmic dynein intermediate chain and targets nuclear membrane. *J. Virol.* **74,** 1355-1363.

Chapter 3: Function of *Autographa californica* Multiple Nucleopolyhedrovirus EXON0 involves association with β-Tubulin[2]

3.1 Introduction

The Baculoviridae is a family of rod-shaped viruses with large circular, covalently closed, double-stranded DNA genomes of approximately 80-180 kb. This family is taxonomically subdivided into two genera, *Nucleopolyhedrovirus* (NPV) and *Granulovirus* (GV) based on the morphology of the occlusion body (Theilmann et al., 2005). Baculoviruses typically have a complex morphogenic pathway that produces two distinct forms of infectious virions in infected cells. ODVs transmit the infection from animal to animal, while BVs mediate the cell-to-cell spread of the infection within the animal and in cell culture.

Baculovirus BVs enter insect and mammalian cells *via* adsorptive endocytosis (Hefferon et al., 1999; Volkman and Goldsmith, 1985). The acidification of late endosome activates the fusogenicity of GP64 and results in the fusion of the viral and endosomal membrane (Blissard and Wenz, 1992; Leikina et al, 1992; Long et al., 2006). After the nucleocapsids are released from the endosomes, the incoming nucleocapsids induce the formation of thick transient actin bundles which are suggested to facilitate the transport of nucleocapsids to the nucleus (Charlton and Volkman, 1991b; Charlton and Volkman, 1993; Lanier and Volkman, 1998b). The depolymerization of microtubules enhances the transgene expression of baculovirus in mammalian cells suggesting that microtubules might be obstacles for the movement of nucleocapsids into the nucleus (van Loo et al., 2001). After the entry to the nuclei, viral transcription and DNA replication occur in a cascade-like fashion. At late time post infection, the progeny nucleocapsids are assembled in the virogenic stroma, transported out of the nucleus and bud at the cytoplasmic membrane to become BV. At very late time post infection, the progeny nucleocapsids are retained, enveloped by the intranuclear membrane and finally occluded

[2] A version of this chapter will be submitted for publication. Fang M., Nie Y. and Theilmann D. Function of Autographa Californica Multiple Nucleopolyhedrovirus EXON0 involves association with β-tubulin.

into polyhedra to form ODV. The mechanism by which the nucleocapsids are shuttled so that they are destined to become BV or retained in the nucleus to become ODV is unknown. In particular, how the nucleocapsids are transported from the nucleus to the cell membrane is poorly understood.

Microtubules are key actors in the cytoskeleton of eukaryotic cells. They play an important role in organelle transport, cell shape maintenance, mitosis, motility, and cell division (Jordan and Wilson, 2004b). Microtubules are highly dynamic polymers of heterodimers of α- and β-tubulin, arranged parallel to a cylindrical axis to form tubes of 24 nm diameter that may be many mimimeters long. The association between viruses and host cell cytoskeletal elements was first observed by electron microscopy (Granados, 1978; Luftig and Weihing, 1975). In the last decade, the involvement of microtubules in virus transport has been a new interest and reported for a number of viruses. Microtubules are required for many viruses for their efficient targeting to their replication sites, notably herpes simplex virus (Sodeik et al, 1997), vaccinia virus (Carter et al., 2003), adenovirus (Ad) (Suomalainen et al., 1999), parvoviruses (Seisenberger et al., 2000), simian virus 40 (SV40) (Pelkmans et al, 2001), hepatitis B virus (Funk et al., 2004), human immunodeficiency virus (HIV) (McDonald et al., 2002), influenza virus (Lakadamyali et al., 2003). In addition, quite a few specific viral proteins that interact directly with microtubules or with microtubule motor proteins have been identified. These include the tegument protein VP22 of herpes simplex virus type 1 (Elliott and O'Hare, 1998; Martin et al., 2002a), A36R membrane protein of vaccinia virus (Ward and Moss, 2004), M protein of Sendai virus (Ogino et al., 2003), protein p54 of African swine fever virus (Alonso et al., 2001), spike protein VP4 of rotavirus (Nejmeddine et al., 2000).

AcMNPV, the archetype of the *Baculoviridae,* has a genome of approximately 134 kbp and encodes 154 predicted genes. *Exon0* (*orf141*) is a conserved gene found in all lepidopteran baculoviruses of the genus *Nucleopolyhedrovirus*. The deletion of *exon0* reduces the level of BV production up to 99% and the infection of Sf9 cells with the *exon0* KO virus is restricted to a single cell or a few neighbouring cells. However, viral

replication and polyhedra production are unaffected, suggesting that *exon0* plays a key role specific to BV production pathway (Dai et al., 2004).

As shown in Chapter 2 of this study EXON0 is a structural component of both BV and ODV that localizes to the nucleocapsid fraction. During infection, EXON0 shows a double ring pattern of localization, in the ring zone of infected nucleus where nucleocapsids are assembled and also in the cytoplasm concentrated towards the plasma membrane. Electron micrographs revealed that EXON0 is required for efficient transport of progeny nucleocapsids from the nucleus to the cytoplasm.

To futher dissect how EXON0 plays its critical role in the viral infection cycle the objective of this chapter was to identify additional proteins with which it interacts. Using 3×FLAG-6×His tandem affinity purification and LC-MS/MS we have identified that the cellular β-tubulin associates with EXON0. This interaction was confirmed using co-IP, confocal microscopy and microtubule inhibitor drugs. These results suggest that microtubules play an important role in BV production and their association with EXON0 may facilitate the transport of nucleocapsids from the nucleus to the plasma membrane.

3.2 Materials and Methods

3.2.1 Cells and Viruses

Cells and viruses were maintained as described in Chapter 2.

3.2.2 Construction of 3×FLAG-6×His-tagged EXON0 and repaired virus

To tag EXON0 with 3×FLAG-6×His at the N-terminus for tandem affinity purification, 3×FLAG-6×His tag was amplified with primer 1215 (5'-GCGGAGATCTATGGACTACAAAGACCATGAC -3') and 1216 (5'-GCGGAGATCTGCTGCCGCGCGGCAC -3') from pCaSpeR-hs-act-Tetra tag plasmid (Yang et al, 2006) and *exon0* was amplified using primers 1213 (5'-GCGGAGATCTTACCCCTACGACGTGCCC -3') and 1214 (5'-GCGGAGATCTGTTGCGTTGCCCGTTATC -3') by inverse polymerase chain reaction (PCR) using p2ZeoKS-HA-exon0 (Chapter II) as a template. The two amplified linear fragments were digested by *Bgl*II, gel purified, ligated for 1 hr at room temperature and transformed into DH5α competent cells. Zeocin resistant colonies were picked and identified by restriction digestion and confirmed by sequencing. The resulting plasmid was named p2Zeo-3×FLAG-6×His-HA-exon0. To transiently express EXON0, the *exon0* gene was cut from p2ZeoKS-HA-EXON0 (Chapter 2) by *Bgl*II and *Xba*I and inserted into the *Bam*HI and *Xba*I sites of pHA-N, named pHA-exon0. In this plasmid, *exon0* was under the control of OpMNPV *ie2* promoter (Theilmann and Stewart, 1992). The correct plasmid construction of pHA-exon0 was confirmed by restriction digestion and sequencing.

To introduce *exon0* into bMON 14272 *exon0* KO, the rescue transfer vector was constructed using the plasmid backbone pFAcT (Dai et al., 2004). pFAcT contains two Tn*7* transposition excision sites that allow the genes cloned between the sites to be transposed into the mini ATT region located in the AcMNPV bacmid (Luckow et al., 1993). p2Zeo-3×FLAG-6×His-HA-exon0 was digested with *Xho*I and *Xba*I. The excised fragment, containing the native late promoter of *exon0,* 3×FLAG-6×His-HA-exon0 and an OpMNPV *ie1* poly(A), was cloned into the *Xho*I and *Xba*I sites of pFAcT

to generate pFAcT-3×FLAG-6×His-HA-exon0. In addition to the cloned gene of interest, the pFAcT backbone contains AcMNPV *polyhedrin*, which is included in the transposed DNA cassette. The recombinant AcMNPV bacmids containing the 3×FLAG-6×His-HA-exon0 was generated by Tn*7*-mediated transposition as previously described (Luckow et al., 1993). The repaired virus was named *exon0* KO-3×FLAG-6×His-HA-EXON0. Virus stock was prepared and titered.

3.2.3 3×FLAG-6×His tandem affinity purification and protein identification

Sf9 cells (3 x 10^8) were infected with *exon0* KO-3×FLAG-6×His-HA-EXON0 or control virus *exon0* KO-HA-EXON0 (Chapter 2) with a multiplicity of infectivity (MOI) of 10. The affinity purification was adapted from Yang et al (2006). At 24 hours post infection (hpi) cells were harvested and washed with phosphate buffered saline (PBS, 137 mM NaCl, 10 mM phosphate, 2.7 mM KCl, pH 7.4), centrifuged at 800 x g for 5 min. Cells were resuspended in 2 ml lysis buffer (15 mM HEPES pH 7.6, 10 mM KCl, 0.1 mM EDTA, 0.5 mM EGTA,1 mM DTT, 1% proteinase inhibitor cocktail (Sigma)), passed twice through a French press at 8.27 MPa (1000 psi) at 4 ^oC. The cell lysate was centrifuged at 13,000 *g* for 10 min and the supernatant was transferred to equilibrated anti-FLAG M2 affinity beads and incubated overnight at 4 ^oC on an orbiting platform. The beads were then transferred to Bio-Rad columns, washed once with 1 ml cold lysis buffer and 6 times with 1 ml TBS buffer (50 mM HEPES, pH 7.6, 150 mM NaCl, 0.1% Triton). Protein was eluted from the FLAG affinity beads with 500 µL of 300 µg/mL 3×FLAG peptide (Sigma) in TBS. The FLAG eluate was incubated with 50 µL Talon cobalt resin (BD Biosciences Clontech) for 1 h at 4 ^oC. The resin was washed 4 times with 1 ml TBS and eluted with 300 µL TBS containing 300 mM imidazole. The eluate was vacuum concentrated to 80 µL, mixed with 80 µL 2× protein sample buffer (PSB, 0.25 M Tris-Cl, pH6.8, 4% SDS, 20% glycerol,10% 2-mercaptoethanol, 0.02% bromophenol blue), boiled at 100 ^oC for 5 min, subjected to sodium dodecyl sulfate polyacrylamide gel electrophoresis (SDS-PAGE), silver staining and western blot. Protein bands specific to the 3×FLAG-6×His-HA-EXON0 were cut from the gel, subjected to in-gel digestion and identified by Liquid Chromatography Mass

Spectrometry/Mass Spectrometry (LC-MS/MS) at Proteomics Core Facility of University of British Columbia.

3.2.4 Immunoprecipitation (IP)

Sf9 cells (3×10^8) were infected with either WT AcMNPV E2 or *exon0* KO-HA-EXON0 at a MOI of 10. For microtubule inhibitor treatment, cells were incubated with 10 μM colchicine (Sigma) or 100 μg/ml nocodazole (Sigma) for 4 hrs before infection and throughout the infection. These drugs were also included in the following lysis and washing buffer. At 24 hpi, cells were collected and following steps were as described in Chapter 2.

3.2.5 Immunofluorescence

Sf9 or Tn368 cells were infected with *exon0* KO-HA-EXON0 using a MOI of 10. For the microtubule inhibitor treatment, cells were incubated with 10 μM colchicine (Sigma) or 100 μg/ml nocodazole (Sigma) for 4 hrs before infection and throughout infection. At 24, 36 and 48 hpi, the supernatant was removed and the cells were washed three times in PBS, followed by fixation in ice-cold 100% methanol for 5 min. The fixed cells were washed three times with PBS for 10 min, and were then blocked for 60 min in the blocking buffer (2% bovine serum albumin in PBS). Cells were incubated with rabbit polyclonal anti-HA antibody (1:200) (Abcam) and mouse monoclonal anti-β-tubulin antibody (1:200) (Abcam, TU06), or incubated with rat monoclonal anti-HA antibody (1:500) (Roche) and mouse monoclonal anti-α-tubulin antibody (1:200) (Sigma, T9026). The cells were washed three times for 10 min each time in blocking buffer, followed by 1 hr incubation with Alexa 488-conjugated goat anti-rabbit IgG (1:500) (Molecular Probe) and Alexa 635-conjugated goat anti-mouse antibody (1:500) (Molecular Probe), or with Alexa 488-conjugated goat anti-rat IgG (1:500) (Molecular Probe) and Alexa 635-conjugated goat anti-mouse antibody (1:500) (Molecular Probe). Cells were subsequently washed three times for 10 min each time in PBS, followed by staining with

200 ng/ml DAPI (4', 6'-diamidino-2-phenylindole) (Molecular Probe) and examined using a Leica confocal Microscope.

3.2.6 Western blot analysis

The protein eluates from the 3×FLAG-6×His purification and co-IP were analyzed by Western blots and probed with one of the following primary antibodies: (i) mouse monoclonal HA antibody (Covance, HA11), 1:1,000; (ii) mouse monoclonal β-tubulin antibody (Abcam, TU-06). Following steps as described in Chapter 2.

3.2.7 BV production assay

Sf9 cells (1.0 x 10^6 cells/35mm diameter well of a six-well plate) were infected with *exon0* KO-HA-EXON0 at MOI of 10 at the presence or absence of microtubule polymerization inhibitor 10 μM colchicine or 100 μg nocodazole. BV titers at 48 and 72 hpi were analyzed by end point dilution method as described in Chapter 2.

3.3 Results

3.3.1 Construction of EXON0 fusion protein repaired viruses

EXON0 has been shown to be required for the high level production of BV and for the efficient egress of nucleocapsids from the nucleus to the cytoplasmic membrane (Dai et al., 2004) (Chapter 2). To investigate the molecular basis for these observations and better characterize the function of EXON0, we attempted to identify cellular binding partners for the protein. We therefore used tandem affinity purification (TAP) coupled with proteomic identification which has been successfully demonstrated to identify the protein interactions (Puig et al., 2001; Rigaut et al., 1999).

The bMON 14272 *exon0* KO (Chapter 2) was repaired by fusion constructs of EXON0 that placed the IgG-CBP, GFP and 3×FLAG-6×His TAP protein tags at the N- or C-terminus of EXON0 respectively (Fig.3.1A). The titers of *exon0* KO-NTAP-HA-EXON0 (1.54×10^8 $TCID_{50}$/ml) and *exon0* KO-3×FLAG-6×His-HA-EXON0 (3.3×10^8 $TCID_{50}$/ml) at 96 hpi was similar to *exon0* KO-HA-EXON0 at 96 hpi, indicating that the addition of either tag did not affect the function of EXON0 and could fully rescue the KO bacmid. Fusion of GFP protein at the N-terminal of EXON0 resulted in a virus that produced a reduced titer of 2.2×10^7 $TCID_{50}$/ml. These three functioning fusion proteins were all detected at correct size by western blot (Appendix Fig. 2). C-terminal fusion protein of EXON0 with CBP-IgG and GFP could not rescue the KO bacmid and neither fusion protein was detected by western blot. These results indicate that two C-terminal fusion tags interfered with the function of EXON0 and were therefore not used for TAP purification.

3.3.2 Identification of β-tubulin as the interacting partner of EXON0

In the first attempt at TAP purification utilizing the IgG-CBP tag Sf9 cells infected with *exon0* KO-NTAP-HA-EXON0 and control virus *exon0* KO-HA-EXON0 were harvested at 24 hpi and subjected to IgG-CBP tandem affinity purification. Extensive IgG-CBP tandem affinity purifications with the N-terminal IgG-CBP-EXON0 repaired virus did

not reveal major specific protein bands for EXON0 (Appendix Fig. 3). The reason for this is unclear but may be due to a lower binding efficiency of CBP to calmodulin resin in insect cells as has been previously demonstrated (Yang et al, 2006). Recently, the 3×FLAG-6×His tandem affinity purification has been shown to be very efficient in insect cells (Yang et al, 2006). Therefore, the 3×FLAG-6×His tandem affinity purification was utilized in further TAP purifications. Results of using 3×FLAG-6×His-HA-EXON0 are shown in Fig 3.1B. Compared to cells infected with a control virus that expressed an untagged EXON0 this purification was efficient and there was one strong specific band of about 50 kDa that co-purified with 3×FLAG-6×His-HA-EXON0. The 50 kDa band was excised and subjected to LC-MS/MS for protein identification. It was determined that there were significant homologies of the specific protein with the drosophila cytoskeletal protein β-tubulin.

3.3.3 Co-immunoprecipitation analysis of EXON0 and β-tubulin

To further examine the physical association between EXON0 and β-tubulin, we performed co-IP studies. Sf9 cells were infected with virus *exon0* KO-HA-EXON0 (Chapter 2) or the control virus AcMNPV-E2 which does not express an HA epitope tagged EXON0. After immunoprecipitation with HA agarose beads, β-tubulin was detected from lysate of *exon0* KO-HA-EXON0 infected cells strongly, but not from WT E2 infected cells (Fig. 3.2). This result therefore agrees with the TAP purification results and supports the conclusion that EXON0 interacts with β-tubulin either directly or in a complex.

3.3.4 Co-localization of EXON0 and β-tubulin

To further investigate the association of EXON0 with β-tubulin, colocalization studies were performed using confocal microscopy. Sf9 cells were infected with *exon0* KO-HA-EXON0 and fixed at 24 hpi. To detect HA-EXON0 and β-tubulin, a rabbit polyclonal anti-HA antibody and the mouse monoclonal anti-β-tubulin antibody (TU-06) were used.

In healthy Sf9 cells the rabbit polyclonal anti-HA antibody produced some background fluorescence. However in infected cells, significantly more intense fluorescence and the double ring localization of EXON0 was observed which was consistent with the previous mouse monoclonal anti-HA antibody (Chapter 2). This indicated that the rabbit polyclonal anti-HA antibody was suitable for this study (Fig.3.3A). The β-tubulin antibody detected microtubule structures from healthy Sf9 cells that predominantly extend from the perinuclear region to the cytoplasmic periphery with very little in the nucleus. However, in infected cells the microtubules signal was also detected in the nucleus localizing to the virogenic stroma. This suggested that AcMNPV infection induced reorganization of the microtubule within the nucleus. At 24 hpi, EXON0 showed strong co-localization with microtubules in the cytoplasm but weak co-localization in the nucleus. Sf9 cells were also probed with a mouse monoclonal anti- α-tubulin antibody, but no clear microtubule network structures were produced.

The Sf9 cell colocalization of microtubules were consistant but difficult to visulize individual microtubules. To clearly visualize the microtubules and confirm the colocalization of EXON0 and β-tubulin, immunofluorescence was performed in Tn368 cells with a rat monoclonal anti-HA antibody and a mouse monoclonal anti-α-tubulin antibody. In comparison to Sf9 cells Tn368 cells have bigger cytoplasms and most have long cytoplasmic extensions. Analysis of the healthy Tn368 cells shows that the network of microtubules structures were clearly visualized (Fig. 3.3B). After infection with *exon0* KO-HAEXON0 at 24 hpi, the cytoplasm volume decreased dramatically but microtubule networks remain visible and EXON0 clearly co-localized with microtubules predominantly in cytoplasm.

3.3.5 BV production in the presence of microtubule inhibitors

To investigate whether the cellular microtubules have an impact on BV production, the infection of Sf9 cells with *exon0* KO-HA-EXON0 was performed in the presence of 10 μM colchicine or 100 μg nocodazole. Both colchicine and nocodazole inhibit microtubule polymerization so if intact microtubules are required for BV transport then

BV titres should be reduced. At 72 hpi, the BV supernatants of treated and untreated cells were assayed by end point dilution. As shown in Fig. 3.4, the average BV production in the presence of colchicine (6×10^7 $TCID_{50}$/ml) or nocodazole (7.2×10^7 $TCID_{50}$/ml) showed a reduction of 81.25% and 77.5%, respectively compared to BV level (3.2×10^8 $TCID_{50}$/ml) without drugs. This was consistent with previously published results which showed that 10 μM colchicine or 20 μM taxol treatment reduced AcMNPV BV production by 75% and 84% respectively (Volkman and Zaal, 1990b). These results indicate that microtubules and their dynamics have an impact on AcMNPV BV production.

3.3.6 Co-localization of EXON0 with microtubules in the presence of microtubule inhibitors

To further investigate the interaction of EXON0 and microtubules the effect of microtubule inhibitors on their co-localization was tested. Sf9 cells were treated with 10 μM colchicine or 100 μg nocodazole for 4 hrs prior to infection and throughout the infections. Cells were infected with *exon0* KO-HA-EXON0 the co-localization of EXON0 and β-tubulin was monitored at 24 hpi by confocal immunofluorescence microscopy. In the untreated Sf9 cells, the normal nuclear and cytoplasmic ring pattern of EXON0 co-localized extensively with microtubules. In the presence of colchicine, microtubule integrity was impaired and showed partial depolymerization in the cytoplasm (Fig. 3.5). Notably the RING pattern of EXON0 in cytoplasm was also impaired at the same position as microtubules. Nocodazole treatment reduced the co-localization of EXON0 and β-tubulin but to a much lesser degree than colchicine. These results strongly suggest that β-tubulin and the integrity of microtubules is required for the normal distribution of EXON0 during infection.

3.3.7 Co-immunoprecipitation of EXON0 and β-tubulin in the presence of microtubule inhibitors

To investigate if the microtubule depolymerizing drugs inhibit the association of EXON0 with microtubules, Sf9 cells were treated with colchicine followed by infection with

exon0 KO-HA-EXON0 and harvested at 24 hpi for co-IP. Tubulin was detected from treated and untreated total cells, however more tubulin was detected from the lysate supernatant of treated cells (Fig. 3.6). This suggests that colchicine depolymerised the microtubules and generated more free tubulins heterodimers. Non-depolymerized microtubules are pelleted with cell debris and not detected in the supernatant lysate. Co-IP with HA antibody of proteins from the cell lysates also resulted in a much stronger β-tubulin signal from colchicine treated cells than from untreated cells. These results show that the drug treatment does not inhibit the interaction of EXON0 with α- and β-tubulin. EXON0 therefore may associate either directly or in a complex with α- and β-tubulin heterodimers.

3.3.8 Interaction of EXON0 and β-tubulin in transient expression

As described above the association of EXON0 with β-tubulin may require a complex of proteins that could be both cellular and viral. To determine if other viral proteins are required *exon0* was transiently expressed in Sf9 cells using the expression vector pHA-exon0. This resulted in the expression of EXON0 in the absence of other viral proteins which was analyzed by co-IP at 24 hpt. The results showed that, after immunoprecipitation with anti-HA antibody, β-tubulin was detected from pHA-exon0 transfected cells but not from non-transfected cells (Fig. 3.7). This result suggested that for association between EXON0 and tubulin additional viral proteins are not essential.

3.4 Discussion

EXON0 is a conserved protein in all the lepidopteran NPVs and is required for the efficient egress of nucleocapsids from the nucleus to cytoplasmic membrane in the BV pathway (Chapter 2). How the nucleocapsids of lepidopteran NPVs are transported to the plasma membrane is an important question and has not been solved. In this study EXON0 has been shown to associate with a component of the microtubule skeleton and that microtubule dynamics and integrity have an important impact on the BV production. This suggests that the transport of the nucleocapsids may be facilitated by or based on the microtubules. Viruses are dependent on the machinery of the cell for both trafficking and transport as they are obligate intracellular parasites. As nucleocapsids are very large structures often greater than 500 kDa or 50 nm in length their free diffusion is restricted in the cytoplasm (Seksek et al., 1997; Stidwell and Greber, 2000). To overcome this barrier viruses have developed transport mechanisms that are based on microtubules and this is a common strategy used by a diversity of viruses (reviewed by Dohner et al (2005)) The transport of baculovirus nucleocapsids on microtubules therefore could be a reasonable mechanism for facilitating the egress of nucleocapsids from the nucleus to the cytoplasmic membrane.

In this study the TAP purification identified β-tubulin as a cellular protein that complexes with EXON0 and therefore suggesting a possible interaction with microtubules. The role of microtubules on the BV production was investigated using the inhibitors colchicine and nocodazole. These inhibitors depolymerized the Sf9 microtubules to a different extent but both reduced the BV yield by 77-81% (Fig. 3.4). This is greater than the 20-50% inhibition in human herpesvirus 8 titres which is already considered to be significant (Naranatt et al., 2005). The results support the conclusion that microtubules are required for nucleocapsid egress that is potentially facilitated by the EXON0-β-tubulin interaction. The effect of microtubule inhibitors on BV production is not as great as deleting EXON0 yet the drug treatments do not cause a complete depolymerization of the microtubule cytoskeletal structures (Fig. 3.5). The surviving structures could provide a limited transport of nucleocapsids.

In Sf9 cells the microtubule skeletons were shown to extend from perinuclear region to cytoplasmic periphery (Fig. 3.3A), which is similar to previous studies using an antibody against α-tubulin (Patmanidi et al., 2003; Volkman and Zaal, 1990a). The subtle network structure of microtubules was not well visualized in this study using the pig anti-β-tubulin antibody. In addition, using antibodies against α-tubulin also did not achieve clear microtubule structures in Sf9 cell (data not shown). However, Tn368 cells produced clear microtubules networks using the anti-α-tubulin antibody (Fig. 3.3B). In Tn368 cells it was possible to show that EXON0 colocalized along the microtubules.

In this study, treatment with colchicine depolymerised microtubules and under these conditions it resulted in greater amounts of β-tubulin co-immunoprecipitating EXON0 (Fig. 3.6). This suggests that EXON0 associates with heterodimers of α- and β-tubulin. In addition, transient expression experiments showed that β-tubulin interacts with EXON0 in the absence of other viral proteins. EXON0 therefore potentially binds directly to the tubulin dimers or may require cellular proteins to bridge their association.

Microtubule associated proteins (MAPs) are a large diverse group that typically have 3 or 4 imperfect tandem repeats of a 31 amino acid sequence motif and flanking proline-rich sequences that are known to bind microtubules (Ferralli et al., 1994; Ludin et al., 1996). Analysis of EXON0 did not reveal any amino acid similarity to the repeat motifs of MAPs suggesting that it does not belong to this class of proteins. The absence of an obvious tubulin binding domain in EXON0 does not exclude the possibility of direct binding of EXON0 to tubulin. However anterograde transport on microtubules to the cell periphery usually requires kinesin motors which encompass a super family of 45 members in humans. A number of viral proteins have been shown to utilize kinesin motor proteins for anterograde transport. For example, the HSV tegument protein US11 interacts with conventional kinesin heavy chain and plays a major role in the anterograde transport of unenveloped capsids in axons (Diefenbach et al., 2002a). To futher understand the mechanism by which EXON0 facilitates transport of AcMNPV nucleocapsids to the plasma membrane future work will have to determine the nature of the interaction with β-tubulin.

Figure 3.1 Identification of β-tubulin as an interacting partner of EXON0.
(A). Construction of EXON0 fusion proteins and repaired viruses. Schematic diagrams showing the bMON 14272 *exon0* KO repair constructs that fused the IgG-CBP, 3×FLAG-6×His TAP tags and the GFP tag to EXON0 at the N- or C-terminal of EXON0. The ability to rescue bMON 14272 *exon0* KO is shown on the right. All constructs included an insertion of the HA epitope. (B). TAP purification of complexes associated with 3×FLAG-6×His–HA-EXON0. Sf9 cells were infected with the *exon0* KO-3×FLAG-6×His-HA-EXON0 (FLAG-His) or *exon0* KO-HA-EXON0 (control) and harvested at 24 hpi, subjected to affinity purification (see methods). The specific band was identified by LC-MS/MS. The bold residues of β-tubulin represent the peptide fragments of β-tubulin covered by LC-MS/MS.

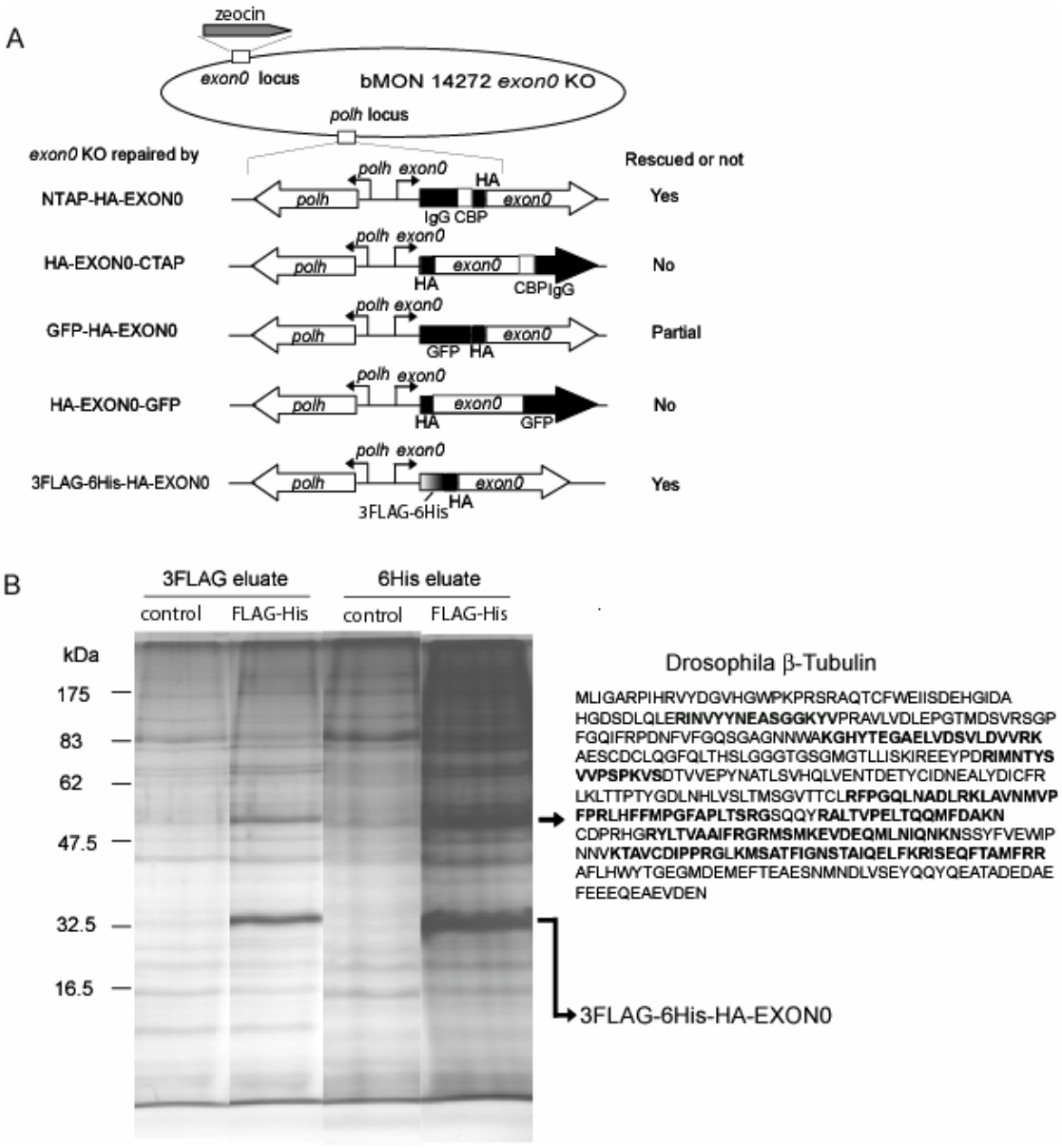
A
zeocin
exon0 locus
bMON 14272 exon0 KO
polh locus
exon0 KO repaired by
Rescued or not
NTAP-HA-EXON0
Yes
IgG CBP
HA-EXON0-CTAP
No
CBP IgG
GFP-HA-EXON0
Partial
GFP HA
HA-EXON0-GFP
No
HA GFP
3FLAG-6His-HA-EXON0
Yes
3FLAG-6His HA
polh
exon0
B
3FLAG eluate
6His eluate
control
FLAG-His
control
FLAG-His
kDa
175
83
62
47.5
32.5
16.5
Drosophila β-Tubulin
MLIGARPIHRVYDGVHGWPKPRSRAQTCFWEIISDEHGIDA
HGDSDLQLERINVYYNEASGGKYVPRAVLVDLEPGTMDSVRSGP
FGQIFRPDNFVFGQSGAGNNWAKGHYTEGAELVDSVLDVVRK
AESCDCLQGFQLTHSLGGGTGSGMGTLLISKIREEYPDRIMNTYS
VVPSPKVSDTVVEPYNATLSVHQLVENTDETYCIDNEALYDICFR
LKLTTPTYGDLNHLVSLTMSGVTTCLRFPGQLNADLRKLAVNMVP
FPRLHFFMPGFAPLTSRGSQQYRALTVPELTQQMFDAKN
CDPRHGRYLTVAAIFRGRMSMKEVDEQMLNIQNKNSSYFVEWIP
NNVKTAVCDIPPRGLKMSATFIGNSTAIQELFKRISEQFTAMFRR
AFLHWYTGEGMDEMEFTEAESNMNDLVSEYQQYQEATADEDAE
FEEEQEAEVDEN
3FLAG-6His-HA-EXON0

Figure 3.2 Co-immunoprecipitation of EXON0 and β-tubulin.

Sf9 (2×10^8) cells were infected with WT AcMNPV E2 (E2) or *exon0* KO-HA-EXON0 (HA) with MOI of 10. Cells were harvested at 24 hpi and subjected to co-IP. Samples were separated by 10% SDS-PAGE and analyzed by western blot. For IP input 0.125% total cell lysate was loaded, and 5% IP eluate was loaded. The antibody used for western blot is shown on the left (WB).

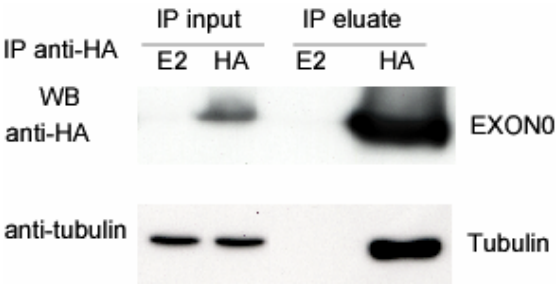

Figure 3.3 The co-localization of EXON0 with β-tubulin and microtubule in infected cells.

Sf9 (A) or Tn368 (B) cells were infected with *exon0* KO-HA-EXON0 virus at MOI of 10 and fixed at 24 hpi. In panel A, Sf9 cells were probed with a rabbit polyclonal anti-HA antibody and a mouse monoclonal anti-β-tubulin antibody and visualized with Alexa 488 conjugated goat anti-rabbit IgG and Alexa 635 conjugated goat anti-mouse IgG . In panel B, Tn368 cells were probed with a rat monoclonal anti-HA antibody and a mouse anti-α-tubulin antibody and visualized with Alexa 488 conjugated goat anti-rat IgG and Alexa 635 conjugated goat anti-mouse IgG. For nuclear visualization the cells were also stained with DAPI.

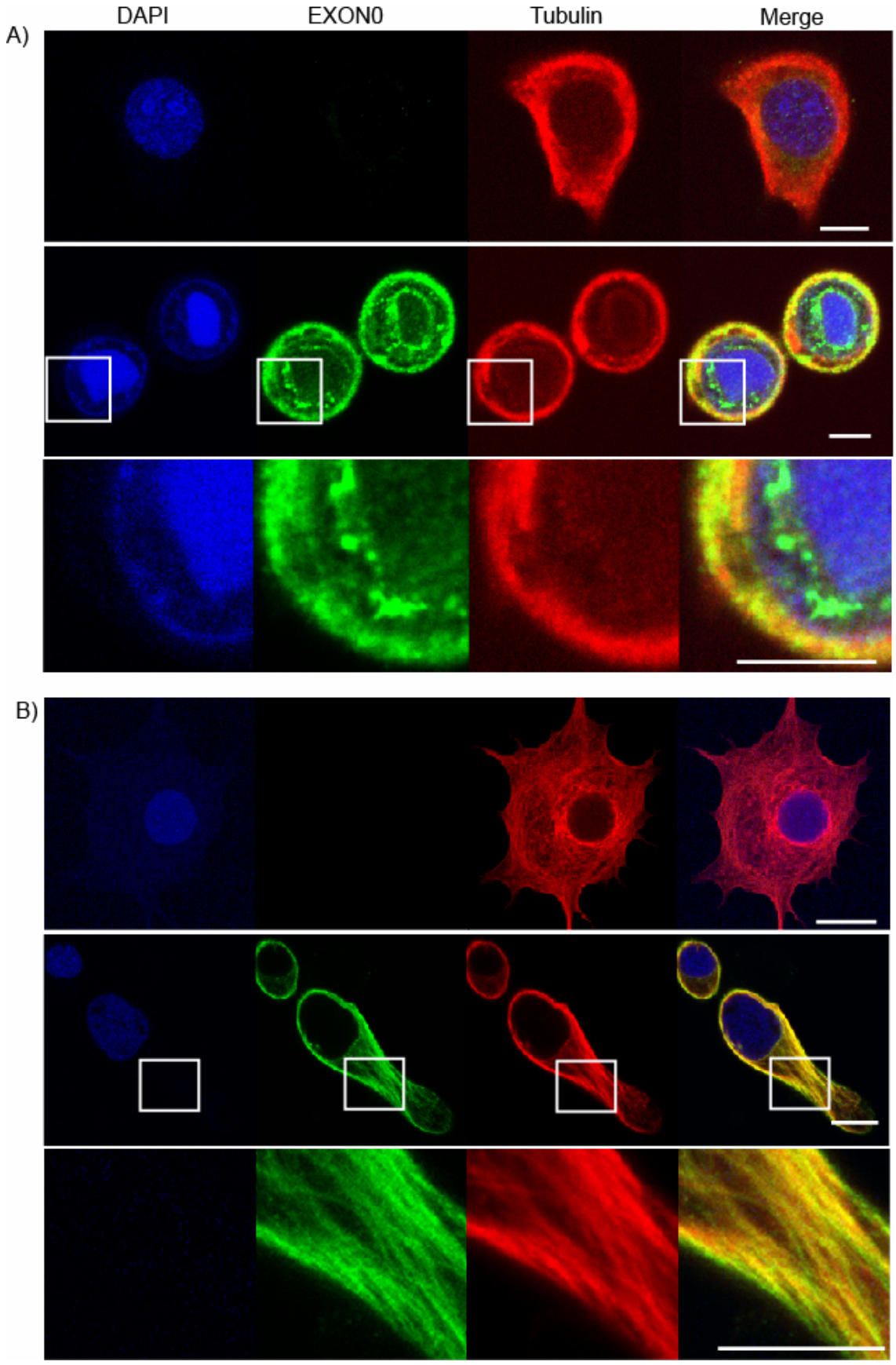
A)
DAPI
EXON0
Tubulin
Merge
B)

Figure 3.4 Microtubule inhibitors reduced the BV production.

Sf9 cells were infected with *exon0* KO-HA-EXON0 in the presence of the microtubule inhibitors 10 μM colchicine or 100 μg nocodazole at an MOI of 10. Supernatents were harvested at 72 hpi and viral titres were determined. The experiment was done in duplicate and average titers are shown. The titres are shown as a percentage of the control which contained no microtubule inhibitors.

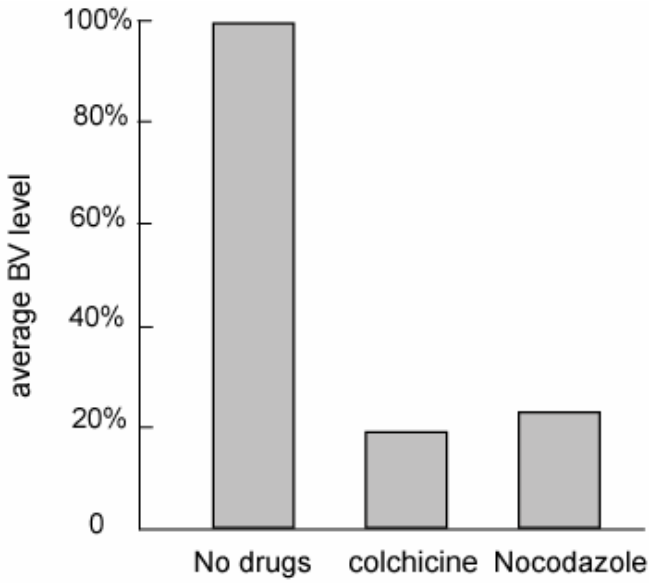

Figure 3.5 Microtubule inhibitors affect the localization of EXON0.

Sf9 cells were treated without (A) or with (B) 10μM colchicine and infected with *exon0* KO-HA-EXON0 and immunofluorescent confocal microscopy was performed at 24 hpi as described in Fig. 3.3 for detection of EXON0 and β-tubulin. Lower parts of panel A and B are the blowout of the square in upper cell. For nuclear localization the cells were also stained with DAPI. Bars = 10 μm.

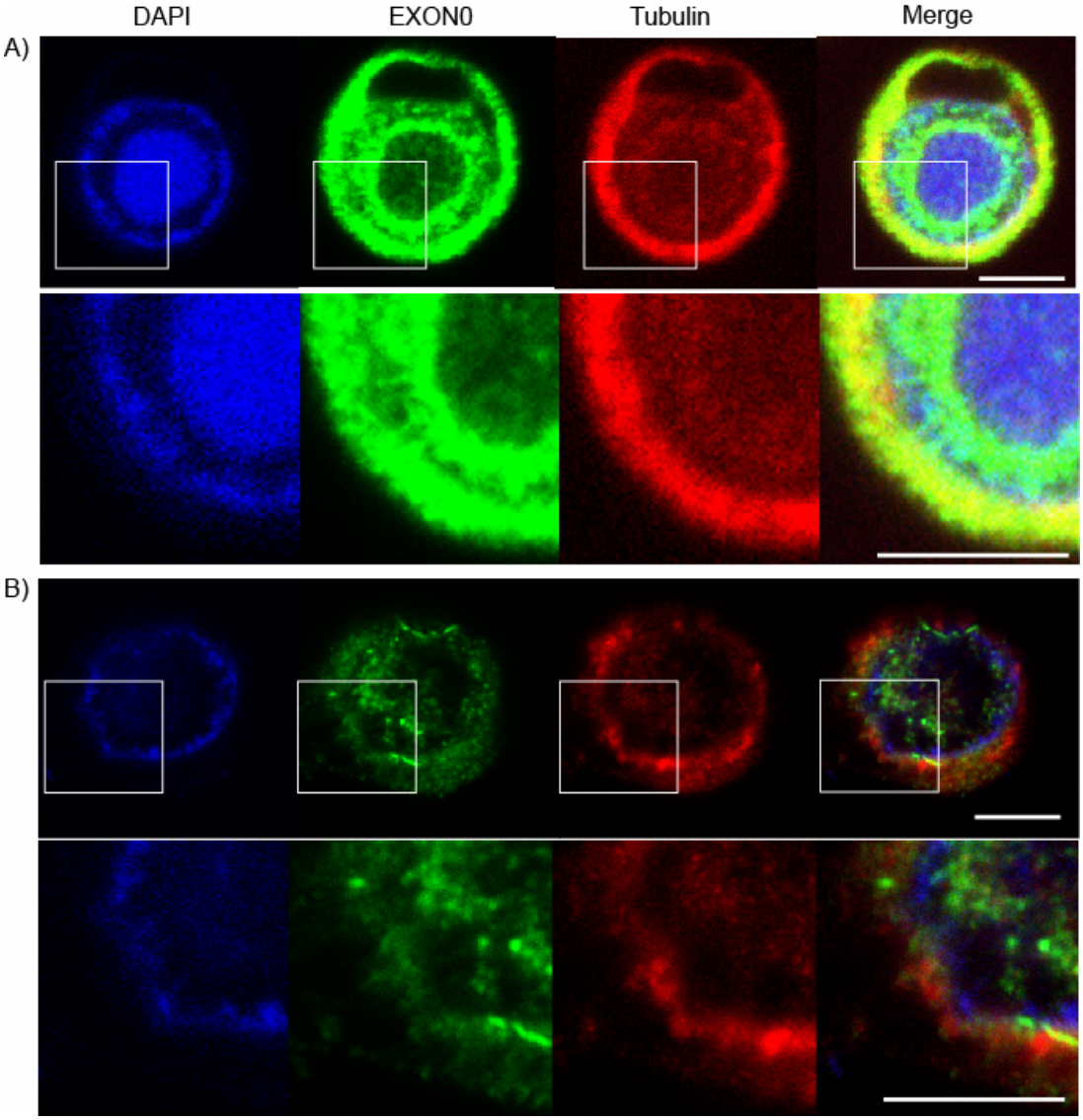

Figure 3.6 EXON0 appears to bind free heterodimers of tubulin

Sf9 cells were infected with *exon0* KO-HA-EXON0 at an MOI of 10 in the presence of 10 μM colchicine throughout infection. Cells were harvested at 24 hpi for IP. Total protein (1% of the total IP input) or immunopreciptated (20% of the total IP eluate) samples were separated by 10% SDS-PAGE and detected by western blot using an anti-HA and anti-β-tubulin antibodies. The left lane were cells infected with control virus *ie1* KO-IE1, the middle and right lanes were cells infected with *exon0* KO-HA-EXON0 in the absence and presence of colchicine, respectively. -, no drug; Col, 10 μM colchicine.

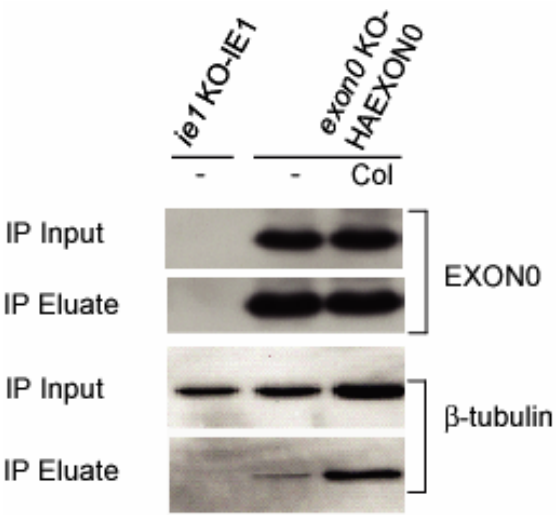

Figure 3.7 Association of EXON0 with β-tubulin does not require other viral proteins.

Sf9 cells were transfected with pHA-exon0 to transiently express *exon0*. Cells were harvested at 24 hpt and proteins were immunoprecipitated with anti-HA antibody. Total protein (IP input) or immunopreciptated (IP eluate) samples were separated by 10% SDS-PAGE and detected by western blot. For IP input, 3% of the total cell lysate was loaded and 50% of the total IP eluate was loaded. β-tubulin was detected from pHA-exon0 transfected cells but not from non-transfected Sf9 cells.

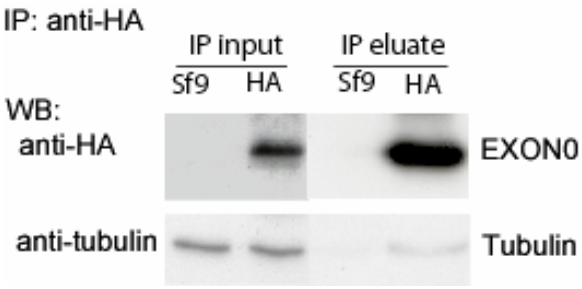

3.5 References

Alonso, C., Miskin, J., Hernaez, B., Fernandez-Zapatero, P., Soto, L., Canto, C., Rodriguez-Crespo, I., Dixon, L., and Escribano, J. M. (2001). African swine fever virus protein p54 interacts with the microtubular motor complex through direct binding to light-chain dynein. *J. Virol.* **75,** 9819–9827.

Blissard, G. W., and Wenz, J. R. (1992). Baculovirus GP64 envelope glycoprotein is sufficient to mediate pH-dependent membrane fusion. *J. Virol.* **66**(11)**,** 6829-6835.

Carter, G. C., Rodger, G., Murphy, B. J., Law, M., Krauss, O., Hollinshead, M., and Smith, G. L. (2003). Vaccinia virus cores are transported on microtubules. *J.Gen. Virol.* **84,** 2443-2458.

Charlton, C. A., and Volkman, L. E. (1991). Sequential rearrangement and nuclear polymerization of actin in baculovirus-infected *Spodoptera frugiperda* cells. *J Virol.* **65,** 1219-1227.

Charlton, C. A., and Volkman, L. E. (1993). Penetration of *Autographa californica* nuclear polyhedrosis virus nucleocapsids into IPLB Sf 21 cells induces actin cable formation. *Virology* **197,** 245-254.

Dai, X., Stewart, T. M., Pathakamuri, J. A., Li, Q., and Theilmann, D. A. (2004). *Autographa californica* multiple nucleopolyhedrovirus *exon0* (*orf141*), which encodes a RING finger protein, is required for efficient production of budded virus. *J. Virol.* **78**(18)**,** 9633-9644.

Diefenbach, R. J., Miranda-Saksena, M., Diefenbach, E., Holland, D. J., Boadle, R. A., Armati, P. J., and Cunningham, A. L. (2002). Herpes simplex virus tegument protein US11 interacts with conventional kinesin heavy chain. *J. Virol.* **76,** 3282-3291.

Dohner, K., Nagel, C. H., and Sodeik, B. (2005). Viral stop-and-go along microtubules: taking a ride with dynein and kinesins. *Trends Microbiol.* **13,** 320-327.

Elliott, G., and O'Hare, P. (1998). Herpes simplex virus type 1 tegument protein VP22 induces the stabilization and hyperacetylation of microtubules. *J. Virol.* **72,** 6448-6455.

Ferralli, J., Doll.T., and Matus, A. (1994). Sequence analysis of MAP2 function in living cells. *J. Cell Sci.* **107**.

Funk, A., Mhamdi, M., Lin, L., Will, H., and Sirma, H. (2004). Itinerary of hepatitis B viruses: delineation of restriction points critical for infectious entry. *J. Virol.* **78,** 8289-8300.

Granados, R. R. (1978). Early events in the infection of Hiliothis zea midgut cells by a baculovirus. *Virology* **90**(1)**,** 170-174.

Hefferon, K. L., Oomens, A. G., Monsma, S. A., Finnerty, C. M., and Blissard, G. W. (1999). Host cell receptor binding by baculovirus GP64 and kinetics of virion entry. *Virology* **258,** 455-468.

Jordan, M. A., and Wilson, L. (2004). Microtubules as a target for anticancer drugs. *Nat. Rev. Cancer* **4,** 253-265.

Lakadamyali, M., Rust, M. J., Babcock, H. P., and Zhuang, X. (2003). Visualizing infection of individual influenza viruses. *Proc. Natl. Acad. Sci. U.S.A.* **100,** 9280-9285.

Lanier, L. M., and Volkman, L. E. (1998). Actin binding and nucleation by Autographa californica M nucleopolyhedrovirus. *Virology* **243,** 167-177.

Leikina, E., Onaran, H. O., and Zimmerberg, J. (1992). Acidic pH induces fusion of cells infected with baculovirus to form syncytia. *FEBS Lett.* **304**(2-3)**,** 221-224.

Long, G., Pan, X., Kormelink, R., and Vlak, J. M. (2006). Functional entry of baculovirus into insect and mammalian cells is dependent on clathrin-mediated endocytosis. *J. Virol.* **80**(17)**,** 8830-8803.

Lowe, J., Li, H., Downing, K. H., and Nogales, E. (2001). Refined structure of alpha beta-tubulin at 3.5 A resolution. *J. Mol. Biol.* **313,** 1045-1057.

Luckow, V. A., Lee, S. C., Barry, G. F., and Olins, P. O. (1993). Efficient generation of infectious recombinant baculoviruses by site-specific transposon-mediated insertion of foreign genes into a baculovirus genome propagated in *Escherichia coli*. *J. Virol.* **67**(8)**,** 4566-4579.

Ludin, B., Ashbridge, K., Funfschilling, U., and Matus, A. (1996). Functional analysis of the MAP2 repeat domain. *J. Cell Sci.* **109,** 91-99.

Luftig, R. B., and Weihing, R. R. (1975). Adenovirus binds to rat brain microtubules *in vitro*. *J. Virol.* **16,** 696-706.

Martin, A., O'Hare, P., McLauchlan, J., and Elliott, G. (2002). Herpes simplex virus tegument protein VP22 contains overlapping domains for cytoplasmic localization, microtubule interaction, and chromatin binding. *J. Virol.* **76,** 4961-4970.

McDonald, D., Vodicka, M. A., Lucero, G., Svitkina, T. M., Borisy, G. G., Emerman, M., and Hope, T. J. (2002). Visualization of the intracellular behavior of HIV in living cells. *J. Cell Biol.* **159,** 441-452.

Naranatt, P. P., Krishnan, H. H., Smith, M. S., and Chandran, B. (2005). Kaposi's sarcoma-associated herpesvirus modulates microtubule dynamics via RhoA-GTP-diaphanous 2 signaling and utilizes the dynein motors to deliver its DNA to the nucleus. *J. Virol.* **79,** 1191-1206.

Nejmeddine, M., Trugnan, G., Sapin, C., Kohli, E., Svensson, L., Lopez, S., and Cohen, J. (2000). Rotavirus spike protein VP4 is present at the plasma membrane and is associated with microtubules in infected cells. *J. Virol.* **74,** 3313–3320.

Nogales, E. (2001). Structural insights into microtubule function. *Annu. Rev. Biophys. Biomol. Struct.* **30,** 397-420.

Ogino, T., Iwama, M., Ohsawa, Y., and Mizumoto, K. (2003). Interaction of cellular tubulin with Sendai virus M protein regulates transcription of viral genome. *Biochem. Biophys. Res. Commun.* **311,** 283–293.

Patmanidi, A. L., Possee, R. D., and King, L. A. (2003). Formation of P10 tubular structures during AcMNPV infection depends on the integrity of host-cell microtubules. *Virology* **317,** 308-320.

Pelkmans, L., Kartenbeck, J., and Helenius, A. (2001). Caveolar endocytosis of simian virus 40 reveals a new two-step vesicular-transport pathway to the ER. *Nat. Cell Biol.* **3,** 473-483.

Puig, O., Caspary, F., Rigaut, G., Rutz, B., Bouveret, E., Bragado-Nilsson, E., Wilm, M., and Seraphin, B. (2001). The tandem affinity purification (TAP) method: a general procedure of protein complex purification. *Methods* **24,** 218-229.

Rigaut, G., Shevchenko, A., Rutz, B., Wilm, M., Mann, M., and Seraphin, B. (1999). A generic protein purification method for protein complex characterization and proteome exploration. *Nat. Biotechnol.* **10,** 1030-1032.

Seisenberger, G., Ried, M. U., Endress, T., Buning, H., Hallek, M., and Brauchle, C. (2000). Real-time single-molecule imaging of the infection pathway of an adeno-associated virus. *Science* **294,** 1929-1932.

Seksek, O., Biwersi, J., and Verkman, A. S. (1997). Translational diffusion of macromolecule-sized solutes in cytoplasm and nucleus. *J. Cell Biol.* **138,** 131-142.

Sodeik, B., Ebersold, M. W., and Helenius, A. (1997). Microtubule-mediated transport of incoming herpes simplex virus 1 capsids to the nucleus. *J. Cell Biol.* **136,** 1007-1021.

Stidwell, R. P., and Greber, U. F. (2000). Intracellular virus trafficking reveals physiological characteristics of cytoskeleton. *News Physiol. Sci.* **15,** 67-71.

Suomalainen, M., Nakano, M. Y., Keller, S., Boucke, K., Stidwill, R. P., and Greber, U. F. (1999). Microtubule-dependent plus- and minus end-directed motilities are competing processes for nuclear targeting of adenovirus. *J. Cell Biol.* **144,** 657-672.

Theilmann, D. A., Blissard, G. W., Bonning, B., Jehle, J. A., O'Reilly, D. R., Rohrmann, G. F., Thiem, S., and Vlak, J. M. (2005). Baculoviridae. *In* "Virus Taxonomy - Eighth Report of the International Committee on Taxonomy of Viruses" (M. M. A. Fauquet C.M., Maniloff J., Desselberger U., and B. L.A. (ed.), Ed.), pp. 177-185. Elsevier/Academic Press, London.

van Loo, N. D., Fortunati, E., Ehlert, E., Rabelink, M., Grosveld, F., and Scholte, B. J. (2001). Baculovirus infection of nondividing mammalian cells: mechanisms of entry and nuclear transport of capsids. *J. Virol.* **75,** 961-970.

Volkman, L. E., and Goldsmith, P. A. (1985). Mechanism of neutralization of budded *Autographa californica* nuclear polyhedrosis virus by a monoclonal antibody: inhibition of entry by adsorptive endocytosis. *Virology* **143,** 143-185.

Volkman, L. E., and Zaal, K. J. (1990b). Autographa californica M nuclear polyhedrosis virus: microtubules and replication. *Virology* **175,** 292-302.

Ward, B. M., and Moss, B. (2004). Vaccinia virus A36R membrane protein provides a direct link between intracellular enveloped virions and the microtubule motor kinesin. *J. Virol.* **78,** 2486–2493.

Yang, P., Sampson, H. M., and Krause, H. M. (2006). A modified tandem affinity purification strategy identifies cofactors of the Drosophila nuclear receptor dHNF4. *Proteomics* **6,** 927-935.

Chapter 4: Identification of the domains of *Autographa californica* multiple nucleopolyhedrovirus EXON0 (ORF141) required for the efficient production of budded virus, dimerization and association with β-tubulin, FP25 and BV/ODV-C42[3]

4.1 Introduction

Autographa californica multiple nucleopolyhedrovirus (AcMNPV) is a large enveloped double-stranded DNA virus that is highly pathogenic for specific species of lepidopteran insects and is the archetype NPV of the *Baculoviridae* (Theilmann et al., 2005). After entry into the host cell, AcMNPV nucleocapsids are transported to the nucleus of infected cells, where viral transcription and DNA replication are initiated. Gene expression from the viral genome can be subdivided into three major phases during the infection cycle: early, late, and very late (Friesen, 1997). NPVs produce two types of virions that play distinctly different roles during a biphasic cycle. ODVs are produced in the nucleus, encased in occlusion bodies, and are responsible for the transmission of infection from animal to animal. In contrast BVs are responsible for the cell-to-cell spread of infection within an infected animal and in cell culture. To date there is little information concerning the mechanism by which nucleocapsids are shuttled into either ODV or BV. In addition, it is also unclear how nucleocapsids are transported to the plasma membrane to become BV. At the plasma membrane a number of elegant studies have shown that the BV specific protein GP64 is required for the successful budding of infectious virions (Blissard and Wenz, 1992; Monsma and Blissard, 1995; Monsma et al, 1996; Oomens and Blissard, 1999b).

[3] A version of this chapter will be submitted for publication. Fang M., Nie Y., Dai X. and Theilmann D. Identification of the domains of *Autographa californica* multiple nucleopolyhedrovirus EXON0 (ORF141) required for the efficient production of budded virus, dimerization and association with β-tubulin, FP25 and BV/ODV-C42.

In other viral systems numerous studies have shown how specific viral genes are responsible for the production of progeny virus through the process of budding. For example in both positive- and negative-stranded enveloped RNA viruses specific amino acid sequences called Late domains have been identified within structural proteins are required for the virion egress (Craven et al., 1999; Gottlinger et al., 1991; Harty et al., 2000; Perez et al, 2003; Wills et al., 1994). Herpesvirus maturation includes primary envelopment of capsids by budding at the inner nuclear membrane, de-envelopement by fusion with the outer nuclear membrane followed by re-envelopement by budding into vesicles of the trans-Golgi network (Mettenleiter, 2004). The herpes simplex virus has a very complex structure, consisting of over 15 proteins in its tegument and over 12 proteins in its envelope and many of these structural genes have been shown to be required for normal production of infectious progeny virus (Mettenleiter, 2002b).

Exon0 (*orf141*) is a highly conserved gene found in all lepidopteran NPVs and is required for the efficient production of BV (Dai et al., 2004). In Chapter 2, EXON0 has been shown to be a structural component of nucleocapsids and interact with FP25 and BV/ODV-C42. In addition, EXON0 is required for the efficient egress of nucleocapsids from the nucleus to the cytoplasmic membrane. In Chapter 3, it is shown that EXON0 interacts with β-tubulin and microtubules and this association has an important impact on BV production. In this study, domains of EXON0 that are required for the efficient production of BV and association with β-tubulin, FP25 and BV/ODV-C42 are mapped by deletion mutagenesis. Yeast 2-hybrid assays and immunoprecipitation also demonstrate that EXON0 forms dimers *in vitro* and *in vivo*. Further point mutations reveal the conserved residues are essential for its association with these proteins and the residues which are required for the dimer formation are also essential for the efficient BV production.

4.2 Materials and Methods

4.2.1 Viruses and cells

As described in Chapter 2.

4.2.2 Construction of HA- and FLAG-tagged EXON0 and EXON0 mutants

To tag EXON0 with the influenza HA epitope (CYPYDVPDYASL) at the C-terminus *exon0* was amplified using the plasmid p2ZeoKS-exon0 (Dai et al., 2004) as a template with the primers 880 (5'-TTAAGATCTGGCGTAGTCGGGCACGTCGTAGGGGTATTTATACGATGTCCTGCAC -3') and 881 (5'-GCGATTGTTGGTGGAGCA-3'). p2ZeoKS-exon0 was also used as a template to tag EXON0 with the FLAG epitope (DYLDDDDL) at the C-terminus with primers 879 (5'-TTAAGATCTCTTGTCGTCGTCGTCCTTGTAGTCTTTATACGATGTCCTGCAC -3') and 881. Inverse polymerase chain reaction (PCR) was used to amplify linear fragments which were treated with T4 polynucleotide kinase and gel purified. Amplified fragments were self-ligated overnight at 16°C and transformed into DH5α competent cells. Zeocin resistant colonies were picked and identified by restriction digestion and confirmed by sequencing. The resulting plasmids were named p2Zeo-exon0-HA and p2Zeo-exon0-FLAG.

Using p2Zeo-HA-exon0 (Chapter 2) as the template and inverse PCR as described above, six pairs of primers were used to delete each of six putative domains of EXON0. Namely primer 624 (5'-GGCGTAGTAGTCGGGCACGT-3') and 813 (5'-GTAATGATCGATAACTTTGT-3) for the deletion of IE0-NH (1-37 aa), primer 624 (5'-GGCGTAGTAGTCGGGCACGT-3') and 625 (5'-GCAAAGCTGCAATGCGGC-3') for the deletion of acidic domain I (AI), 626 (5'-TGCGTCAATTTGTATGTCGG-3') and 627 (5'-TTTTTTTATTACTATGATCAATGT-3') for the deletion of charged region (C), 628 (5'-GGCACATTGATCATAGTAATAA-3') and 629 (5'-GCCCAACGTATTATTCAATG-3') for the deletion of acidic domain II (AII), 630 (5'-ATTGCCGCGATCACGCAC-3') and 631 (5'-TTGTACGAATGCAATGTTTGTA-3')

for the deletion of the leucine zipper domain (Leu), 640 (5'-TTCGTACAAAACCAAATTGT-3') and 641 (5'-AGGACATCGTATAAATAA-3') for the deletion of the RING finger domain (RING) (Fig. 4.1). The plasmids containing deletion mutants of EXON0 were named as p2Zeo-HA-exon0-△IE0-NH, -△AI, -△C, -△AII, -△Leu, -△RING. All the mutants were sequenced to confirm the correct deletion.

The N-terminally tagged HA-EXON0 produced an extra band of about 40 kDa besides of the predicted band in size of 30 kDa (Fig. 4.2A). This 40 kDa band was not detected when the EXON0 was tagged with the HA epitope at the C-terminal (Fig. 4.6A). The C-terminal EXON0-HA repaired virus had a $TCID_{50}$ of 2.89×10^8 (Fig. 4.6C), similar to 1.54×10^8 $TCID_{50}$ of *exon0* KO-HA-EXON0 (Chapter 2). Therefore the HA epitope at either C or N terminus did not affect EXON0 function. To make point mutants of EXON0, inverse PCR was used with p2Zeo-exon0-HA as a template. The following primers were used: primer 1384 (5'-GGCAGCAGCGTTATCGATCATTACCTG-3') and 1385 (5'-TTTCACGCGTACAACGCCGA-3') for F44F46M49/AAA, 1386 (5'-CAGCGCTGCGTCAATTTG-3') and 1387 (5'-CAATGCGGCGTGGCCTCG-3') for K59R65/AA, 1388 (5'-CGAGCGCGCGCCGCATTG-3') and 1389 (5'-GCCGCGGCTGCAATGGCCGAC-3') for V64F69I72/AAA, 1390 (5'-ACGTTGGGCATCAAAAGCAAAATG-3') and 1391 (5'-GCTATTCAATGTGCTAAAGAGAT -3') for I116I122I126/AAA, 1392 (5'-CGCGCCGTCGTCATCG -3') and 1393 (5'-GCCTGTCACCATTTTATTTTTGAT-3') for C111/A, 1392 and 1394 (5'-TGCTGTGCCCATTTTATTTTTGAT-3') for H113/A, 1374 (5'-CGCTATTGCATTGCCGCGATC-3') and 1375 (5'-TTTTATCCGTACGCGAAACAG-3') for V141V143L148/AAA, 1376 (5'-AGAGTTTTTAATTAGCTTCGCCGC -3') and 1377 (5'-GCAGCGTGTTGTTTTAAAATTGCAAAT-3') for L155F162I169/AAA, 1378 (5'-CTTCAACGCGTCTCGCAA-3') and 1379 (5'-GCAATTAAAAACTCTTTTGCGTGT-3') for L157/A, 1380 (5'-GCAATTTGATATTAACTCGTTCGCGTA-3') and 1381 (5'-CTGTTGTTTATTGAAAAGGCGGAAAC-3') for V176L190/AA, 1382 (5'-GCAATTTGATATTAACTCGTTCGGGTA-3') and 1383 (5'-

CTGTTGTTTATTGAAAAGCCGGAAAC-3') for L190/A. The C230C231/AA mutant was provided by Dr. Dai (unpublished results). The resulting plasmids were named as p2zeo-exon0-HA-F44F46M49/AAA, -K59R65/AA, -V64F69I72/AAA, -I116I122I126/AAA, -C111/A, -H113/A, -V141V143L148/AAA, -L155F162I169/AAA, -L157/A, -V176L190/AA, -L190/P. The correct substitutions were all confirmed by sequencing.

To introduce *exon0* mutants into AcBac *exon0* KO, rescue transfer vectors were constructed in the plasmid backbone pFAct-GFP (Dai et al., 2004). pFAct-GFP contains two Tn*7* transposition excision sites that allow the genes cloned between the sites to be transposed into the mini ATT region located in AcMNPV bacmid (Luckow et al., 1993). The plasmids of *exon0*-FLAG, six deletion and eleven point mutants were digested with *Xho*I and *Xba*I. The excised fragments containing the native late promoter of *exon0*, *exon0* ORF and an OpMNPV *ie1* poly(A), were cloned into the *Xho*I and *Xba*I sites of pFAct-GFP, to generate pFAct-GFP-exon0-FLAG, pFAct-GFP-HA-exon0-△IE0-NH, -△AI, -△C, -△AII, -△Leu, -△RING, pFAct-GFP-exon0-HA-F44F46M49/AAA, -K59R65/AA, -V64F69I72/AAA, -I116I122I126/AAA, -C111/A, -H113/A, -V141V143L148/AAA, -L155F162I169/AAA, -L157/A, -V176L190/AA, -L190/P. In addition to the cloned gene of interest, the pFAcT-GFP backbone contains AcMNPV polyhedrin and green fluorescent protein (GFP), both of which are included in the transposed DNA cassette (Fig. 4.2).

4.2.3 Construction of AcMNPV bacmids containing the full-length and mutants of exon0

AcMNPV bacmids containing the cassettes between the two Tn7 sites were generated as previously described by Luckow *et al.* (Luckow et al., 1993). Electrocompetent DH10B cells containing both pMON7124 (Invitrogen Life Technologies) and bacmid bMON 14272 *exon0* KO (Chapter 2) or WT AcMPNV bacmid (AcBac) bMON14272 (Invitrogen Life Technologies) were transformed with one of the transfer plasmid pFAcT-GFP-*exon0*-FLAG, pFAcT-GFP-HA-*exon0*-△IE0-NH, -△AI, -△C, -△AII, -

△Leu, -△RING, pFAcT-GFP-*exon0*-HA-F44F46M49/AAA, -K59R65/AA, -V64F69I72/AAA, -I116I122I126/AAA, -C111/A, -H113/A, -V141V143L148/AAA, -L155F162I169/AAA, -L157/A, -V176L190/AA, -L190/P. The transformed cells were incubated at 37°C for 4 h in 3 ml of SOC medium and placed onto agar medium containing 30 µg of zeocin per ml, 50 µg of kanamycin per ml, 7 µg of gentamicin per ml, 10 µg of tetracycline per ml, 100 µg of 5-bromo-4-chloro-3-indolyl-ß-D-galactopyranoside (X-Gal) per ml, and 40 µg of isopropyl-ß-D-thiogalactopyranoside (IPTG) per ml. Plates were incubated at 37°C for a minimum of 48 h, and white colonies resistant to kanamycin, gentamicin and tetracycline, were selected and streaked onto new plates to confirm the phenotype and then verified by PCR. Transposition events were also confirmed by GFP expression and occlusion body formation in bacmid DNA-transfected Sf9 cells.

4.2.4 Time course analysis of BV production

Sf9 cells (1.0 x 10^6 cells/35-mm-diameter six-well plate) were transfected with 1.0 µg of each bacmid (*exon0* KO, *exon0* KO-HA-EXON0, *exon0* KO-HA-EXON0-△IE0-NH, -△AI, -△C, -△AII, -△Leu, -△RING, and control virus *ie1* KO-IE1). At various hours post transfection (hpt), supernatant containing BV was harvested and cell debris was removed by centrifugation (8,000 x *g* for 5 min). BV was titrated in duplicate by end point dilution in Sf9 cells with 96-well microtiter plates, which was also used for the titration of *exon0* KO repaired by the point mutants of EXON0.

4.2.5 Western blot assay

Protein samples from Sf9 cell pellets or from IP elulate were subjected to Western blot as described in Chapter 2. The used antibodies are: (i) mouse monoclonal anti-HA antibody (HA.11, Covance), 1:1,000; (ii) mouse monoclonal anti-FLAG antibody (M2, Sigma), 1:15,000; (iii) rabbit polyclonal FP25 antibody 1:5,000; (v) rabbit polyclonal BV-ODV C42 antibody 1:5,000.

4.2.6 Plaque assay

Sf9 cells (3.0 x 10^6 cells/ 60-mm-diameter dish) were incubated with viral inoculums for 1 h with gentle rocking at room temperature. The viral inoculums were removed, and the cells were washed with 1 ml of Grace's medium. Cells were overlaid with 4 ml of TC-100 medium containing 1.5% low-melting-point agarose (SeaPlaque) pre-equilibrated to 37°C, followed by incubation at 27°C for 5 days until observation.

4.2.7 Yeast two hybrid assay

The *Saccharomyces cerevisiae* strains YRG2 (MATa *ura3-52 his3-200 ade2-101lys2-801 trp1-901 leu2-3 112 gal4-542gal80-538* LYS2::UAS GAL1-TATA GAL1-HIS3URA3::UAS GAL4 17mers(x3)-TATACYC1-*lacZ*) (Stratagene) was used for two-hybrid tests. Plasmid vectors p2Zeo-HA-exon0, -△IE0-NH, -△AI, -△C, -△AII, -△Leu, and -△RING were digested with *Bgl*II and *Xba*I and the *exon0* fragments were cloned into the *Bam*HI and *Xba*I sites of yeast 2-hybrid activation domain (AD) vector pAD-GAL4-2.1 (Stratagene). The bait vectors were constructed using PCR to amplify HA-*exon0*, △IE0-NH, △AI, △C, △AII, △Leu, △RING with the primers 733 (5'-CGGAATTCTACCCCTACGACGTGCCC-3') and 734 (5'-AACTGCAGTTATTTATACGATGTCCTGCA-3') from p2Zeo-HA-exon0, -△IE0-NH, -△AI, -△C, -△AII, -△Leu, and -△RING. The amplified fragments were digested with *Eco*RI and *Pst*I and cloned into the binding domain (BD) vector pBD-GAL4 Cam (Statagene). The resulting AD and BD fusion plasmids were introduced into yeast strain YRG2 by the lithium acetate method according to the recommended procedure (Stratagene). Transformants were screened on medium lacking the appropriate amino acids, and selection for HIS reporter gene activation was performed on histidine, tryptophan, or histidine, tryptophan, leucine-deficient agar plates.

4.2.8 Immunoprecipitation (IP)

For the preparation of cell lysate for IP, 1 μg of the *exon0* KO, six domain deletion mutants and HA-*exon0* bacmid DNA were transfected into 2.0 x 10^6 Sf9 cells, followed by infection of *exon0* KO-EXON0-FLAG virus at a MOI of 10. At 48 hours post

infection (hpi) cells were washed twice with phosphate-buffered saline, collected and subjected to co-IP as described in Chapter 2. Or Sf9 (2.0×10^8) cells were infected with WT AcBac expressing each of the six deletion mutants of HA-EXON0 or the 12 point mutants of EXON0-HA at an MOI of 10, harvested at 24 hpi, followed co-IP as described in Chapter 2.

4.3 Results

4.3.1 Construction of deletion mutants of EXON0 and repaired viruses

AcMNPV *exon0* encodes a protein of 261 residues and six putative domains in EXON0 have been identified by analysis of the amino acid sequence (Fig. 4.1A). At the N-terminal, there is an acidic domain (AI) which consists of the first 53 amino acids. The AI domain also contains the first 37 amino acids of the transcriptional transactivator IE0 coded by the first exon of *ie0* that is spliced onto the 5' end of *ie1* mRNA to form *ie0* mRNA. So to determine if the IE0 amino acids play a role in EXON0 function we constructed a second deletion of only the first 37 amino acids (IE0-NH). Next to AI is a region rich in charged amino acids (C) from residue 65-87 followed by a second acidic region (AII) from residue 93-118. From residue 143-202 is a predicted coiled-coil or leucine zipper like domain (Leu) and at the C-terminal there is a RING finger-like domain (RING) from residue 209-261. To determine which of the putative domains of EXON0 were required for efficient budding, we constructed six mutants in which each one of the domains described above were deleted individually.

The bMON 14272 *exon0* KO bacmid (Chapter 2) was repaired with full length *exon0* or the six *exon0* deletion constructs which had all been tagged with the HA epitope at the N-terminus (Fig. 4.1B). The repair bacmids also contained *polyhedrin* and constitutively expressed *gfp* as a marker.

4.3.2 Analysis of EXON0 deletion mutant expression

Western blot analyses were performed to determine the expression of the six deletion mutants (Fig. 4.2A). Consistent with our previous study EXON0 was expressed at late times pt (Dai et al., 2004), HA-EXON0 in size of 30 kDa was detected at 24 hpt, peaked at 48 hpt and maintained a steady level up to 96 hpt. Analysis of the six EXON0 deletion mutants also detected a major band at the predicted sizes, but protein levels of these six mutants varied which is likely partially related to the BV production and further infection of cells beyond those originally transfected. *Exon0* KO-HA-EXON0-△RING showed

the highest levels of expression, followed by -△C and -△Leu, -△AI and -△IE0-NH. The exceptionally high level of EXON0-△RING and the high molecular forms of EXON0-△RING were consistent with the point mutants of EXON0 in the RING finger (Dai, et al, unpublished results), suggesting that the mutations of RING finger appear to increase the stability and affect the modification of EXON0. In addition to the major bands of the predicted sizes, the full length HA-EXON0, HA-EXON0-△C, -△AII, -△Leu, and -△RING also produced a band of a fixed size of about 40 kDa. However, HA-EXON0-△IE0-NH and -△AI which do not contain the IE0 splicing donor sequence did not produce the 40 kDa band, suggesting this band may be an artefact from non-specific splicing.

4.3.3 Plaque assay analysis

The initial analysis of BV production was done by comparing plaque size of *exon0* KO, *exon0* KO-HA-EXON0 and the six deletion mutant viruses (Fig. 4.2B). By 5 days pi, *exon0* KO-HA-EXON0 produced large WT like plaques. In comparison, the *exon0* KO plaques consisted primarily of a single cell or a few adjoining cells. All six mutant viruses showed much smaller plaques than full-length EXON0 virus but were generally larger than the *exon0* KO virus. The *exon0* KO-HA-EXON0-△C virus had the biggest plaque, followed by the *exon0* KO-HA-EXON0-△IE0-NH and *exon0* KO-HA-EXON0-△AII deletion viruses, *exon0* KO-HA-EXON0-△AI deletion virus showed the smallest plaque.

4.3.4 Virus growth curves

The BV production from each of the mutant EXON0 viruses was analyzed by comparing the growth curves (Fig. 4.2C). The BV production by *exon0* KO, *exon0* KO-HA-EXON0 (Chapter 2) virus and the control virus *ie1* KO-IE1 (Stewart et al., 2005) have been characterized and showed similar levels as previously described. The six EXON0 deletion viruses showed lower BV levels than *exon0* KO-HA-EXON0 virus, but levels were higher than *exon0* KO, suggesting that the mutants of EXON0 retained limited functionality. The BV production of the six deletion mutant viruses peaked at 72 hpt

between $1x10^5$ and $1x10^7$ $TCID_{50}$/ml, 2-4 logs lower than *exon0* KO-HA-EXON0 at 72 hpt. The *exon0* KO-HA-EXON0-△C and *exon0* KO-HA-EXON0-△AII viruses had the highest titers, while the *exon0* KO-HA-EXON0-△AI and *exon0* KO-HA-EXON0-△Leu viruses had the lowest titers of the six EXON0 deletion mutants. Interestingly, at 24 hpt, the titers of *exon0* KO-HA-EXON0-△C and *exon0* KO-HA-EXON0-△RING viruses were almost 100x higher than the other four deletion mutants. These two mutants therefore had a much more rapid production of BV between 12-24 hpt than △AI, △IE0-NH, △AII, and △Leu. However, despite this more rapid production of BV △C and △RING still only reached 1% of levels produced by full length EXON0. The domain mapping results therefore showed that all the six predicted domains were required for the efficient production of BV, but the deletion of the AI, and Leu domains had the greatest impact on the BV production.

4.3.5 Yeast two hybrid analysis of EXON0

The presence of a predicted leucine zipper domain in EXON0 suggested that EXON0 may form dimers or oligomers with itself or with other leucine zipper proteins. Initially the yeast 2-hybrid system was used to investigate if EXON0 forms homodimers or oligomers. The full length EXON0 was used as bait and the full length or mutant EXON0s were used as targets. Control experiments showed that EXON0 fused with BD transactivated the histidine reporter gene, allowing limited growth in the absence of an interacting partner (Fig. 4.3A). This suggested that full length EXON0 possessed a region that acted as a transactivation domain in yeast.

To find a construct that did not auto-transactivate but could still be used to investigate 2-hybrid formation, the six EXON0 mutants were fused with the GAL4 BD and transformed into YRG2 yeast cells. On the tryptophan and histidine dropout plates (Fig. 4.3B), EXON0-△IE0-NH, -△C, -△AII and -△Leu did not grow, suggesting that the deletion of each of these domains eliminated transactivation in yeast when fused to the BD domain. Interestingly, deletion of the AI domain appeared to enhance the growth, suggesting that the residues between 38 and 53 inhibited the auto-transactivation activity.

Therefore for 2-hybrid analysis EXON0-△IE0-NH which had the majority of the domains intact was used as the GAL4 BD fusion bait construct as it did not have any auto-transactivation activity.

The bait vector pBD-EXON0-△IE0-NH was co-transformed into YRG2 yeast cells with the empty AD vector or with the AD fused to full length or deletion mutant EXON0s. Colony growth on the Leu-Trp-His dropout plates indicated protein-protein interaction or dimer formation (Fig. 4.3C). Full length EXON0 showed strong growth, indicating that EXON0 forms dimers in yeast. The results also showed that deletion of the first 37 amino acids (EXON0-△IE0-NH) and the RING finger (EXON0-△RING) permitted yeast growth, indicating that these domains were not required for 2-hybrid formation. Deletion of AI, C, AII and Leu domains abolished the homodimerization of EXON0, suggesting that these domains were essential for the 2-hybrid formation.

4.3.6 Immunoprecipitation analysis of EXON0 dimer formation

To confirm the yeast 2-hybrid results, co-IP was used to show the dimer formation of EXON0 *in vivo*. A virus *exon0* KO-EXON0-FLAG was constructed which expressed EXON0 tagged at C-terminus with the FLAG epitope (Fig. 4.1B). To prepare cell lysate for co-IP, viral bacmid DNA of *exon0* KO, or *exon0* KO repaired by the six EXON0 domain deletion mutants and full length EXON0 were transfected into Sf9 cells, followed by the infection with *exon0* KO-HA-EXON0-FLAG. At 48 h pi, cells were collected and lysed for co-IP. The total expression (input) of EXON0-FLAG, the domain deletion mutants and full length HA-EXON0 was analyzed by western blot. The results showed all proteins were expressed (Fig. 4.4A). Cell lysates were immunoprecipitated with the anti-HA antibody and the, the purified proteins were collected and analyzed by western blot using the anti-FLAG antibody (Fig. 4.4B). The presence of EXON0-FLAG in the anti-HA immunoprecipitate indicated that the mutant or full length protein formed protein-portein complexes EXON0-FLAG was immunoprecipitated by full length HA-EXON0, confirming homodimers or multimers form *in vivo* (Fig. 4.4B). Of the six domain deletion mutants, HA-EXON0-△IE0-NH, -△AI, and -△RING

immunoprecipitated with EXON0-FLAG, whereas HA-EXON0-△C, -△AII and -△Leu did not. This result showed that *in vivo* the C, AII and Leu domains were required for EXON0-EXON0 interaction.

4.3.7 Identification of residues of EXON0 required for the efficient budding and dimerization

Deletion mutation of EXON0 can potentially disrupt tertiary structures of a protein and therefore have indirect effects on function and protein-protein interactions. Therefore to complement the EXON0 domain deletion results site directed point mutations were constructed that maintained the full length protein. To categorize critical amino acids in each domain a clustalW analysis was performed on the homologues of EXON0 from lepitopteran NPVs to identify highly conserved residues (Fig. 4.5). Highly conserved amino acids in each domain were mutated to either a alanine or a proline and eleven point mutants were generated in HA-EXON0 covering the AI , C, AII, and Leu domains. Each of the amino acid changes made for each mutant are shown in Fig. 4.5. The RING domain which is unique has been analyzed in much greater details by point mutation in another study (Dai et al., manuscript in preparation). As a control, a neutral mutant within the leucine zipper region was constructed where the non-conserved L157, which is predicted not to be in a critical position of the heptad repeat, was mutated to alanine (L157/A). The EXON0 point mutants were introduced into the bMON14272 *exon0* KO bacmid by transposition.

The repaired bacmids were transfected into Sf9 cells and BV supernatants and cells were collected at 96 hpt. Western blot analysis of infected cells showed that all point mutants were expressed and migrated at the predicted size of 30 kDa (Fig. 4.6A). The protein levels varied which is likely due to the varying abilities to produce BV and to generate secondary infections.

Yeast 2-hybrid analysis and IP above showed that EXON0 interacted with itself to form dimers or multimers. To further analyze this homologous interaction and to determine

the critical residues of EXON0 required for dimerization, the effects of EXON0's point mutations on dimer formation were analyzed by non-reducing SDS-PAGE and western blot as previously described (Monsma and Blissard, 1995). Under non-reducing conditions the WT HA-EXON0 produced the 30 kDa monomeric form (Fig.4.6B, lane 1). In addition, higher molecular weight forms of WT EXON0 were detected of approximately 60, 64 and 68 kDa of which the latter two were detected in smaller proportion. This would agree with the predicted size of an EXON0 dimer of approximately 60 kDa. This result, combined with the yeast two-hybrid results that EXON0 interacted with itself directly (Fig. 4.4), suggests EXON0 forms homodimers (Dimer I). The 64 and 68 kDa higher molecular weight forms of EXON0 could also be dimers (Dimer II and III) whose migration is affected by post-translational modifications or the binding of other molecules in the non-reducing condition.

The eleven point mutants of EXON0 were also examined for their ability to form dimers as indicated by the formation of the 60 kDa product in non-reducing gels (Fig. 4.6B). The neutral control mutant L157/A (lane 9) and C231C232/AA mutant (lane 12) in the RING finger domain showed the same high molecular weight dimers as WT EXON0, suggesting the RING finger is not required for the dimerization. Of 10 other point mutants, the mutants in Leu domain, L155F162I169/AAA, V176L190/AA and L190/P abolished the dimers, seven other mutants reduced the dimer formation, indicating the L155, F162, I169, V176 and L190 which are on the critical position of heptad repeat are required for the dimer formation, other conserved residues in AI, C, and AII domain help the dimerization. The mutation of single leucine (L190/P) in the predicted heptad repeat of the leucine zipper also eliminated dimer formation (lanes11, Fig. 4.6B). This strongly supports the conclusion that this region is forming a classic leucine zipper structure as predicted. In addition, the C230C231/AA mutant still produced three bands of 60, 64 and 68 kDa, confirming the RING finger is not required for dimerization.

The effects of all the point mutations of EXON0 on BV production were examined by determining the $TCID_{50}$ of each virus at 96 hpt. All mutants except for the control neutral mutant L157/A exhibited significantly lower titres (2 to 4 logs) of BV compared

to the EXON0-HA. Mutant L190/P, in which the substituted proline could cause the disruption of the predicted α-helix of the coiled-coil region, produced the lowest BV level compared to other alanine substitution mutants in the Leu domain which may weaken the hydrophobic interaction and dimer formation. The $TCID_{50}$ assays revealed the conserved residues in C, AII and Leu domain are essential for the efficient BV production as well as dimer formation.

4.3.8 Identification of domains and residues of EXON0 required for the association with β-tubulin, FP25 and BV/ODV-C42

In Chapter 2 and 3, EXON0 has been shown to interact with β-tubulin, FP25 and BV/ODV-C42. To determine the domains of EXON0 required for the association with above three proteins, Sf9 cells were infected with WT AcBac expressing the deletion and point mutants of EXON0 to obtain large-scale infection and high protein levels of EXON0 mutants. Cells were collected at 24 hpi and lyzed for co-IP. After immunoprecipitation with anti-HA beads (Fig. 4.7), β-tubulin was detected from WT EXON0, EXON0-ΔIE0-N, -ΔAI and –ΔRING, but not –ΔC, -ΔAII and –ΔLeu, suggesting these three domains are involved in the association with β-tubulin. Results also showed that the deletion of C, AII and Leu domains reduced the interaction with both BV/ODV-C42 and FP25. For FP25, the absence of AI also reduced its association.

The effects of EXON0 point mutation on the association with these three proteins were also investigated. After immunoprecipitation with HA antibody, β-tubulin, FP25 and BV/ODV-C42 were all detected from WT EXON0, L157/A and C231C232/AA mutants, suggesting L157, C231, C232 do not impact on the association of EXON0 with these three proteins (Fig. 4.8). F44F46M49, K59R65/AA, C111/A, V141V143L148/AAA reduced the association with β-tubulin, while V64F69I72/AAA, I116I122I126/AAA, L155F162I169/AAA, V176L190/AA and L190/P abolished the β-tubulin association. The point mutation of conserved residues in the Leu domain reduced association with both BV/ODV-C42 and FP25. The K59R65 abolished the association with BV/ODV-C42. In addition, the C111/A and H113/A mutants also reduced the association with

BV/ODV-C42. In summary, the Leu domain which is required for dimerization is also essential for association with β-tubulin, BV/ODV-C42 and FP25, and the conserved residues in AI, C, and AII domains contribute to the associations.

4.4 Discussion

Recently we showed that AcMNPV *exon0* is a key late gene as it is required for the efficient production of BV (Dai et al., 2004). In Chapter 2 and 3 I showed that nucleocapsid protein FP25, BV/ODV-C42 and cellular β-tubulin interacted with EXON0. In this study, regions and critical residues of EXON0 were mapped that are required for efficient BV production and association with above three proteins by constructing viruses that express different mutants that have domain deletions and amino acid substitutions. Mutation of the acidic I (AI) domain and the leucine zipper domain (Leu) caused the greatest reduction in BV production. However, all domains impacted on BV production suggesting that EXON0 may have a complex structure and may require interactions with multiple proteins for complete functionality. In addition, yeast 2-hybrid, co-IP and non-reducing SDS-PAGE show that EXON0 forms dimers. The domains of EXON0 required for the efficient budding, dimerization, association with β-tubulin, FP25 and BV/ODV-C42 are summarized in Fig. 4.9. The IE0-N and RING finger domains at the two terminals are not required for either dimerization, or the association with β-tubulin, FP25 and BV/ODV-C42 although they are required for the BV production at WT levels. The Leu domain is required for the dimerization, the association with β-tubulin and BV/ODV-C42 and is also essential for interaction with FP25. The conserved residues in C, AII domains are also important as their changes to alanines abolished or reduced the dimerization, association with β-tubulin and BV/ODV-C42. The deletion of C, AII domains also abolished the dimerization (Fig. 4.3 and 4.4) and association with β-tubulin (Fig. 4.7), suggesting the absence of these two domains has more significant effects than the point mutations (Fig. 4.6 and 4.8). No specific domain abolished association with FP25 suggesting some of the residues of EXON0 that were not deleted in this study are responsible for or the combination of C, AII and Leu domains participates in the interaction. Another possibility is that EXON0 could interact with FP25 both directly and indirectly. Alternatively, as all the point mutants were expressed with a background of WT EXON0 present it is possible that mutant-WT EXON0 dimers were formed that retained the ability to bind FP25.

The presence of a predicted leucine zipper domain suggested that EXON0 may form dimers or oligomers with itself or with other leucine zipper proteins. Using the yeast 2-hybrid system and co-immunoprecipitation, and point mutations we showed that EXON0 forms homodimers that requires the leucine zipper (Fig. 4.3, 4.4, and 4.6). However, the results also showed that the conserved residues in C and AII domains help dimer formation (Fig. 4.6). This is unlike many leucine zipper proteins whose dimerization usually only requires a coiled-coil domain (Kouzarides et al., 1991; Landschulz, Johnson, and McKnight, 1988; Sinclair and Farrell, 1992). In baculoviruses for example, only the C-terminal leucine zipper of *Bombyx mori* NPV IE2 has been shown to be required for the dimerization and foci formation (Imai et al, 2005). Mutation or deletion of the leucine zipper of AcMNPV IE2 reduced or abolished the transactivation activity showing the importance of dimer formation for functionality (Yoo and Guarino, 1994). For EXON0, the requirement of the Leu domain in combination with the C, and AII domains for optimal dimerization reflects that a unique conformation of EXON0 and/or the interaction with other proteins may be required for its dimer formation.

Yeast 2-hybrid assays showed that full-length EXON0 fused with the GAL4 BD contained a potential transcriptional transactivating domain (Fig. 4.3). The regions of EXON0 required for transactivation in yeast were mapped to the IE0-NH, C, AII and Leu domains. The residues between amino acid 38 and 53, however, inhibited the transactivation activity. A herpesvirus protein UL48 that is required for virion egress also has transactivation activity on viral early gene promoters but also interacts with other tegument proteins. Deletion of UL48 results in impaired cytoplasmic assembly of virions (Newcomb et al., 1993). It is therefore possible that one of the functions of EXON0 may include activation of gene expression. Further studies will, however, have to be performed to determine if transcriptional transactivating activity of EXON0 is observed in insect cells during infection.

EXON0 also contains a novel RING domain (Dai et al., 2004) which suggests that the ubiquitin pathway may play a role in the function of this protein. The deletion of the

RING domain results in a significant drop in BV production, showing that it is required. In addition, the appearance of more high molecular weight bands and more accumulation of RING finger mutants (Fig. 4.2 and Dai, personal communication) suggest aberration of the RING finger changes the post-translational modification and stability of EXON0. RING domains have been shown to be consistently associated with E3 ubiquitin ligases and it is required for binding E2 ubiquitin conjugating enzymes. Loss of the RING domain therefore may abolish interactions with proteins involved in the ubiquitination pathway that are required for BV production. In support of this it has been clearly shown that ubiquitination processes are required for retrovirus budding (Bashirova et al., 2006; Stanke et al., 2005).

For other DNA viruses, viral egress and budding has been shown to require many different proteins that are involved in diverse functions. In HSV-1 infected cells approximately 25 different genes may play a role in HSV-1 nucleocapsid transport from the nucleus and budding from the plasma membrane (Mettenleiter, 2002b). This includes UL31 and UL34 which if knocked out create viruses deficient in plaque formation, and titers are reduced more than 100-fold similar to the AcMNPV *exon0* knockout phenotype. UL31 and UL34 have been shown to associate with each other by yeast 2-hybrid and glutathione-*S*-transferase pull down assays. These proteins are associated with the nuclear membrane and may be required for partial dismantling of the nuclear lamina allowing nucleocapsid transport to the cytoplasm (Fuchs et al., 2002b; Mettenleiter, 2002b; Schnee et al., 2006).

It is clear from other viral systems that the process of baculovirus nucleocapsid egress from the nucleus to the plasma membrane and budding is likely to involve many viral proteins in addition to EXON0. Baculoviruses also have the additional complexity of having to direct nucleocapsids to two final destinations, ODV formation in the nucleus and BV budding from the plasma membrane. EXON0 appears to play a key role in the latter. In this study the domains of EXON0 which interact with the viral proteins FP25, ODV-C42, and the cellular protein β-tubulin are identified. In addition, it is unknown at what point in the pathway of BV egress that these interactions with EXON0 are required.

Figure 4.1 Schematic diagrams of the domains of AcMNPV EXON0, EXON0 mutants and repair viruses.

(A) EXON0 domain deletions were constructed and tagged with either the FLAG or HA-epitopes at the C-terminal of EXON0. IE0-NH domain consists of the first 37 residues which form the amino terminal of the transactivator IE0 due to an early splicing event. The first 53 residues are rich in acidic residues and is designated Acidic domain I (AI). ΔC deletes residues 65 to 85 which contain a domain rich in charged amino acids. ΔAII deletes the second acidic domain (AII) located from residue 93 to 118. The ΔLeu deletes the predicted leucine zipper domain (residue 143 to 202) and ΔRING deletes the unique C-terminal C3YC4 RING finger (residue 209 to 261). EXON0 was also tagged at the C-terminus with the FLAG epitope (EXON0-FLAG) and the HA epitope (EXON0-HA). A series of point mutations were generated in the AI, C, AII, and Leu domains in the C-terminus tagged EXON0-HA (EXON0-HA point mutants). (B) Schematic diagrams of *exon0* KO repaired viruses showing the genes inserted into the polyhedrin (*polh*) locus by Tn*7*-mediated transposition. This includes the six deletion mutants *exon0* KO-HA-EXON0-ΔIE0-NH, -ΔAI, -ΔC, -ΔAII, -ΔLeu, -ΔRING, *exon0* KO-EXON0-FLAG, *exon0* KO -EXON0-HA and EXON0-HA point mutants. HA, HA-epitope tag, FLAG, FLAG-epitope tag, polh, *polyhedrin*; GFP, green fluorescent protein.

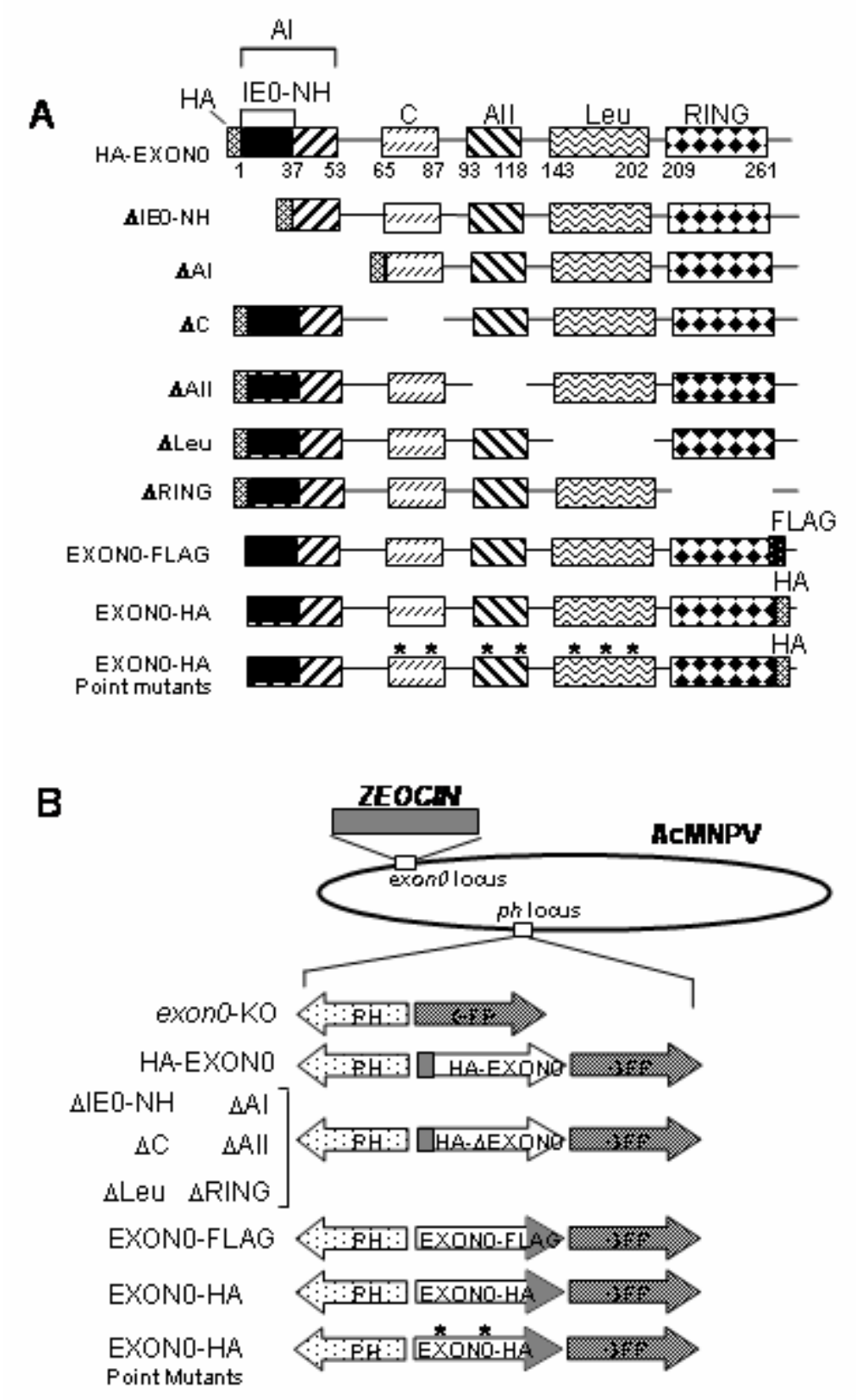
A
AI
HA
IE0-NH
C
AII
Leu
RING
HA-EXON0
1 37 53 65 87 93 118 143 202 209 261
ΔIE0-NH
ΔAI
ΔC
ΔAII
ΔLeu
ΔRING
FLAG
EXON0-FLAG
HA
EXON0-HA
HA
EXON0-HA
Point mutants
B
ZEOCIN
AcMNPV
exon0 locus
ph locus
exon0-KO
PH
GFP
HA-EXON0
HA-EXON0
ΔIE0-NH
ΔAI
ΔC
ΔAII
ΔLeu
ΔRING
HA-ΔEXON0
EXON0-FLAG
EXON0-FLAG
EXON0-HA
EXON0-HA
EXON0-HA
Point Mutants

Figure 4.2 Domains of EXON0 required for the efficient BV production.
(A) Western blot analysis of full length HA-EXON0 and EXON0 domain deletions. Bacmid-transfected Sf9 cells were collected at designated times post transfection, EXON0 proteins were detected with anti-HA monoclonal antibody which recognizes the HA-tag on each construct. The full-length and all EXON0 deletion proteins were detected and migrated at the predicted sizes. (B) Plaque assay analysis of *exon0* KO, *exon0* KO-HA-EXON0 and six EXON0 domain deletion viruses in infected Sf9 cells. Fluorescence micrographs of plaques formed by each virus in infected Sf9 cells at 5 days p.i. (C) BV growth curves of the six EXON0 domain deletion viruses in transfected Sf9 cells. Sf9 cells were transfected with 1.0 μg of bacmid DNA of each virus, and the cell culture supernatants were harvested and assayed for the production of infectious virus by $TCID_{50}$ assays. Each data point represents the average titer derived from two independent $TCID_{50}$ assays.

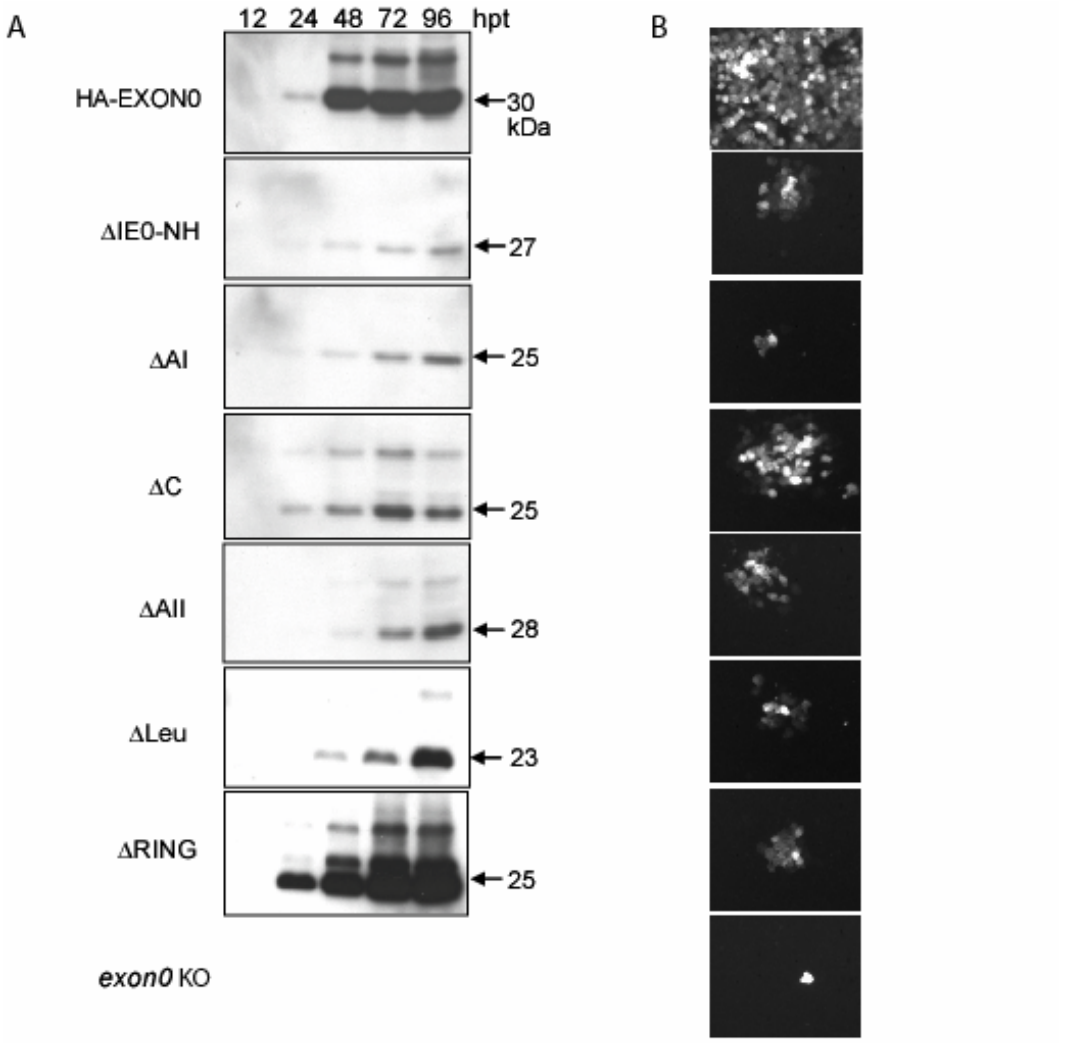
A
12 24 48 72 96 hpt
HA-EXON0
30 kDa
ΔIE0-NH
27
ΔAI
25
ΔC
25
ΔAII
28
ΔLeu
23
ΔRING
25
exon0 KO
B
C
TCID 50 (log)
hours post transfection
0 12 24 36 48 60 72 84 96
0 1 2 3 4 5 6 7 8 9
HA-EXON0
exon0 KO
ie1 KO-IE1
ΔIE0-NH
ΔAI
ΔC
ΔAII
ΔLeu
ΔRING

Figure 4.3 Yeast 2-hybrid analysis of EXON0.

(A) Autoactivation analysis of full-length EXON0 fused to the binding domain or activation domain of GAL4 using the yeast vectors pBD-Gal4Cam and pAD-Gal4-2.1 respectively. The fusion plasmids were transformed into YRG2 yeast cells and plated on Tryptophan, Leucine and Histidine dropout SD plate. (B) Autoactivation analysis of the EXON0 deletions fused to the GAL4 binding domain to identify domains of EXON0 responsible for transcriptional transactivation in yeast. Plasmids were transformed into YRG cells and selected on Tryptophan and Histidine dropout SD plate in triplicate**.** (C) Yeast 2-Hybrid analysis showing interactions between pBD-△IE0-NH and EXON0 domain deletion constructs cloned into pAD-Gal4-2.1. Plasmids were cotransformed into yeast YRG cells and selected on Tryptophan, Leucine and Histidine dropout SD plate in triplicate.

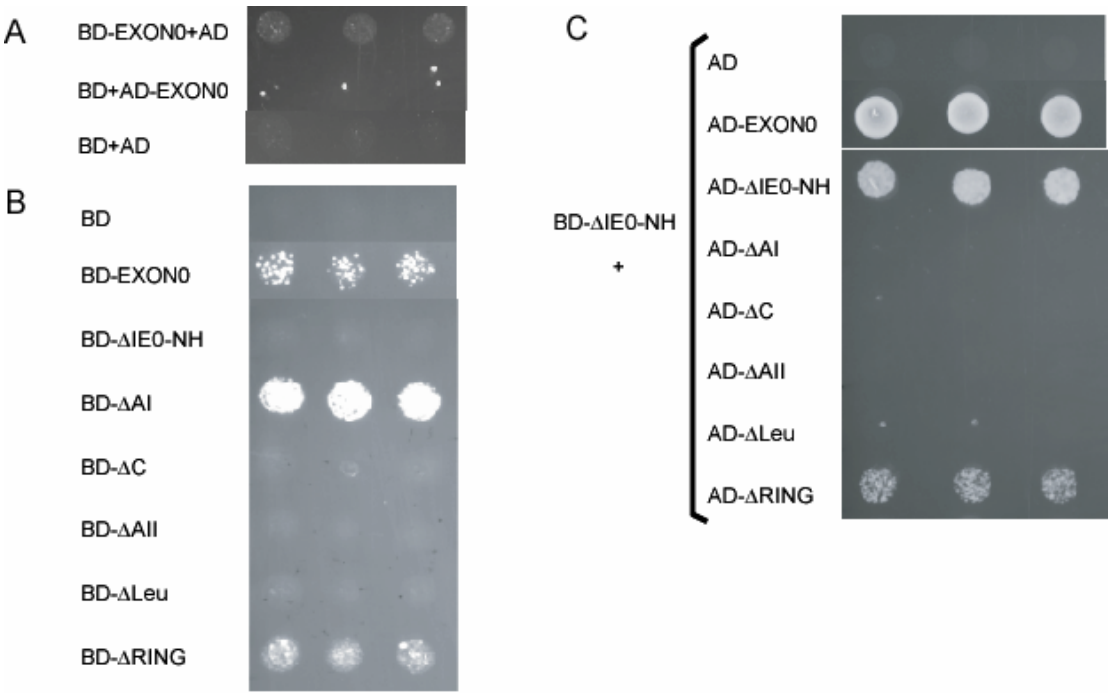

Figure 4.4 Co-IP to confirm homodimer formation of EXON0 in vivo.
Sf9 cells were transfected with bacmid DNA of *exon0* KO, *exon0* KO-HA-EXON0 and the six HA-EXON0 domain deletion viruses followed by infection with *exon0* KO-EXON0-FLAG virus (Fig. 4.2) at an MOI of 10. At 48 hpi, cells were collected and lysed for IP. (A) Western blot analysis of 1.25% of the total cell lysate to confirm expression of input proteins probed with either anti-FLAG (upper panel) or anti-HA (lower panel) antibodies. (B) Proteins were immunoprecipitated using anti-HA antibodies and samples were analysed by Western blot using anti-FLAG (upper panel) and anti-HA antibodies (lower panel). For Western blot, 25% of the IP eluate was loaded.

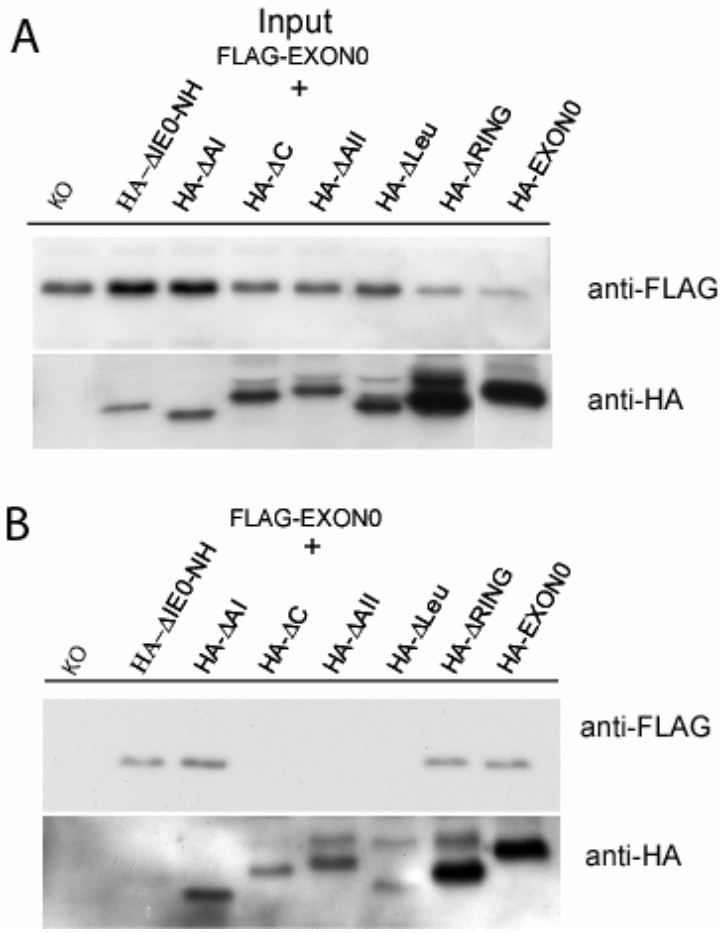

Figure 4.5 Alignment of EXON0 homologs and location of point mutations.
ClustalW (Thompson et al, 1994) alignment of EXON0 homologues from 21 lepidopteran NPVs. Amino acids with a black background show 100% conservation, dark grey represents 80% and light grey for 60%. The conserved residues of EXON0 in C, AII and Leu domains were mutated to alanines or proline as indicated with asterisks. The predicted AI, C, AII, Leu and RING finger domains are shown above the domains. Rules to assign conservation are as: A = G = S = T, V = L = I = M = F = Y = W, N = Q = D = E, and R = K = H. Mutants are #1 F44F46M49/AAA, #2 K59R65/AA, #3 V64F69I72/AAA, #4 I116I122I126/AAA, #5 C111/A, #6 H113/A, #7 V141V143L148/AAA, #8 L155F162I169/AAA, #9 L157/A, #10 V176L190/AA, #11 L190/A. Genbank number of these EXON0s are following: NP_703128 for RaouMPNV (Raou), NP_054172 for AcMNPV (Ac), YP_203292 for EppoNPV (Eppo), NP_046294 for OpMNPV (Op), NP_932743 for CfMNPV (Cf), YP_803531 for AngeMNPV (Ange), YP_473204 for HycuNPV (Hycu), YP_610986 for AnpeNPV (Anpe), YP_ 529822 for AgseNPV (Agse), NP_075077 for HaSNPV (Ha), NP_047657 for LdMNPV (Ld), NP_613251 for MacoNPV-A (MacoA), NP_037898 for SeMNPV (Se), NP_258276 for SpliMNPV (Spli), NP_818672 for AdhoNPV (Adho) , YP_249614 for ChchNPV (Chch), YP_717549 forClbiNPV (Clbi), YP_874205 for EcobNPV (Ecob), YP_758305 for LeseNPV (Lese), YP_308899 for TniSNPV (Tni).

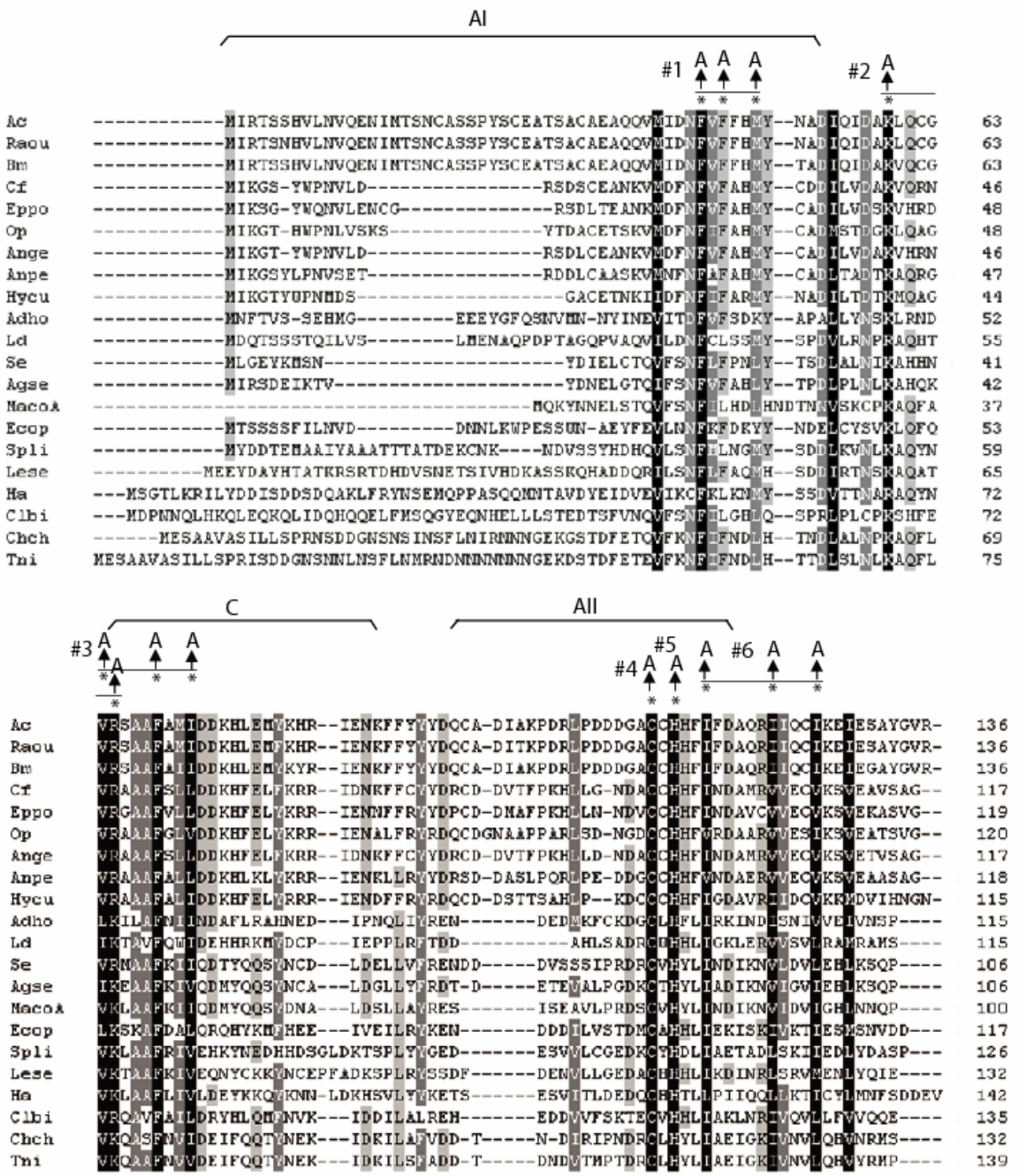
AI
#1
#2
C
AII
#3
#4
#5
#6
Ac
Raou
Bm
Cf
Eppo
Op
Ange
Anpe
Hycu
Adho
Ld
Se
Agse
MacoA
Ecop
Spli
Lese
Ha
Clbi
Chch
Tni

Fig. 4.5 continued

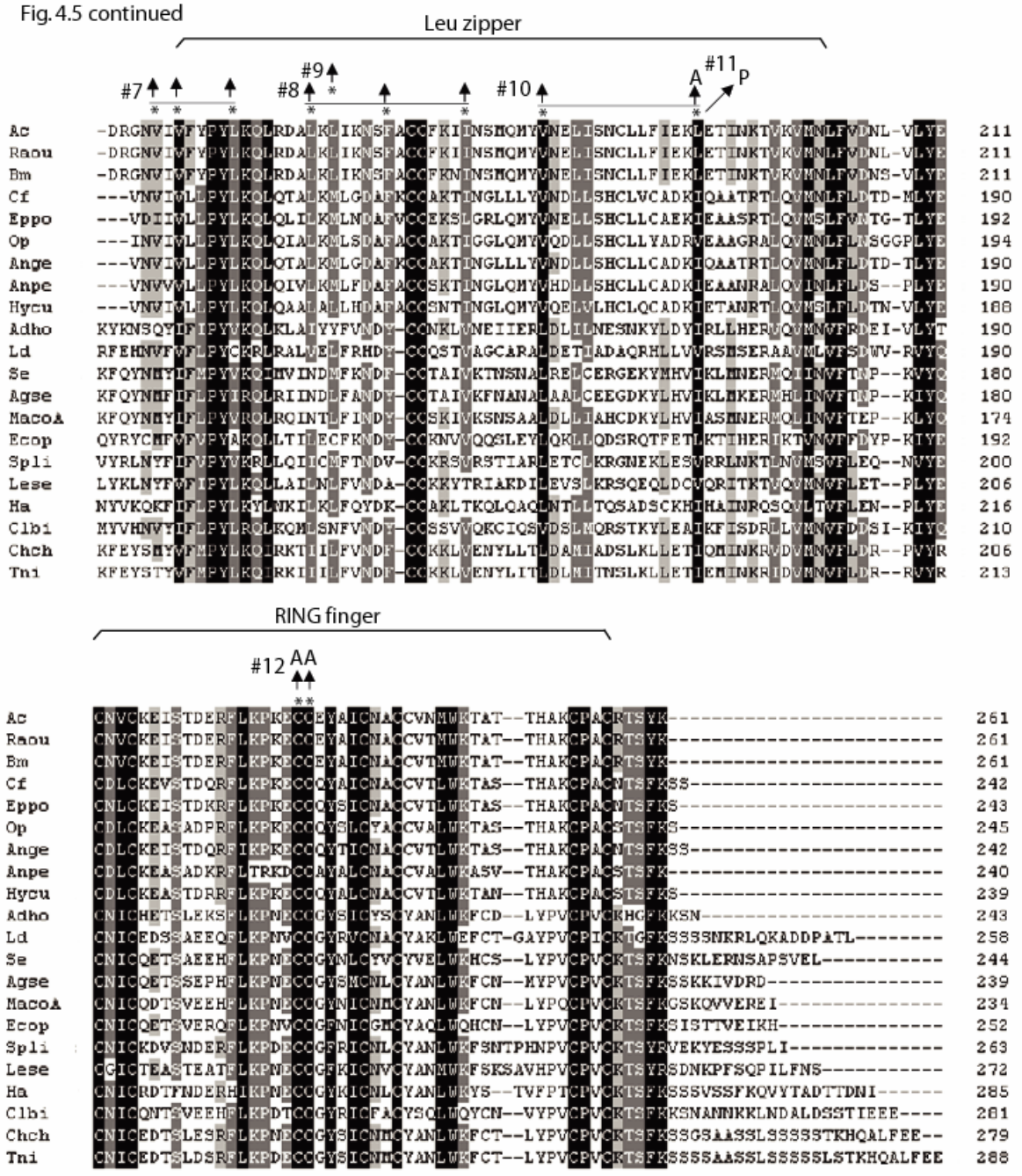

Figure 4.6 Analysis of EXON0 point mutations on EXON0 dimerization and BV production.

Western blot analysis of a (A) reducing and a (B) non-reducing SDS-PAGE gel of Sf9 cells transfected with EXON0 point mutants at 96 hpt. In panel A, approximately 5×10^4 transfected cells were loaded each lane. In panel B, to get similar protein level of EXON0, varible amount of cells ($5\text{-}15\times10^4$) were loaded into each lane. Monomeric EXON0 is detected at 30 kDa and dimers are observed at approximately 60 kDa of which there are three forms (Dimer I, II, and III). EXON0 point mutants were detected with anti-HA monoclonal antibody. Molecular weight markers are shown on the left in kDa. (C) Titration of HA-EXON0 and point mutant BV at 96 hpt from the supernatants of the samples in A as determined by end point dilution assays. The changed residues of each mutant are shown at the bottom of the graph. Titers were done in duplicate and average titers are shown. Lane WT, WT EXON0-HA; Lane 1, F44F46M49/AAA; Lane 2, K59R65/AA; Lane 3, V64F69I72/AAA; Lane 4, I116I122I126/AAA; Lane 5, C111/A; Lane 6, H113/A; Lane 7, V141V143L148/AAA; Lane 8, L155F162I169/AAA; Lane 9, L157/A; Lane10, V176L190/AA; Lane 11, L190/A; CC/AA, C230C231/AA.

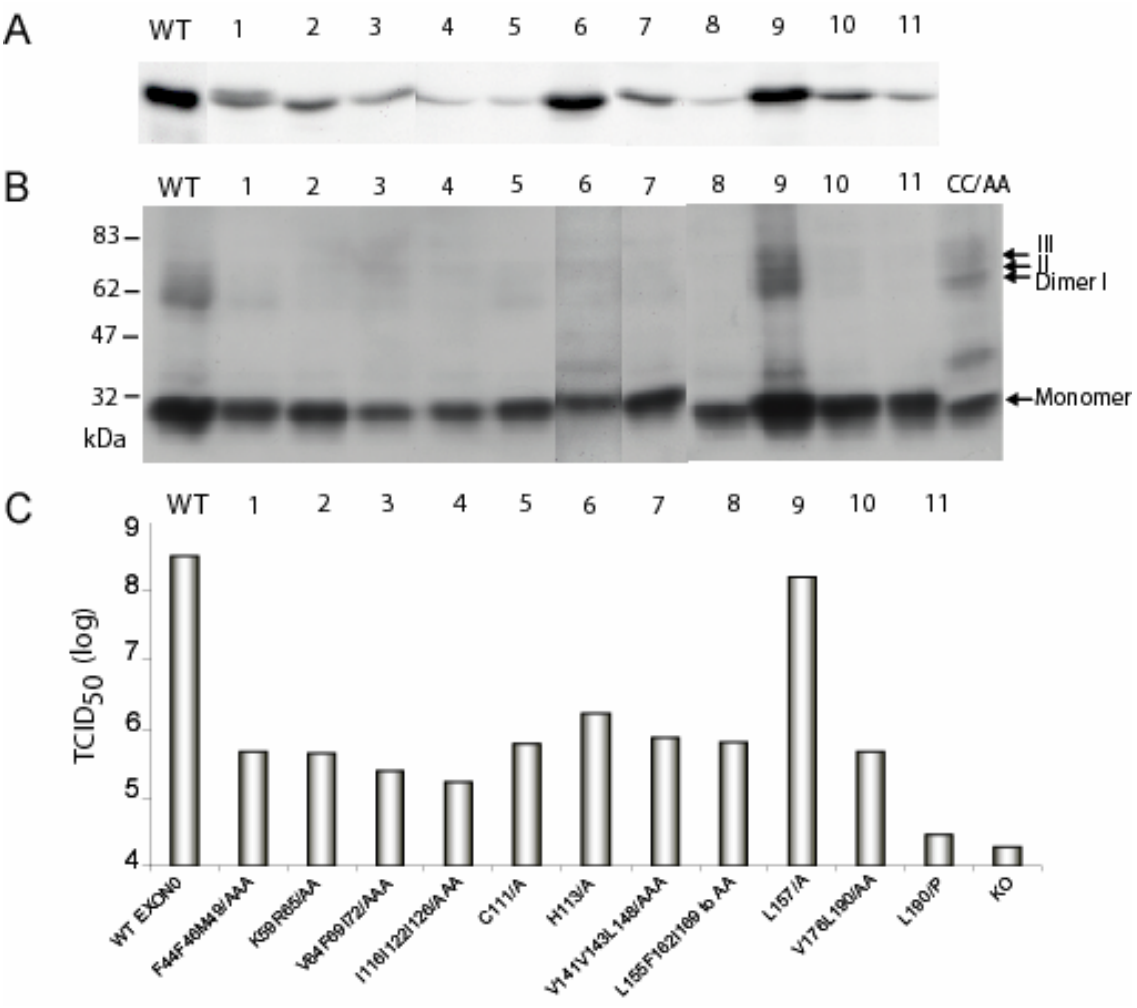
A
WT 1 2 3 4 5 6 7 8 9 10 11
B
WT 1 2 3 4 5 6 7 8 9 10 11 CC/AA
83
62
47
32
kDa
III
II
Dimer I
Monomer
C
WT 1 2 3 4 5 6 7 8 9 10 11
TCID50 (log)
9
8
7
6
5
4
WT EXON0
F44F46M49/AAA
K59R65/AA
V64F69I72/AAA
I116I122I126/AAA
C111/A
H113/A
V141V143L148/AAA
L155F162I169 to AA
L157/A
V176L180/AA
L190/P
KO

Figure 4.7 Domains of EXON0 required for the association with β-tubulin, BV/ODV-C42 and FP25.

Sf9 cells were infected with WT AcBac (-) or WT AcBac expressing HA-EXON0 or the six HA-EXON0 domain deletion viruses at an MOI of 10. At 24 hpi, cells were collected and lysed for IP. Upper panel, IP input, Western blot analysis of total cell lysate (0.025% of total sample) to confirm expression of input proteins probed with anti-HA, -β-tubulin, -BV/ODV-C42 and -FP25 antibodies. Lower panel, IP eluate, proteins immunoprecipitated with anti-HA antibodies were analysed by Western blot using anti-HA, -β-tubulin, -BV/ODV-C42 and -FP25 antibodies. Approximately 8.75% of the total IP eluate was loaded for each lane. Protein size markers are indicated on the left.

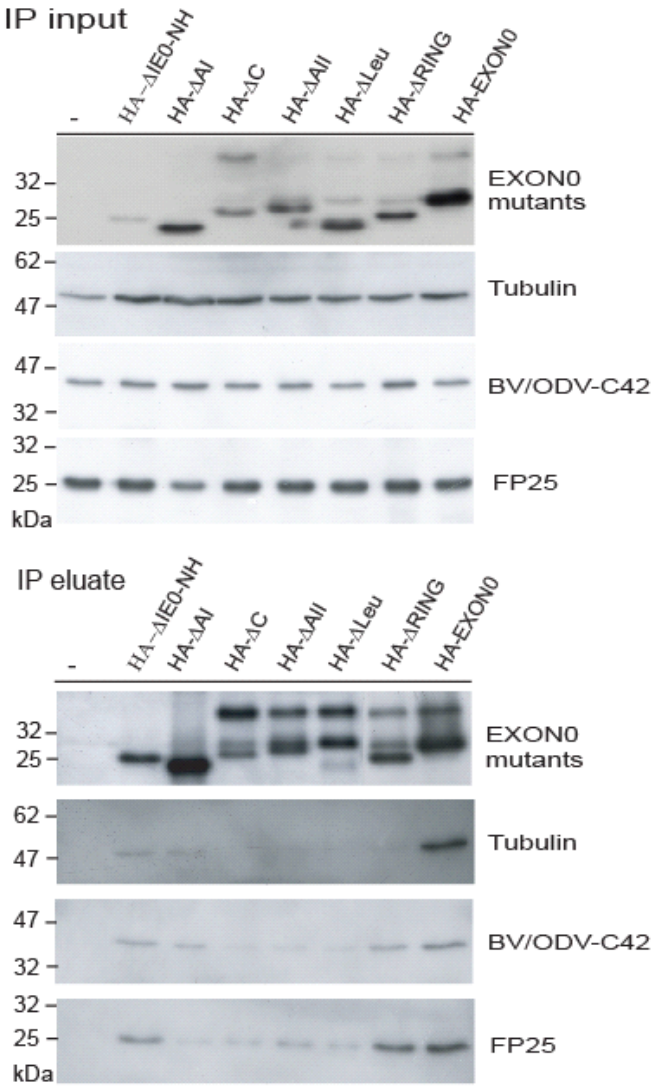

Figure 4.8 Co-immunoprecipitation of EXON0 mutants with β-tubulin, BV/ODV-C42 and FP25.

The ability of EXON0 point mutants to co-immunoprecipitate β-tubulin, BV/ODV-C42 or FP25 was examined by infecting Sf9cells with WT AcBac (-) or WT AcBac expressing EXON0-HA and the 12 point mutants of EXON0-HA at an MOI of 10. At 24 hpi, cells were collected and lysed for IP. Upper, 0.025 % of the total cells lysate was loaded in each lane. After immunoprecipitated with anti-HA antibodies, 10% of the total eluates were analysed by Western blot using anti-HA, anti-β-tubulin, anti-BV/ODV-C42 or anti-FP25 antibodies. Lanes: -, no HA tag; WT, WT EXON0-HA; 1, F44F46M49/AAA; 2, K59R65/AA; 3, V64F69I72/AAA; 4, I116I122I126/AAA; 5, C111/A; 6, H113/A; 7, V141V143L148/AAA; 8, L155F162I169/AAA; 9, L159/A; 10, V176L190/AA; 11, L190/P; 12, C230C231/AA. Protein markers were indicated on the left.

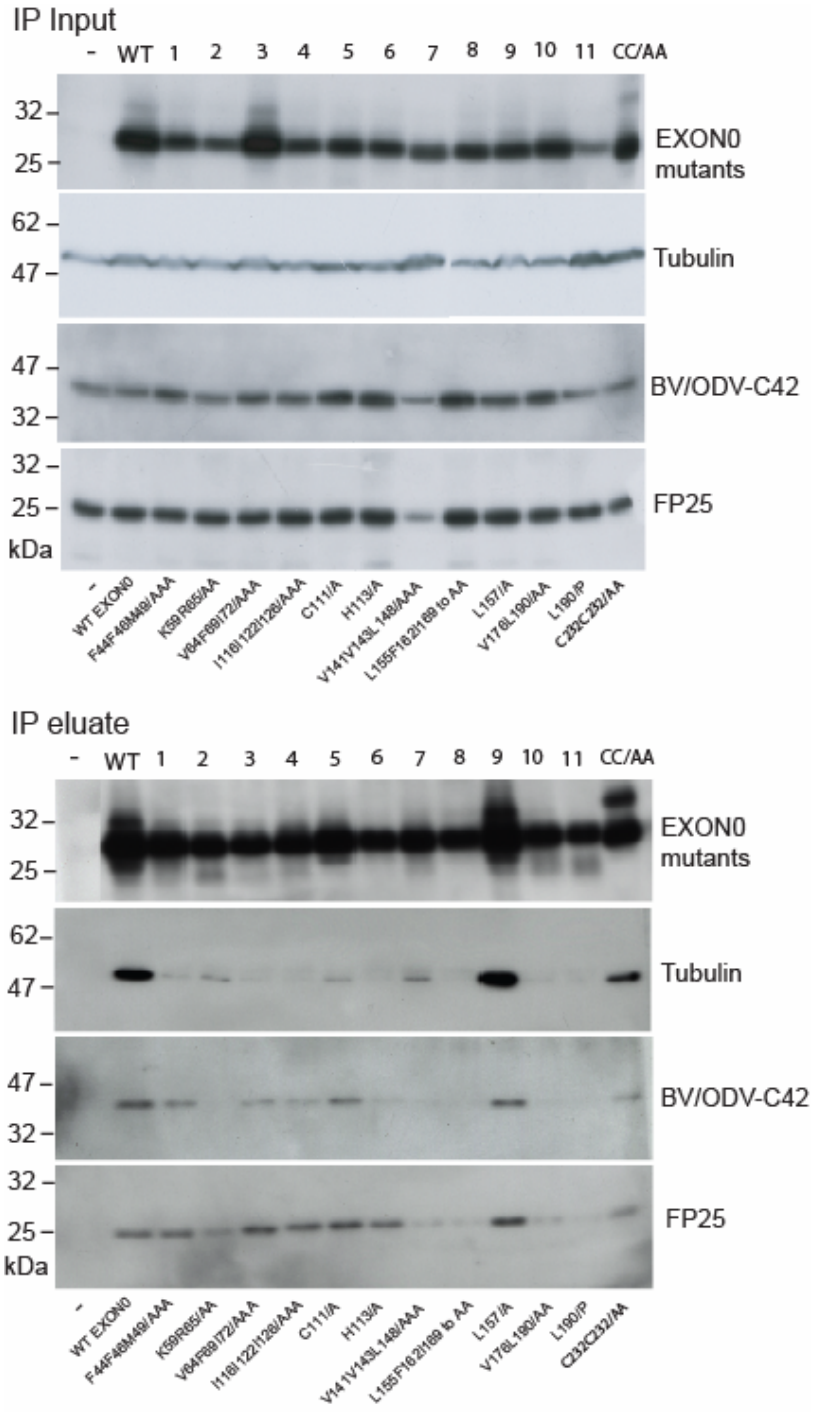
IP Input
- WT 1 2 3 4 5 6 7 8 9 10 11 CC/AA
32
25
EXON0 mutants
62
47
Tubulin
47
32
BV/ODV-C42
32
25
kDa
FP25
-
WT EXON0
F44F46M46I/AAA
K59R65/AA
V64F68I72/AAA
I116I122I126I/AAA
C111/A
H113/A
V141V143L148/AAA
L155F162I169 to AA
L157/A
V176L190/AA
L190/P
C232C232/AA
IP eluate
- WT 1 2 3 4 5 6 7 8 9 10 11 CC/AA
32
25
EXON0 mutants
62
47
Tubulin
47
32
BV/ODV-C42
32
25
kDa
FP25
-
WT EXON0
F44F46M46I/AAA
K59R65/AA
V64F68I72/AAA
I116I122I126I/AAA
C111/A
H113/A
V141V143L148/AAA
L155F162I169 to AA
L157/A
V176L190/AA
L190/P
C232C232/AA

Figure 4.9 Summary of EXON0 domains required for efficient production of BV, dimerization, association with β-tubulin or BV/ODV-C42, and transactivation in yeast.

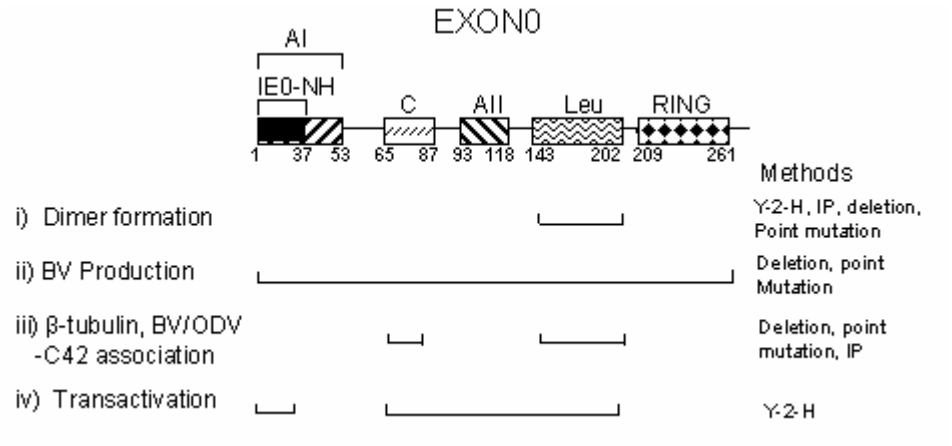

4.5 References

Bashirova, A. A., Bleiber, G., Qi, Y., Hutcheson, H., Yamashita, T., Johnson, R. C., Cheng, J., Alter, G., Goedert, J. J., Buchbinder, S., Hoots, K., Vlahov, D., May, M., Maldarelli, F., Jacobson, L., O'Brien S, J., Telenti, A., and Carrington, M. (2006). Consistent effects of TSG101 genetic variability on multiple outcomes of exposure to human immunodeficiency virus type 1. *J. Virol.* **80**(14)**,** 6757-6763.

Blissard, G. W., and Wenz, J. R. (1992). Baculovirus gp64 envelope glycoprotein is sufficient to mediate pH-dependent membrane fusion. *J. Virol.* **66**(11)**,** 6829-6835.

Craven, R. C., Harty, R. N., Paragas, J., Palese, P., and Wills, J. W. (1999). Late domain function identified in the vesicular stomatitis virus M protein by use of rhabdovirus-retrovirus chimeras. *J. Virol.* **73**(4)**,** 3359-3365.

Dai, X., Stewart, T. M., Pathakamuri, J. A., Li, Q., and Theilmann, D. A. (2004). *Autographa californica* multiple nucleopolyhedrovirus exon0 (orf141), which encodes a RING finger protein, is required for efficient production of budded virus. *J. Virol.* **78**(18)**,** 9633-9644.

Friesen, P. D. (1997). "Regulation of baculovirus early gene expression." Baculovirus (L. K. Miller, Ed.) Plenum Publishing Corporation, New York.

Fuchs, W., Klupp, B. G., Granzow, H., Osterrieder, N., and Mettenleiter, T. C. (2002). The interacting UL31 and UL34 gene products of pseudorabies virus are involved in egress from the host-cell nucleus and represent components of primary enveloped but not mature virions. *J. Virol.* **76**(1)**,** 364-378.

Gottlinger, H. G., Dorfman, T., Sodroski, J. G., and Haseltine, W. A. (1991). Effect of mutations affecting the p6 gag protein on human immunodeficiency virus particle release. *Proc. Natl. Acad. Sci. U. S. A.* **88**(8)**,** 3195-3199.

Harty, R. N., Brown, M. E., Wang, G., Huibregtse, J., and Hayes, F. P. (2000). A PPxY motif within the VP40 protein of Ebola virus interacts physically and functionally

with a ubiquitin ligase: implications for filovirus budding. *Proc. Natl. Acad. Sci. U. S. A.* **97**(25)**,** 13871-13876.

Imai, N., Matsumoto, S., and Kang, W. (2005). Formation of *Bombyx mori* nucleopolyhedrovirus IE2 nuclear foci is regulated by the functional domains for oligomerization and ubiquitin ligase activity. *J. Gen. Virol.* **86**(Pt 3)**,** 637-644.

Kouzarides, T., Packham, G., Cook, A., and Farrell, P. J. (1991). The BZLF1 protein of EBV has a coiled coil dimerisation domain without a heptad leucine repeat but with homology to the C/EBP leucine zipper. *Oncogene* **6**(2)**,** 195-204.

Landschulz, W. H., Johnson, P. F., and McKnight, S. L. (1988). The leucine zipper: a hypothetical structure common to a new class of DNA binding proteins. *Science* **240**(4860)**,** 1759-1764.

Luckow, V. A., Lee, S. C., Barry, G. F., and Olins, P. O. (1993). Efficient generation of infectious recombinant baculoviruses by site-specific transposon-mediated insertion of foreign genes into a baculovirus genome propagated in Escherichia coli. *J. Virol.* **67**(8)**,** 4566-4579.

Mettenleiter, T. C. (2002). Herpesvirus assembly and egress. *J. Virol.* **76**(4)**,** 1537-1547.

Mettenleiter, T. C. (2004). Budding events in herpesvirus morphogenesis. *Virus Res.* **106**(2)**,** 167-180.

Monsma, S. A., and Blissard, G. W. (1995). Identification of a membrane fusion domain and an oligomerization domain in the baculovirus GP64 envelope fusion protein. *J. Virol.* **69**(4)**,** 2583-2595.

Monsma, S. A., Oomens, A. G., and Blissard, G. W. (1996). The GP64 envelope fusion protein is an essential baculovirus protein required for cell-to-cell transmission of infection. *J. Virol.* **70**(7)**,** 4607-4616.

Newcomb, W. W., Trus, B. L., Booy, F. P., Steven, A. C., Wall, J. S., and Brown, J. C. (1993). Structure of the herpes simplex virus capsid. Molecular composition of the pentons and the triplexes. *J. Mol. Biol.* **232**(2)**,** 499-511.

Oomens, A. G. P., and Blissard, G. W. (1999). Requirement for GP64 to Drive Efficient Budding of *Autographa californica* Multicapsid Nucleopolyhedrovirus. *Virology* **254,** 297-314.

Perez, M., Craven, R. C., and de la Torre, J. C. (2003). The small RING finger protein Z drives arenavirus budding: implications for antiviral strategies. *Proc. Natl. Acad. Sci. U. S. A.* **100**(22)**,** 12978-12983.

Schnee, M., Ruzsics, Z., Bubeck, A., and Koszinowski, U. H. (2006). Common and specific properties of herpesvirus UL34/UL31 protein family members revealed by protein complementation assay. *J Virol* **80**(23)**,** 11658-66.

Sinclair, A. J., and Farrell, P. J. (1992). Epstein-Barr virus transcription factors. *Cell Growth Differ.* **3**(8)**,** 557-563.

Stanke, N., Stange, A., Luftenegger, D., Zentgraf, H., and Lindemann, D. (2005). Ubiquitination of the prototype foamy virus envelope glycoprotein leader peptide regulates subviral particle release. *J. Virol.* **79**(24)**,** 15074-15083.

Stewart, T. M., Huijskens, I., Willis, L. G., and Theilmann, D. A. (2005). The Autographa californica multiple nucleopolyhedrovirus ie0-ie1 gene complex is essential for wild-type virus replication, but either IE0 or IE1 can support virus growth. *J. Virol.* **79**(8)**,** 4619-4629.

Theilmann, D. A., Blissard, G. W., Bonning, B., Jehle, J. A., O'Reilly, D. R., Rohrmann, G. F., Thiem, S., and Vlak, J. M. (2005). Baculoviridae. *In* "Virus Taxonomy - Eighth Report of the International Committee on Taxonomy of Viruses" (M. M. A. Fauquet C.M., Maniloff J., Desselberger U., and B. L.A. (ed.), Ed.), pp. 177-185. Elsevier/Academic Press, London.

Thompson, J. D., Higgins, D. G., and Gibson, T. J. (1994). Improved sensitivity of profile searches through the use of sequence weights and gap excision. *Comput Appl Biosci* **10**(1)**,** 19-29.

Wills, J. W., Cameron, C. E., Wilson, C. B., Xiang, Y., Bennett, R. P., and Leis, J. (1994). An assembly domain of the Rous sarcoma virus Gag protein required late in budding. *J. Virol.* **68**(10)**,** 6605-6618.

Yoo, S., and Guarino, L. A. (1994). Functional dissection of the *ie2* gene product of the baculovirus *Autographa californica* nuclear polyhedrosis virus. *Virology* **202**(1)**,** 164-172.

Chapter 5: General discussion and future perspectives

5.1 Summary and hypothesis

Baculoviruses have a biphasic replication cycle, in which two types of virions are formed (Blissard, 1996; Rohrmann, 1992). After DNA replication but prior to occlusion body formation, progeny nucleocapsids are destined to be transported to the cytoplasmic membrane and become budded virus which spread the secondary infection and accelerate the systemic infection in the host larvae. At the very late stage of infection, the progeny nucleocapsids are retained in the nucleus, become singly or multiply enveloped and occluded in polyhedra. Polyhedra, also know as occlusion bodies, can be stable and survive for years in the soil under natural conditions until they are ingested by another host and initiate the next round of infection. This biphasic life cycle perfectly matches the fitness of baculovirus. The extensive study of ODV specific proteins and the formation of polyhedra have been a persistent interest and extensively studied for over two decades (Funk et al, 1997; Braunagel et al, 2003). However, the events in the BV pathway are not well studied and the mechanism that determines the fate of the progeny nucleocapsids to be either shuttled out of or retained in the nucleus is unknown. In addition, the mechanism by which the nucleocapsids are transported from the nucleus to cytoplasmic membrane has not been studied.

EXON0 is found in all the members of the lepidopteran NPV sequenced to date and has been shown to be required for the efficient production of BV. Deletion of *exon0* however does not affect the DNA replication or polyhedra formation indicating that EXON0 has a role specific to the BV pathway (Dai et al., 2004). In this thesis, the molecular mechanism by which EXON0 is required for the efficient BV production was investigated. The results of these investigations have shown that EXON0 facilitates the efficient transport of nucleocapsids from the ring zone of the virogenic stroma in the

nucleus to the plasma membrane to become BV. EXON0 was shown to associate with microtubules and this interaction was demonstrated to play an essential role which may be similar to egress mechanisms used by other animal viruses. The utilization of microtubules for viral egress by baculoviruses was previously unknown. The domains of EXON0 required for the efficient budding were also mapped for dimer formation and association with other proteins. This thesis is the first study to show functional mechanisms of a baculovirus protein that is specific for the BV pathway and significantly enhances our understanding of baculovirus life cycle.

The conservation of EXON0 in all lepidopteran NPVs (the proposed alphabaculovirus genus (Jehle et al., 2006) suggests EXON0 facilitates a common transport pathway in the BV production for this group of baculoviruses. The genomes of granuloviruses and NPVs of Sawflies that have been sequenced to date do not contain an *exon0* homolog. The question therefore arises as why these baculoviruses do not contain EXON0 and if they use an alternate mechanism for BV transport. Potentially these other groups do not produce an equivalent BV phenotype. For example it is interesting to note that the CpGV in tissue culture system produces very low titers of extracellular virus compared to lepidopteran NPVs (Winstanley and Crook, 1993). In addition, the particles described as BV are not produced until very late times post infection which is significantly different from lepidopteran NPV BV production. The Sawfly NPVs whose host Hymenopterans are more ancient insects have been shown to be restricted to midgut tissue and no BV have been described (Federici, 1997). It is therefore possible that EXON0 may be a relatively recent acquisition by the lepidopteran NPVs for the rapid and high-level production of BV for the quick dissemination of virus from the initial midgut foci of infection.

Like maturation of herpesvirus (Mettenleiter, 2002; 2004), the egress pathway of baculovirus BV nucleocapsids is a complicated process, they have to egress through not only nucleus and cytoplasm, but also penetrate the nuclear membrane and bud at plasma membrane. The EM studies form previous studies (Williams and Faulkner, 1997) and my data have suggested following pathway of nucleocapsid egress, which can be dissected

into five steps (Fig. 5.1A). The first step is the egress of nucleocapsid in the nucleus from virogenic stroma to the nuclear membrane, followed by the packaging of nucleocapsids in the nuclear membrane. The third step is pinching off of nucleocapsids from nuclear membrane and the formation of transport vesicle in the cytoplasm. In step 4 of de-envelopment, the nuclear membrane-derived vesicle is lost during egress and naked nucleocapsids are found in the cytoplasm. The step 5 is the migration of un-enveloped nucleocapsids to plasma membrane. The EM picture in Fig. 5.1A also shows the close association of nucleocapsids with apparent microtubules during egress.

Little is know about the mechanism of nucleocapsid egress in above 5 steps. From my research, EXON0 has been found to be the component of transported nucleocapsids, EXON0 associates with microtubules, microtubule dynamics and integrity are essential for BV production. Nucleocapsids apparently associate with microtubules during egress. Therefore, my hypothesis is that the transport of BV nucleocapsids is based on microtubules, and EXON0 bridges the nucleocapsids and microtubules to facilitate the efficient transport of nucleocapsids in Step 1 and Step 5 of nucleocapsids egress pathway (Fig. 5.1B). This is my contribution to the understanding of the egress pathway of baculovirus nucleocapsids.

5.2 Functions of EXON0

EXON0 was shown to be a nucleocapsid protein that interacts and colocalizes with the nucleocapsid proteins FP25 and BV/ODV-C42. Deletion of FP25 results in a virus that produces fewer occlusion bodies and fewer virions per occlusion body, but releases more BV into the media (Fraser and Hink, 1982; MacKinnon et al., 1974; Potter et al, 1976; Ramoska and Hink, 1974). The association between FP25 with EXON0 therefore suggests that these two proteins may be jointly involved in regulating the BV production. Additional studies have also shown that the deletion of *fp25* alters not only the expression and accumulation profile of several viral proteins including the major capsid protein VP39, GP64, and BV/ODV-E26, and, alters the transport of ODV-E66 to intranuclear

membranes during infection (Braunagel et al., 1999; Rosas-Acosta et al, 2001). It is yet to be determined if the absence of EXON0 also changes the expression and transport of these proteins.

A surprising result of this study was to show that even though EXON0 is a structural component of nucleocapsids it is not required for the assembly of progeny nucleocapsids. This was determined by electron microscopy which showed that nucleocapsids were produced in equivalent numbers, in normal size and were filled with electron-dense viral nucleoprotein. Sections of polyhedra from very late infection show that nucleocapsids of *exon0* KO virus are packaged into polyhedra with no overt differences to the repair virus (data not shown). However, it is unknown if *exon0* KO ODV packaging efficiency or the yield of polyhedra relative to the repaired virus is affected. Further quantitative analysis of mature polyhedra of these two viruses will be necessary to determine if EXON0 has any impact on ODV or polyhedra production.

The specific domains of EXON0 were investigated using deletion and point mutants to show that the leucine zipper domain had the greatest impact on BV production. The single point mutant L190/P which was predicted to cause the disruption of the leucine zipper produces levels of BV similar to the *exon0* KO. The point mutations which abolish the dimerization reveal the requirement of dimer formation for the function of EXON0. This is similar to some microtubule associated proteins such as kinesin and Stu2p for which it has been shown that dimerization is indispensable for association with microtubules (Al-Bassam et al., 2006; Vale and Fletterick, 1997).

5.3 The association between EXON0 and microtubules

EXON0 has been shown to associate with β-tubulin. In addition, the dynamics and integrity of microtubules have significant impact on the BV production, suggesting the implication of microtubule dependent transport of nucleocapsids in BV pathway. As a structural protein of nucleocapsids, EXON0 facilitates the efficient transport of

nucleocapsids to the plasma membrane. This is similar to the transport proteins of vaccinia virus, F12L and A36R and the herpesvirus tegument proteins VP22, VP11, and US11, which are all the structural components of transported capsids and interact with microtubules directly or with kinesin and are involved in the microtubule-dependent egress of capsids (Diefenbach et al., 2002; van Eijl et al., 2002; van Eijl, et al, 2000; Zhang et al, 2000). The transport based on microtubules is a common strategy used by a vast diversity of viruses (reviewed by Dahner et al (2005) and Smith and Enquist (2002)). The transport of baculovirus nucleocapsids on microtubules could be a reasonable mechanism and a good solution for their egress.

In this study, EXON0 has been shown to associate with free heterodimers of tubulin. In addition, the association of β-tubulin with transiently expressed EXON0 suggests no other viral proteins are required for their association. Although these results provide preliminary information on the mechanism of their association it still remains to be determined how EXON0 associates with microtubules in detail. EXON0 might bind directly to the tubulin dimers or other cellular proteins may bridge their association. The herpes simplex virus tegument protein US11 interacts with conventional kinesin heavy chain and plays a major role in the anterograde transport of unenveloped capsids in axons (Diefenbach et al., 2002).

Stu2p is another essential microtubule binding protein identified in yeast which regulates microtubule plus end dynamics and localizes primarily to the spindle pole body and to a lesser extent along microtubules (Al-Bassam et al., 2006; Wang and Huffaker, 1997). The microtubule-binding domain of Stu2p has been localized to a highly basic 100-amino acid region which contains two imperfect repeats and both repeats appear to contribute to microtubule binding to a similar extent (Wang and Huffaker, 1997). The only baculovirus protein P10 which has been shown to bind α-tubulin directly also has a basic C-terminal which is believed to be the putative microtubule-binding domain (Patmanidi et al, 2003; Van Oers and Vlak, 1997). It is interesting to note that the Charged (C) domain of EXON0 (K59 to K87) which is required for tubulin binding is rich in charged amino acids and has a slightly alkaline pI of 8.93. Further alignment analysis between the basic

repeat R1, R2 of Stu2p, P10 and EXON0 did not, however, reveal similarity of primary structure. MAPs are generally believed to associate with microtubules by ionic interaction between the basic microtubule-binding domain and the acidic C-terminus of tubulin (Patmanidi et al, 2003). It is possible that there is tertiary structural similarity between the C domain of EXON0 and the basic microtubule-binding domain of other MAPs that contributes to potential interaction with tubulin.

5.4 The movement of nucleocapsids

In this thesis, EXON0 has been shown to associate with microtubules and the microtubule polymerization drugs affect both the localization of EXON0 and yield of BV. This initial evidence examining the effects of microtubule depolymerizing agents on nucleocapsid egress and BV production provides important progress in the baculovirus field of and a basis for further sophisticated studies.

"Single-virus tracking" is an emerging powerful imaging tool which enables us to visualize and track the steps of virus infection, especially the entry and egress process (Brandenburg and Zhuang, 2007). The mechanisms of virus transport and virus-cell interactions *in vitro* and *in vivo* have been examined in detail from viruses genetically engineered with fluorescent proteins. Labelling virus structural proteins with fluorescent protein has already shown visually the process of herpes virus entry, transport, and egress in detail (Luxton et al., 2005; Sampaio et al., 2005; Smith et al., 2004). The exit mode of vaccinia virus has been successfully studied by the fusion of B5R protein with EGFP. Time-lapse confocal microscopy of live cells infected with vB5R-EGFP has revealed that velocity of IEV transport from perinuclear assembly site to plasma membrane is 40–98 μm/min (mean 60μm/min), similar to that mediated by microtubules but not actin filaments (Rietdorf et al., 2001; Ward and Moss, 2001a; 2001b; 2004).

The EGFP has been fused with major capsids protein VP39 of baculovirus virions at both termini and the fusion protein incorporated successfully into the capsids whose infectivity

is not compromised (Oker-Blom et al, 2003). Other nucleocapsid proteins may also be the amenable candidates for EGFP fusion and virus tracking. It is possible that EGFP labelled baculoviruses will enable the visualization of the nucleocapsid interaction with the cytoskeleton, their trajectory, and velocity of transport. This will build upon the results of this study which is one of the first to identify a viral protein, EXON0, to be directly involved in baculovirus egress.

Figure 5. 1 Hypothesis of the roles of EXON0 in the egress pathway of BV nucleocapsids.

(A). Illustration of BV pathway by EM pictures. The first step is the egress of nucleocapsid to nuclear membrane (1), followed by the packaging of nucleocapsids in nuclear membrane (2), then the formation of transport vesicle in plasma (3) and de-envelopement of nucleocapsids (4), finally the migration of naked nucleocapsids to plasma membrane. Bars, 500 nm in length. (B). The roles of EXON0 in egress of BV nucleocapsids. EXON0 may bridge the nucleocapsids and microtubules to facilitate the efficient transport of nucleocapsids to plasma membrane.

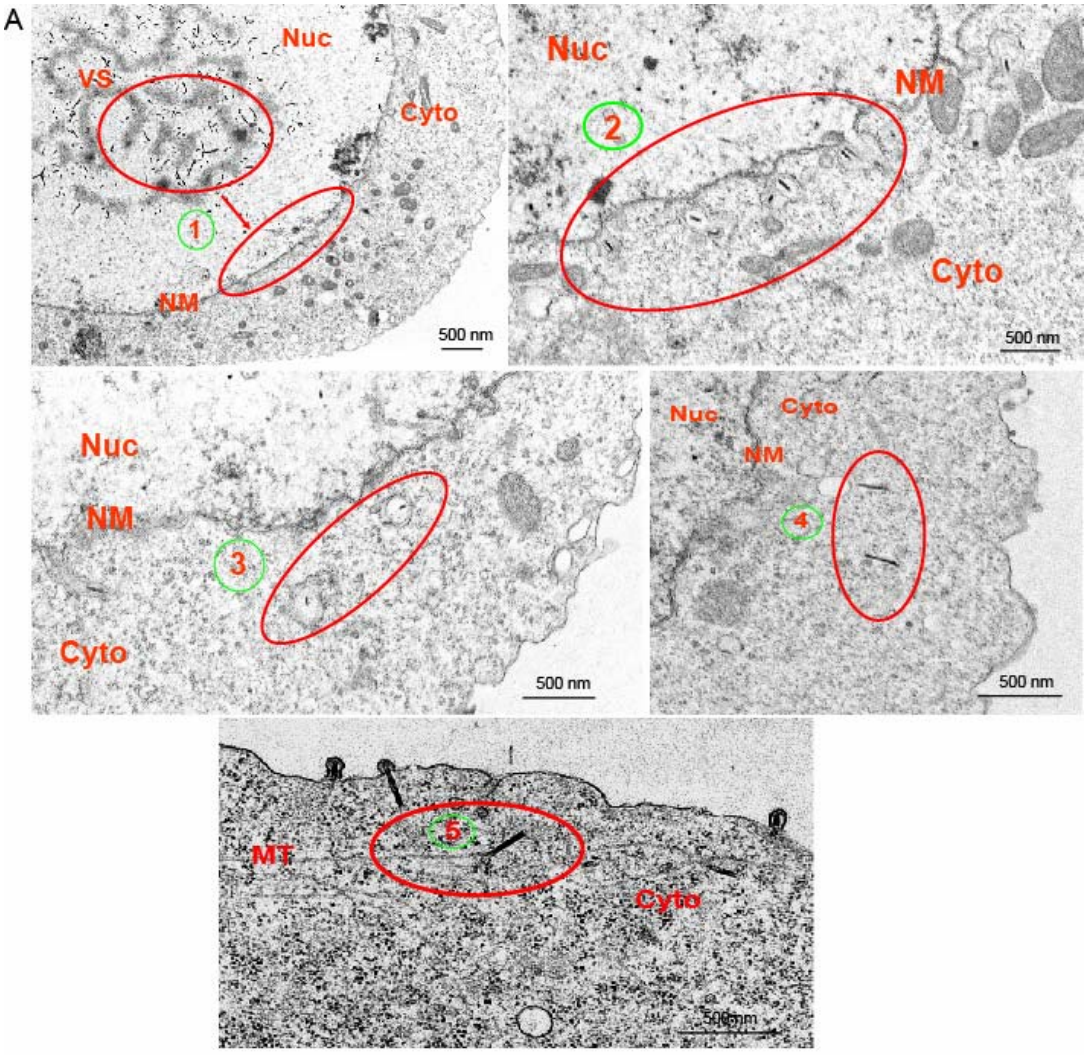
A
Nuc
VS
Cyto
1
NM
500 nm
Nuc
NM
2
Cyto
500 nm
Nuc
NM
3
Cyto
500 nm
Nuc
Cyto
NM
4
500 nm
MT
5
Cyto
500nm

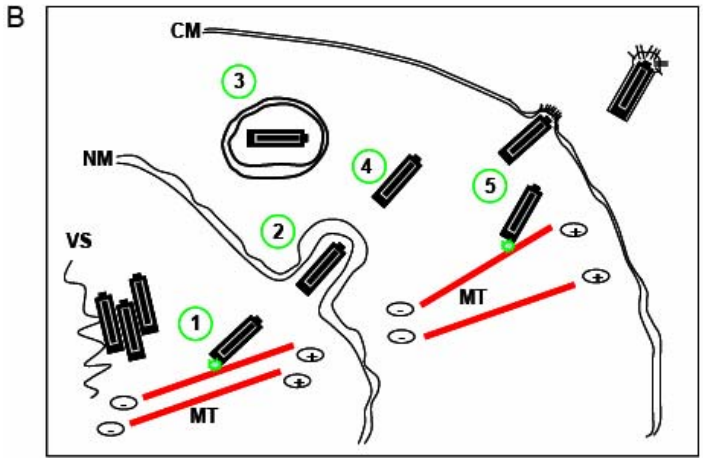
B
CM
3
NM
4
5
2
VS
1
MT
MT

5.5 References

Al-Bassam, J., van Breugel, M., Harrison, S. C., and Hyman, A. (2006). Stu2p binds tubulin and undergoes an open-to-closed conformational change. *J Cell Biol* **172**(7)**,** 1009-22.

Blissard, G. W. (1996). Baculovirus--insect cell interactions. *Cytotechnology* **20**(1-3)**,** 73-93.

Brandenburg, B., and Zhuang, X. (2007). Virus trafficking - learning from single-virus tracking. *Nat Rev Microbiol* **5**(3)**,** 197-208.

Braunagel, S. C., Burks, J. K., Rosas-Acosta, G., Harrison, R. L., Ma, H., and Summers, M. D. (1999). Mutations within the *Autographa californica* nucleopolyhedrovirus FP25K gene decrease the accumulation of ODV-E66 and alter its intranuclear transport. *J. Virol.* **73**(10)**,** 8559-8570.

Braunagel, S. C., Russell, W. K., Rosas-Acosta, G., Russell, D. H., and Summers, M. D. (2003). Determination of the protein composition of the occlusion-derived virus of *Autographa californica* nucleopolyhedrovirus. *Proc. Natl. Acad. Sci. U. S. A.* **100**(17)**,** 9797-9802.

Dai, X., Stewart, T. M., Pathakamuri, J. A., Li, Q., and Theilmann, D. A. (2004). *Autographa californica* multiple nucleopolyhedrovirus *exon0* (*orf141*), which encodes a RING finger protein, is required for efficient production of budded virus. *J. Virol.* **78**(18)**,** 9633-9644.

Diefenbach, R. J., Miranda-Saksena, M., Diefenbach, E., Holland, D. J., Boadle, R. A., Armati, P. J., and Cunningham, A. L. (2002). Herpes simplex virus tegument protein US11 interacts with conventional kinesin heavy chain. *J. Virol.* **76,** 3282-3291.

Dohner, K., Nagel, C. H., and Sodeik, B. (2005). Viral stop-and-go along microtubules: taking a ride with dynein and kinesins. *Trends Microbiol.* **13,** 320-327.

Federici, B. A. (1997). Baculovirus pathogenesis. *In* "The Baculoviruses" (L. K. Miller, Ed.), pp. 33-56. Plenum, New York.

Fraser, M. J., and Hink, W. F. (1982). The isolation and characterization of the MP and FP plaque variants of *Galleria mellonella* nuclear polyhedrosis virus. *Virology* **117,** 366–378.

Funk, C. J., Braunagel, S. C., and Rohrmann, G. F. (1997). Baculovirus structure. *In* "The Baculoviruses" (L. K. Miller, Ed.), pp. 7-32. Plenum, New York.

Jehle, J. A., Blissard, G. W., Bonning, B. C., Cory, J. S., Herniou, E. A., Rohrmann, G. F., Theilmann, D. A., Thiem, S. M., and Vlak, J. M. (2006). On the classification and nomenclature of baculoviruses: a proposal for revision. *Arch Virol* **151**(7)**,** 1257-66.

Luxton, G. W., Haverlock, S., Coller, K. E., Antinone, S. E., Pincetic, A., and Smith, G. A. (2005). Targeting of herpesvirus capsid transport in axons is coupled to association with specific sets of tegument proteins. *Proc Natl Acad Sci U S A* **102**(16)**,** 5832-7.

MacKinnon, E. A., Henderson, J. F., Stoltz, D. B., and Faulkner, P. (1974). Morphogenesis of nuclear polyhedrosis virus under conditions of prolonged passage in vitro. *J Ultrastruct Res* **49**(3)**,** 419-35.

Mettenleiter, T. C. (2002). Herpesvirus assembly and egress. *J. Virol.* **76**(4)**,** 1537-1547.

Mettenleiter, T. C. (2004). Budding events in herpesvirus morphogenesis. *Virus Res.* **106**(2)**,** 167-180.

Oker-Blom, C., Airenne, K. J., and Grabherr, R. (2003). Baculovirus display strategies: Emerging tools for eukaryotic libraries and gene delivery. *Brief Funct Genomic Proteomic* **2**(3)**,** 244-53.

Patmanidi, A. L., Possee, R. D., and King, L. A. (2003). Formation of P10 tubular structures during AcMNPV infection depends on the integrity of host-cell microtubules. *Virology* **317,** 308-320.

Potter, K. N., Faulkner, P., and MacKinnon, E. A. (1976). Strain selection during serial passage of *Trichoplusia ni* nuclear polyhedrosis virus. *J. Virol.* **18,** 1040–1050.

Ramoska, W. A., and Hink, W. F. (1974). Electron microscope examination of two plaque variants from a nuclear polyhedrosis virus of the alfalfa looper, *Autographa californica*. *J. Invert. Pathol.* **23,** 197–201.

Rietdorf, J., Ploubidou, A., Reckmann, I., Holmstrom, A., Frischknecht, F., Zettl, M., Zimmermann, T., and Way, M. (2001). Kinesin-dependent movement on microtubules precedes actin-based motility of vaccinia virus. *Nat Cell Biol* **3**(11)**,** 992-1000.

Rohrmann, G. F. (1992). Baculovirus structural proteins. *J. Gen. Virol.* **73,** 749-761.

Rosas-Acosta, G., Braunagel, S. C., and Summers, M. D. (2001). Effects of deletion and overexpression of the *Autographa californica* nuclear polyhedrosis virus FP25K gene on synthesis of two occlusion-derived virus envelope proteins and their transport into virus-induced intranuclear membranes. *J. Virol.* **75**(22)**,** 10829-10842.

Sampaio, K. L., Cavignac, Y., Stierhof, Y. D., and Sinzger, C. (2005). Human cytomegalovirus labeled with green fluorescent protein for live analysis of intracellular particle movements. *J Virol* **79**(5)**,** 2754-67.

Smith, G. A., and Enquist, L. W. (2002). Break ins and break outs: viral interactions with the cytoskeleton of Mammalian cells. *Annu. Rev. Cell Dev. Biol.* **18,** 135-161.

Smith, G. A., Pomeranz, L., Gross, S. P., and Enquist, L. W. (2004). Local modulation of plus-end transport targets herpesvirus entry and egress in sensory axons. *Proc Natl Acad Sci U S A* **101**(45)**,** 16034-9.

Vale, R. D., and Fletterick, R. J. (1997). The design plan of kinesin motors. *Annu Rev Cell Dev Biol* **13,** 745-77.

van Eijl, H., Hollinshead, M., Rodger, G., Zhang, W. H., and Smith, G. L. (2002). The vaccinia virus F12L protein is associated with intracellular enveloped virus particles and is required for their egress to the cell surface. *J Gen Virol* **83**(Pt 1)**,** 195-207.

van Eijl, H., Hollinshead, M., and Smith, G. L. (2000). The vaccinia virus A36R protein is a type Ib membrane protein present on intracellular but not extracellular enveloped virus particles. *Virology* **271**(1)**,** 26-36.

Van Oers, M. M., and Vlak, J. M. (1997). The baculovirus 10-kDa protein. *J Invertebr Pathol* **70**(1)**,** 1-17.

Wang, P. J., and Huffaker, T. C. (1997). Stu2p: A microtubule-binding protein that is an essential component of the yeast spindle pole body. *J Cell Biol* **139**(5)**,** 1271-80.

Ward, B. M., and Moss, B. (2001a). Vaccinia virus intracellular movement is associated with microtubules and independent of actin tails. *J Virol* **75**(23)**,** 11651-63.

Ward, B. M., and Moss, B. (2001b). Visualization of intracellular movement of vaccinia virus virions containing a green fluorescent protein-B5R membrane protein chimera. *J Virol* **75**(10)**,** 4802-13.

Ward, B. M., and Moss, B. (2004). Vaccinia virus A36R membrane protein provides a direct link between intracellular enveloped virions and the microtubule motor kinesin. *J. Virol.* **78,** 2486–2493.

Williams, G. V., and Faulkner, P. (1997). Cytological changes and viral morphogenesis during baculovirus infection. *In* "The Baculoviruses" (L. K. Miller, Ed.), pp. 61-107. Plenum Press, New York.

Zhang, W. H., Wilcock, D., and Smith, G. L. (2000). Vaccinia virus F12L protein is required for actin tail formation, normal plaque size, and virulence. *J Virol* **74**(24)**,** 11654-62.

Appendix

To show the qualityof the BV purification, the coomassie stained gel of purified BV from Chapter 2 is shown in Fig. 1. The TAP purification using the IgG-CBP tag was ineffective (Chapter 3). The expression of the IgG-CBP, GFP and 3FLAG-6His tagged EXON0 proteins is shown in Fig. 2, and the IgG purification results are shown in Fig. 3.

Figure 1 SDS-PAGE and Coomassie stain of purified BV, nucleocapsid and envelope fraction.

Budded viruses (BV) of *exon0* KO-HA-EXON0 was purified and fractionated into nucleocapsid (NC) and envelope (Env) fraction. Purified BV (15 μg), NC (10 μg) and Env (10 μg) were separated by 10% SDS-PAGE and stained with Coomassie brilliant blue. The major BV envelope protein GP64, major nucleocapsid protein VP39 and a protein band in agreement with the size of EXON0 (30 kDa) were indicated on the right. The sizes of marker bands were indicated on left.

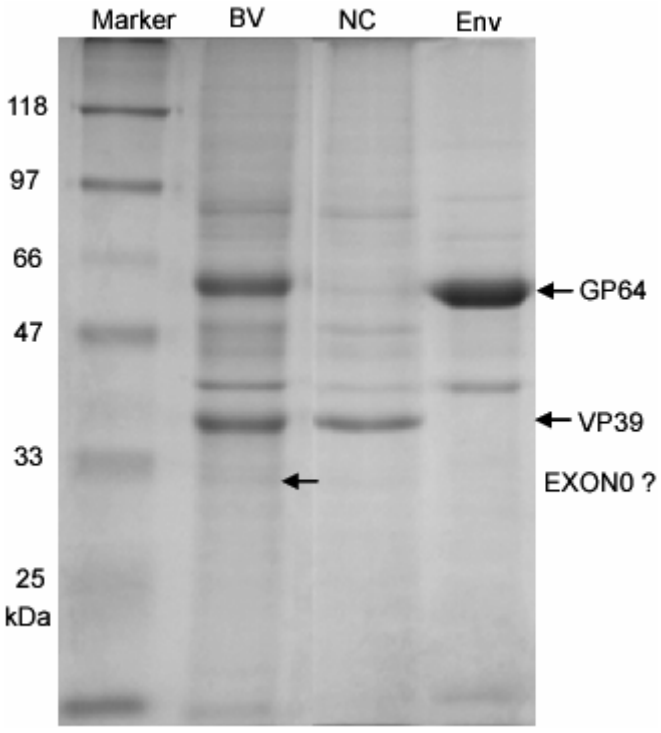

Figure 2 Western blot detection of EXON0 fusion proteins.

Sf9 cells were transfected with *exon0* KO-NTAP-HA-EXON0, *exon0* KO-GFP-HA-EXON0 and *exon0* KO-3FLAG-6His-HA-EXON0 and harvested 96 hpt. Approximately 5×10^5 cells were loaded on 10% SDS-PAGE and probed with anti-HA antibody. The cells transfected with *exon0* KO-HA-EXON0 was also loaded as control. The protein marker is labeled on left and the sizes of detected bands are indicated on right.

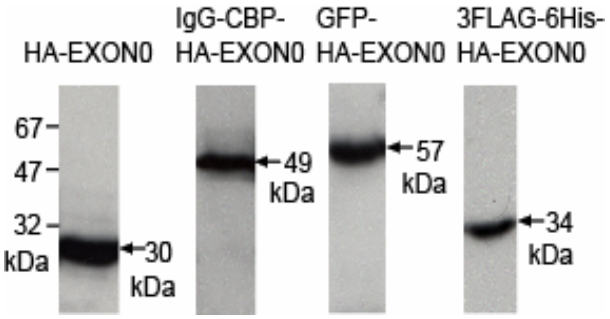

Figure 3 IgG purification of IgG-CBP-EXON0.

Sf9 cells were infected with control virus *exon0* KO-HA-EXON0 or *exon0* KO-IgG-CBP-HA-EXON0 with MOI of 10 and harvested at 24 hpi. Cell lysates were incubated with protein A sepharose beads. After extensive washing, the bound proteins were eluated with TEV protease cleavage. The eluates were analyzed with 4-12% gradient SDS-PAGE and visualized by silver stain. No major specific band was found to IgG-CBP-HA-EXON0.